SPATIAL-TEMPORAL SIGNAL PROCESSING FOR MULTI-USER CDMA COMMUNICATION SYSTEMS

by

Ruifeng Wang

A thesis submitted to the
Department of Electrical and Computer Engineering
in conformity with the requirements
for the degree of Doctor of Philosophy

Queen's University
Kingston, Ontario, Canada
July 1999

Abstract

Among multi-access communications techniques, CDMA (Code Division Multiple Access) is interference-limited. Conventional single-user receivers suffer from the near-far problem in CDMA cellular communications systems. One method to suppress multi-access interference is digital beamforming by using base-station antenna arrays. However, using beamforming alone cannot solve the near-far problem. Verdú demonstrates that multi-user signal detection can be used to eliminate multi-access interference by utilizing all active users' spreading codes at the base-station. This thesis addresses the incorporation of array signal processing with multi-user signal detection in the CDMA terminal to base-station uplink. In particular, this thesis proposes a method - jointly estimating the unknown channel array response vectors and detecting the bits from all users.

We first consider synchronous single-path Rayleigh fading channels. We develop a spatial-temporal decorrelator receiver employing the maximum likelihood criterion based on a novel discrete-time system model and analyze the decorrelator's asymptotic efficiency. It is shown that the spatial-temporal decorrelator is near-far resistant and that using a base-station antenna array significantly increases asymptotic efficiency for either the spatial-temporal decorrelator or the conventional single-user detector. We formulate the expectation-maximization (EM) and the space alternating generalized expectation-maximization (SAGE) algorithms based on the discrete-time model and obtain two receiver structures for joint channel array response vector estimation and bit sequence detection. The receiver's convergence rate is analyzed. We have observed that using base-station antenna array accelerates the SAGE-based receiver's

convergence and improves channel estimation performance. The BER performance of the SAGE-based receiver is shown to be near-far resistant.

A synchronous equivalent discrete-time system model is formulated for asynchronous multipath channels. Based on this model, we exploit multipath diversity by incorporating maximal-ratio combiner into the spatial-temporal decorrelator. It is shown that unlike antenna arrays, using multipath diversity combining does not improve detector's asymptotic efficiency. We exploit the SAGE algorithm to decouple the multi-user signals for bit sequence detection and again decouple the multipath signals to estimate the channel array response vector for each path of each user for given time delays. Timing error effects on the SAGE-based receiver are studied by simulation. Multipath diversity combining is shown to be effective in improving the receiver's bit error rate (BER) performance.

Finally, we extend the techniques developed for single-rate systems to multi-rate systems with base-station antenna arrays over asynchronous multipath fading channels. An iterative multi-user receiver for dual-rate systems is derived. It is shown that unlike the conventional single-user receiver, the proposed receiver's BER relative performances for high-rate and low-rate users are similar. We observed that the BER of high-rate users converges to the derived lower bound as a function of the number of iterations faster than that of low-rate users.

Acknowledgements

It is a great pleasure to thank my supervisor, Dr. Steven Blostein, for his excellent supervision and financial support throughout this research. Without Dr. Blostein's constructive suggestions and knowledgeable guidance in statistical signal processing area, this work would not have been successfully completed.

I would like to thank my defence committee members, Dr. S. G. Akl (Computer Science), Dr. N. C. Beaulieu, Dr J. C. Cartledge and Dr. D. Falconer (Carleton University) for taking time to review this thesis. Prof. Falconer also provides helpful suggestions to the final version of this thesis.

I am indebted to my parents for their continuous encouragement and expectation. Special thanks give my mother for her coming Canada to take care of my baby son.

Finally, I would like to express my appreciation to my wife, Ying, for her understanding, patient and support. I am grateful to my son, Andrew, for the happiness he brings to my family.

This work was supported by the Canadian Institute for Telecommunications Research and the School of Graduate Studies and Research at Queen's University.

Contents

List of Figures

List of Important Symbols

α_k	complex channel attenuation for user k
$\alpha_{k,p}$	complex channel attenuation for user k through pth path
γ_k	signal to noise ratio (SNR) for user k
η_k^c	asymptotic efficiency of conventional detector for user k
η_k^d	asymptotic efficiency of spatial-temporal decorrelator for user k
ρ_{kj}	temporal correlation between user k and user j
σ^2	variance of additive white Gaussian noise
θ_k	direction of arrival (DOA) of user k
$\theta_{k,p}$	direction of arrival (DOA) of user k through pth path
τ_k	relative time delay of user k
$\tau_{k,p}$	relative time delay of user k through pth path
$\mathbf{a}(\theta)$	array response vector with DOA θ
$b_k(i)$	ith bit of kth user
$\mathbf{b}(i)$	ith bit vector
$\mathbf{b}_k^w(i)$	ith sliding window bit vector of kth user
$\mathbf{b}^w(i)$	ith sliding window bit vector
$c_k(t)$	spreading waveform of kth user
c_{kl}	lth chip of kth user
$\mathbf{c}_k$	spreading code vector of kth user
C_k	temporal channel matrix of user k for synchronous single-path channels
$C_{k,p}$	temporal channel matrix of user k through pth path

$\mathbf{f}_k$	channel array response vector of kth user
f_k^m	mth component in $\mathbf{f}_k$
$\mathbf{f}_{k,p}$	channel array response vector of kth user through pth path
$f_{k,p}^m$	mth component in $\mathbf{f}_{k,p}$
f_{kj}	spatial correlation between user k and user j
$F_{k,p}$	spatial channel matrix of user k through pth path
$\mathbf{h}_k$	total impulse response vector of kth user for synchronous single-path channel
H	spatial-temporal channel matrix for synchronous single-path channels
$\mathcal{H}$	spatial-temporal channel matrix for asynchronous multipath channels
H_k	spatial-temporal channel matrix of kth user
$H_{k,p}$	spatial-temporal channel matrix of kth user through pth path
i	bit index
k	user index
K	number of users in the system
l	chip index
L	processing gain
m	antenna array element index
M	number of antenna elements
$\mathbf{n}(.)$	additive white Gaussian noise vector
N	number of bits in each block
p	propagation path index
P	number of propagation paths
$p(t)$	spreading chip pulse
R	spatial-temporal cross-correlation matrix for synchronous single-path channels
R_{kj}	kjth component in R
$\mathcal{R}$	spatial-temporal cross-correlation matrix for asynchronous multipath channels
$\mathcal{R}_{kj}$	kjth sub-matrix in $\mathcal{R}$, denoting cross-correlation between users k and j

Chapter 1

Introduction

1.1 Motivation

Wireless communication systems, which provide an efficient high-quality information exchange between two portable terminals, have great potential for further development in the near future. Cordless and cellular telephony, mobile computing, and satellite communications are facing rapid market demand. With the popularity of wireless communication services, the number of users has been growing dramatically for the past few years. This increase results in a big challenge for wireless technology, i.e., expanding the system capacity for wireless services with the available spectrum.

The cellular concept was conceived to increase the radio channel efficiency by dividing the large service area into several smaller cells and using a subset of the total available radio channels in each cell. Therefore, the radio channels could be reused in different cells which were separated sufficiently to avoid co-channel interference. Hence, system capacity is increased by the spatial characteristics of the channel [27]. Cellular systems exploit handoff techniques to enable a mobile leaving a cell to switch to a new channel available in the next cell automatically. Normally, one base-station is assigned in each cell to serve several mobile users.

For multiple access communication systems, sharing a common channel spectrum can be achieved by frequency division multiple access (FDMA), time division multiple access (TDMA), code division multiple access (CDMA) or their combinations.

While FDMA and TDMA are based on dividing the available frequency spectrum and the transmission time to maintain multiple users, respectively, CDMA systems permit multiple users to transmit in the same frequency band simultaneously by using different spreading codes [70] [100]. Comparative studies show that CDMA can achieve greater system capacity than FDMA and TDMA [21] [39]. Unlike FDMA and TDMA capacities which are primarily bandwidth limited, CDMA capacity is interference limited. Any reduction in interference converts directly into an increase in system capacity. Therefore, multiple access interference (MAI) suppression techniques for CDMA systems have attracted a substantial amount of attention in the past years.

1.1.1 Spatial Signal Processing

A promising approach to suppress MAI is the use of antenna arrays at base-stations [1] [40] [85] [104] [105]. Since base-station antenna arrays capture more signal energy from mobile users and provide spatial diversity for base-station receivers, optimum combining and beamforming technology can be used with a base-station antenna array to increase system capacity for wireless communication systems. Using antenna arrays also permits a less stringent form of power control while maintaining acceptable bit error rate (BER) performance. Performance improvements for CDMA systems with base-station antenna arrays have been studied in [12], [57] and [59]. Combined beamformer-RAKE conventional single-user receivers have been proposed for multipath channels in [35], [41] and [58]. A comprehensive review of antenna array signal processing for wireless communications can be found in [66] and [88].

1.1.2 Multi-user Signal Detection

Because of the relative time delays among the active mobile users for CDMA uplink channels (mobile to base-station), we cannot guarantee orthogonality between the spreading codes. Therefore, CDMA systems suffer from co-channel interference which results in the near-far problem [43]. The near-far effect arises because received

powers from users near the base-station receiver are higher than those from users far away and some users' signals experience deep fading. However, the near-far problem is not inherent to CDMA systems, but due to the conventional single-user receiver which models the interference from other users as noise (see Figure 1.1). The interference

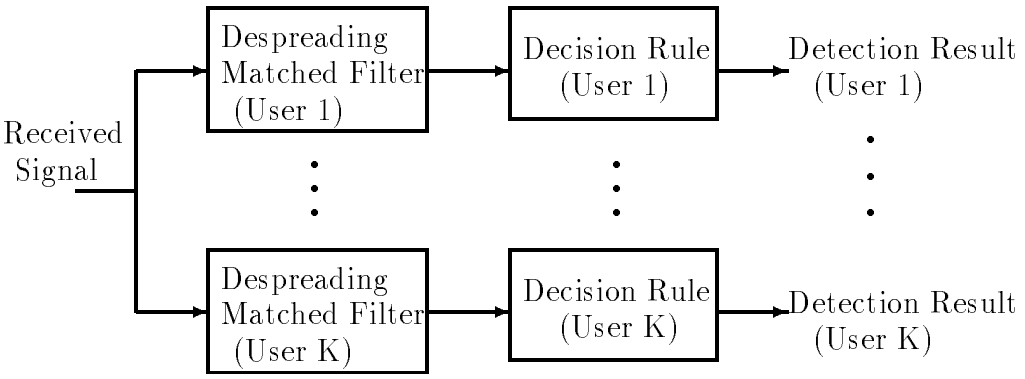

Figure 1.1: Conventional Single-user Detector

modelling loses useful information from interfering users. By jointly detecting all the users' signals, optimum multi-user signal detection for CDMA systems can be made near-far resistant and can achieve significant performance improvement over that of conventional single-user detection [95]. Multi-user signal detection is illustrated in Figure 1.2. Because of the computational complexity of optimum multi-user detec-

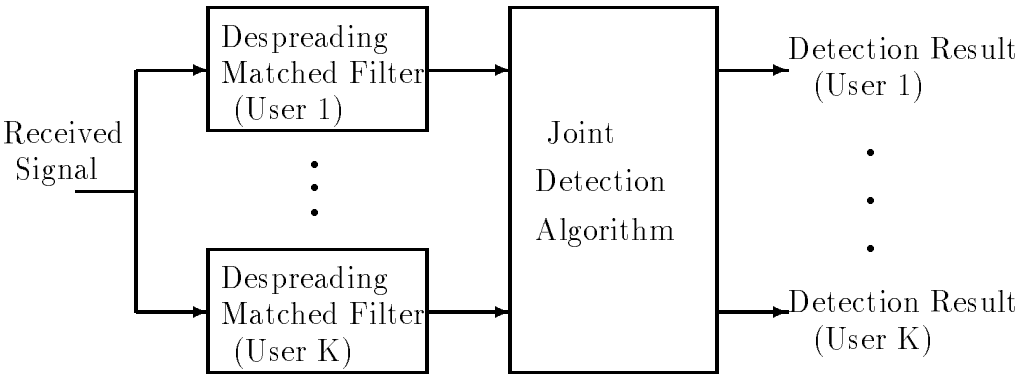

Figure 1.2: Multi-user Signal Detector

tion, several suboptimum multi-user signal detectors have been proposed for additive white Gaussian noise (AWGN) channels, including decorrelating detectors [31] [43]

[107], linear minimum mean-squared error (MMSE) detectors [46] [107], multi-stage detectors [91] [92], decision feedback detectors [9] [10], adaptive multi-user detectors [4] [26] [48] [71] and blind multi-user detectors [24] [102].

The major advantage of multi-user signal detection is its near-far resistance, i.e., the detector's performance is not sensitive to the unequal received signal power from different mobile users. This makes the receiver avoid the sophisticated precise power control currently used in the second generation PCS standard IS-95 [70]. The benefit obtained from multi-user signal detection is three-fold. Firstly, eliminating precise power control directly increases channel spectrum efficiency. Secondly, since no precise power control algorithms are needed, complexity is considerably reduced at the mobile transmitters. This translates into a reduction of mobile power consumption. Finally, even for equal received power from all active mobiles, multi-user signal detectors achieve better bit error rate (BER) performance than the conventional single-user detector, and hence provide greater system capacity.

Matched filtering (MF) methods are proposed to suppress MAI for CDMA systems in [110], which provide a compromise between the noise-whitening MF [52] and linear MMSE detector [46]. A successive interference cancellation approach is analyzed in [98] and [64], and compared with multi-stage detector [91]. As a parallel interference canceller, multi-stage detector outperforms the successive interference canceller for AWGN channels. However, successive interference cancellation can achieve better performance than multi-stage detection for fading channels [65]. Array signal processing concepts [29] can be adapted for multi-user signal detection in single antenna CDMA systems for known channels which are oversampled [76], and provide an extension of the linear MMSE detector in [46].

In [114], [115] and [93], multi-user signal detection is extended to fading channels. The problems of integrating antenna array processing and multi-user signal detection are proposed for known channels in [49] for AWGN channels and in [30] for Rayleigh fading channels. In [37], adaptive antenna array processing and interference cancellation approaches using the least mean squared (LMS) algorithm are analyzed and

the convergence is found to require several hundred training bits. Decorrelating detectors combined with antenna array diversity combining are studied for multipath fading channels in [113], but channel estimation has not been addressed. Overviews of multi-user signal detection can be found in [11], [56] and [97].

1.1.3 Channel Estimation

In order to detect information symbols reliably, we have to estimate channel parameters and antenna array response vectors. Parameter estimators are proposed for AWGN CDMA channels in [94] and [55]. In [36], a channel parameter estimation method is proposed for antenna array CDMA systems, which is not near-far resistant. Joint parameter estimation and multiuser signal detection approaches are studied for single-antenna CDMA systems in [33], [81] and [108]. In [2], [83] and [89] subspace-based channel parameter estimators are proposed for multi-user CDMA systems. Comparative studies for blind channel estimation schemes are provided for multipath CDMA channels in [51]. Recently proposed channel estimation techniques for TDMA systems can be found in [61], [86] and [90]. Most of these estimation methods involve significant matrix computation. Therefore, computationally efficient estimation methods are needed for practical applications.

It is well-known that the expectation-maximization (EM) algorithm provides an efficient numerical solution to the maximum likelihood estimation problem [8]. Applications of the EM algorithm to CDMA systems have been proposed for signal detection [60] and channel estimation [15] [16]. The space-alternating generalized expectation-maximization (SAGE) algorithm has been developed to accelerate the convergence of the EM algorithm [19]. Applications of the SAGE algorithm in multi-user AWGN CDMA channels can be found in [60] for known channels, in [7] for channel parameter estimation and in [78] for joint parameter estimation and signal detection based on the discrete wavelet transform for a single antenna system.

In addition to suffering from the near-far problem, the conventional single-user

receiver also exhibits a nonzero bit error rate (BER) floor even if the background noise level goes to zero. This effect is caused by the contributions from the interfering users at the output of the matched filters (see Figure 1.1). The nonzero BER floor makes it difficult to achieve a low BER required by the multi-rate systems using the conventional single-user receiver without an excessive reduction of system capacity [12] [45]. Therefore, it is important to investigate advanced techniques to eliminate the nonzero BER floor and overcome the near-far problem.

Performance gains provided by multi-user signal detection are achieved at the expense of computational complexity. Therefore, investigation into computationally efficient multi-user signal detection approaches is an important issue. Iterative signal detection and channel estimation approaches have been proposed for fading channels in [16] and [7]. Multi-stage detectors are used to detect information symbols and the maximum-likelihood (ML) channel estimation is implemented by applying the EM-type algorithms in these receivers. However, the multi-stage detector does not guarantee convergence of the receiver to a fixed point and often exhibits slower convergence and oscillatory behaviour [60]. Since the EM-type algorithms have guaranteed convergence, we propose to investigate joint signal detection and channel estimation receivers integrating spatial signal processing with multi-user signal detection by applying the EM-type algorithms to antenna array CDMA systems. We call the combination of spatial signal processing and multi-user signal detection as *spatial-temporal signal processing*.

1.2 Summary of Contributions

This thesis investigates the problem of incorporating array signal processing with multi-user detection. We develop spatial-temporal decorrelating receivers for CDMA systems by incorporating base-station antenna arrays and channel estimation techniques using advanced signal processing algorithms. The new receivers are near-far resistant and also outperform the conventional single-user receiver in terms of bit

error rate (BER). Better BER performance can potentially increase system capacity. The primary contributions are summarized as follows:

- A spatial-temporal decorrelator receiver is derived based on a discrete-time system model for synchronous single-path channels. This decorrelator completely eliminates the multi-access interference (MAI) at the cost of increased background noise.

- Asymptotic efficiencies of the spatial-temporal decorrelator and the conventional single-user detector are derived and compared. Numerical results show that the spatial-temporal decorrelator is near-far resistant and that using a base-station antenna array improves the asymptotic efficiency for either the spatial-temporal decorrelator or the conventional single-user detector.

- Two iterative spatial-temporal decorrelating receivers for joint channel estimation and bit sequence detection are derived by applying the expectation-maximization (EM) and the space alternating generalized expectation-maximization (SAGE) algorithms to the synchronous discrete-time system model, respectively.

- Convergence for the two iterative receivers is analyzed. The SAGE-based receiver is found to converge faster than the EM-based receiver. We have also found that using a base-station antenna array can accelerate convergence of the SAGE-based receiver.

- The bit error rate (BER) of the spatial-temporal decorrelator is derived for known channels. This BER provides a benchmark for the iterative spatial-temporal decorrelating receivers which jointly estimate the channel array response vector and detect the information bit sequence.

- A Cramér-Rao Lower Bound (CRLB) for the channel estimates is derived to assess the performance of the new iterative receivers for synchronous single dominant-path systems.

- A synchronous equivalent discrete-time system model is formulated for asynchronous multipath CDMA systems with base-station antenna arrays.

- A spatial-temporal decorrelator is obtained for asynchronous multipath fading channels by extending the results for the case of synchronous single-path channels. A maximal-ratio combiner (MRC) is incorporated in the new decorrelator to exploit multipath diversity.

- The asymptotic efficiency of the RAKE receiver in multipath fading channels is analyzed. Numerical results show that unlike base-station antenna array, using multipth diversity combining does not improve asymptotic efficiency for multi-user CDMA systems.

- By applying the SAGE algorithm, an iterative receiver is derived for joint channel array response vector estimation and bit sequence detection for asynchronous multipath fading channels. To estimate the channel array response vector for each path of each user, we decouple the multipath received signals for each user after decoupling the multi-access signals.

- A BER lower bound is derived for the spatial-temporal decorrelator for asynchronous multipath CDMA systems with base-station antenna arrays by assuming that the channels for all active users are known and the bit sequences for all the interferers are known.

- A discrete-time model is formulated for multi-rate systems with base-station antenna arrays for asynchronous multipath uplink fading channels.

- An iterative multi-user receiver is derived for multi-rate systems by extending the results obtained for single-rate systems.

- It is observed that multipath diversity can be used to suppress multipath interference for CDMA systems and no multipath interference decorrelator is needed.

1.3 Thesis Overview

This thesis investigates the problem of joint channel estimation and signal detection for multi-user CDMA communication systems with base-station antenna arrays. We use the maximum-likelihood (ML) criterion to solve this problem. Since the computational complexity of direct likelihood maximization is prohibitive, we apply expectation-maximization (EM)-type algorithms to obtain suboptimum solutions. The advantage of the EM-type solutions is that we decompose the K-user coupled optimization problem to K single-user optimization problems. Therefore, using multi-user signal decoupling reduces the computational complexity of direct likelihood maximization while maintaining the improved performance.

Chapter 2 introduces the system model and formulates the problem mathematically. We discuss the characteristics of the wireless fading channel and incorporate the array response vector into the channel models. The transmitted CDMA signals are analyzed in Section 2.3.1. We obtain the received signals for both synchronous single-path channels and asynchronous multipath channels. The problem of joint channel estimation and signal detection is formulated in Section 2.4.

In Chapter 3, we investigate the integration of array signal processing with multi-user signal detection for synchronous single-path channels. A discrete-time model is developed. Based on this model, we derive a spatial-temporal decorrelator for known channels and analyze the decorrelator's asymptotic efficiency. Numerical results show that the spatial-temporal decorrelator is near-far resistant. We apply the EM and SAGE algorithms to the discrete-time model and obtain two iterative receivers. Convergence of the iterative receivers are studied. The SAGE-based receiver converges faster than the EM-based receiver and using base-station antenna array accelerates the SAGE-based receiver's convergence. Analytical BER and Cramér-Rao Lower Bound (CRLB) for the estimated channel are derived to assess the simulation results for the new receivers. Both iterative receivers significantly outperform the conventional single-user receiver. However, the EM-based receiver is not near-far resistant. The SAGE-based receiver has near-far behavior.

We formulate a synchronous equivalent discrete-time system model for asynchronous multipath systems in Chapter 4. Similar to the case of synchronous single-path channels, we derive a spatial-temporal decorrelator for asynchronous multipath channels for given channels. An iterative receiver structure is obtained by applying the SAGE algorithm for joint channel array response vector estimation and bit sequence detection assuming that the time delays are known at the receiver. We derive a BER lower bound for this receiver. We also study the timing error effects on the SAGE-based receiver by simulations.

Chapter 5 extends the results obtained in Chapter 4 for the case of single-rate systems to multi-rate systems. We first formulate a discrete-time system model for dual rate systems with base-station antenna arrays and asynchronous multipath fading channels. We then apply the SAGE algorithm to the dual-rate system model and use the technique developed in Chapter 4 to obtain an iterative receiver for joint channel array response vector estimation and signal detection. The receiver's BER performance is verified using simulations. We observe that using simplified bit detection algorithm without a multipath decorrelator achieves comparable performance to the detector having a multipath decorrelator for both high-rate and low-rate users.

Finally, Chapter 6 summarizes the conclusions obtained in this thesis and provides possible research areas which could need to be further investigated.

Chapter 2

System Model and Problem Formulation

2.1 Introduction

The goal of this thesis is to investigate potential performance improvement for direct-sequence (DS) CDMA communications using advanced signal processing techniques. To this end, we consider the reverse link (mobile to base-station, also called the uplink) of DS-CDMA systems.

This chapter provides the system models which we use to derive receiver structures developed in the following chapters. We first analyze physical mobile channels and formulate statistical channel models. We then introduce the array response vector for base-station antenna array. The received signal models are developed based on the transmitted signals and propagation channel model. Two received signal models are formulated: a synchronous single-path model and an asynchronous multi-path model. Finally, we formulate the problem to be solved in this thesis.

2.2 Wireless Channel Model

Understanding the physical radio propagation channel is crucial to the development of appropriate system models for the applications of spatial-temporal signal processing to wireless communications. A transmitted signal usually arrives at a receiver through

multiple propagation paths with different time delays and different directions of arrival (DOAs). The multipaths are caused by reflection, refraction, diffraction and scattering of the propagating wave due to natural terrain, man-made constructions and possible moving objects in the environment. In this section, we will describe general wireless propagation channel characteristics and provide the statistical channel models used in this thesis. The antenna array response vector is also introduced for CDMA systems with base-station antenna arrays.

2.2.1 Path Loss and Shadowing

Path loss arises from the effect of ground reflection and diffraction of the propagation wave, as well as absorption by water and foliage. Mean propagation loss is range-dependent and changes very slowly. The path loss is defined as the ratio of the received and transmitted powers. In cellular environments, the path loss can be approximated as [27]

$$\mu = \frac{P_r}{P_t} = g_t g_r (\frac{h_t h_r}{d^2})^2 \tag{2.1}$$

where P_t and P_r are the transmitted and received powers, respectively, g_t and g_r are the power gains of the transmit and receive antennas, respectively, d is the distance between the transmit and receive antennas, and h_t and h_r are the heights of the transmit and receive antennas, respectively. The effective path loss follows an inverse fourth power law. In practical environments, this path-loss exponent varies between 2 and 5.

Shadowing is also known as long-term fading or slow fading. It is caused by the shadowing effect of the obstructions in the environment such as buildings and natural features. The envelope of a slow fading signal is determined by the local (sliding-window) mean of the fast fading signal. Experimental studies show that the local mean received power is log-normally distributed and can be modelled as

$$S = 10^{\xi/10} \tag{2.2}$$

where ξ is a Gaussian random variable with distribution which we denote by $N(\nu, \sigma_s^2)$,

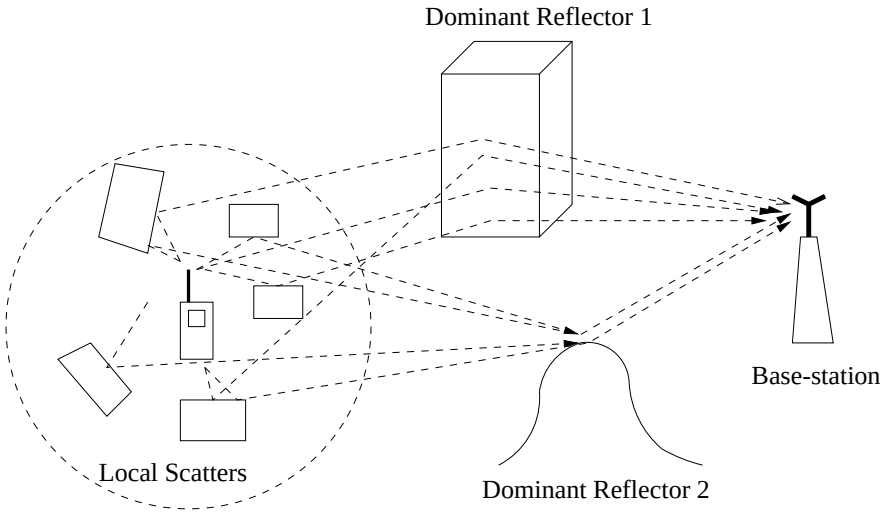

Figure 2.1: Multipath Propagation Channel Environment

where ν is the local area mean and the standard deviation σ_s varies between 4-12 dB depending on the degree of shadowing.

2.2.2 Fast Fading

Fast fading results from local scatters in the vicinity of the mobile. Figure 2.1 illustrates an example of reflection and scattering in the physical propagation environment. Multipath propagation not only causes signal envelope fluctuation, but also results in signal spreading in time. From Figure 2.1, it can be observed that the direction of arrival (DOA) of the transmitted signal to the base-station antenna array may be from an angular region for each specular propagation path. This effect is called angle spread. In addition, the motion of mobile unit introduces spread in frequency, which is known as Doppler spread.

Due to local scatterers, large buildings and natural structures, the radio propagation channel consists of several distinct dominant paths, each of which is a superposition of many component waves. We now proceed with a statistical model for a single dominant path channel. Let the transmitted signal be

$$x(t) = s(t)e^{j2\pi f_c t} \tag{2.3}$$

where $s(t)$ is the baseband signal and f_c is the carrier frequency. If the environment consists of a large number of local scatters, the received noiseless signal can be expressed by

$$\sum_n R_n(t)s(t-t_n)e^{j2\pi f_c(t-t_n)} \tag{2.4}$$

where R_n is the attenuation factor for the signal received from the nth scattering component and t_n is the corresponding time delay. For simplicity, the received signal is modelled as a series of narrow pulses. Doppler spread occurs when the mobile unit is moving with velocity v. The Doppler frequency spread is given by [84]

$$f_{D,n} = v\cos\theta_n/\lambda_c$$

where θ_n is the direction of the nth wave with respect to the velocity vector v and λ_c is the wavelength of the arriving plane wave. The received low-pass equivalent noiseless signal is therefore given by

$$r(t) = \sum_n R_n s(t-t_n)e^{-j2\pi[(f_c+f_{D,n})t_n - f_{D,n}t]} \tag{2.5}$$

We assume that the signal is narrowband with respect to the channel of a single specular path, i.e., its inverse bandwidth 1/B (pulse-width) is much greater than the time delay spread which is the difference between the maximum and the minimum time delays due to local scattering. Thus, we obtain

$$s(t-t_n) \approx s(t-\tau) \tag{2.6}$$

where $\tau \in [\min_n t_n, \max_n t_n]$. Denoting the phase associated with the nth path

$$\phi_n(t) = 2\pi[(f_c + f_{D,n})t_n - f_{D,n}t] \tag{2.7}$$

we obtain the received low-pass noiseless signal as

$$r(t) = s(t-\tau)\sum_n R_n e^{-j\phi_n(t)} \tag{2.8}$$

Letting $\alpha(t) = \sum_n R_n e^{-j\phi_n(t)}$, the channel impulse response is expressed concisely as

$$\alpha(t)\delta(t-\tau) \tag{2.9}$$

where $\delta(.)$ is the Dirac delta function.

Fast fading is primarily the result of time variations of the phases in (2.7). Since $f_c + f_{D,n}(t)$ is very large, a small change in time delay t_n may result in a large change in $\phi_n(t)$. Thus, the received signal components may add constructively or destructively. When the number of scatterers in the channel is large, the channel impulse response, $\sum_n R_n e^{-j\phi_n(t)}$, has a complex Gaussian distribution and the phases $\phi_n(t)$ are uniformly distributed in the interval $[0, 2\pi)$.

In the absence of a line-of-sight (LOS) component, the envelope of the channel impulse response is Rayleigh distributed with probability density function

$$p(r) = \begin{cases} \frac{r}{\sigma^2} \exp(-\frac{r^2}{2\sigma^2}), & r \geq 0 \\ 0, & r < 0 \end{cases} \tag{2.10}$$

where σ^2 is the variance of both real and imaginary parts of the complex fading attenuation. In simulations in the following chapters, we generate fading attenuations as follows: first generating complex channel attenuation with variance 1 for both real and imaginary parts, then scaling the attenuation by $1/\sqrt{2}$ for single-path channels and $1/\sqrt{2}/P$ for multipath channels, where P is the number of paths. This maintains a unit average power level for channel attenuation.

If there exists a LOS component, the channel has nonzero mean and the complex envelope has a Rician distribution with pdf

$$p(r) = \begin{cases} \frac{r}{\sigma^2} \exp(-\frac{r^2+a^2}{2\sigma^2}) I_0(\frac{ar}{\sigma_2}), & r \geq 0 \\ 0, & r < 0 \end{cases} \tag{2.11}$$

where $a \geq 0$ is the peak amplitude of the LOS received signal and $I_0(.)$ is the modified zeroth-order Bessel function.

When there exist P dominant specular paths, the fast fading is modelled as

$$\sum_{p=1}^{P} \alpha_p(t) \delta_p(t - \tau_p) \tag{2.12}$$

We have discussed path loss, shadowing and fast fading for wireless channel environment, a combined channel characteristic is sketched in Figure 2.2 for a single

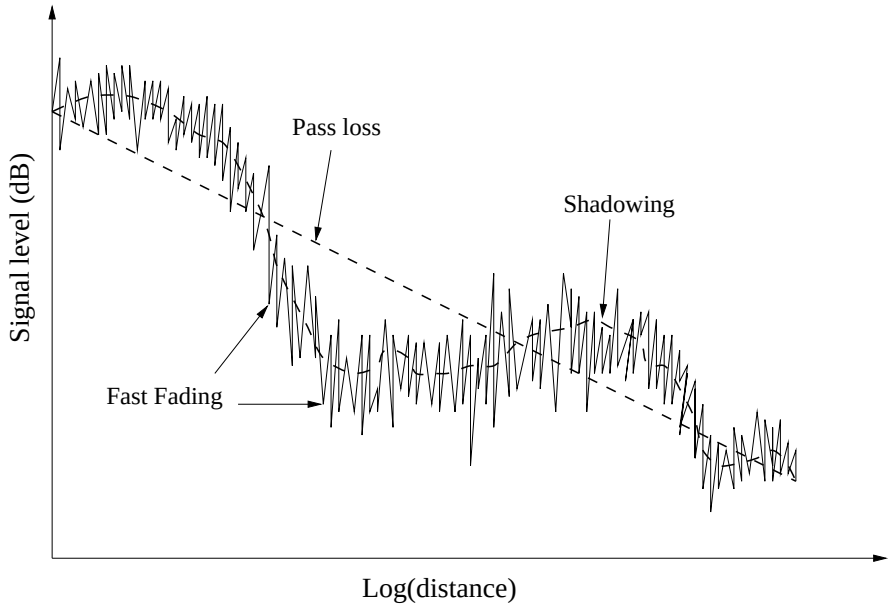

Figure 2.2: Total Fading Signal

dominant path [109]. For multiple dominant (or *multipath*) channels, the channel impulse response can be written as

$$\sum_{p=1}^{P} \sqrt{\mu_p S_p}\alpha_p(t)\delta_p(t-\tau_p) \tag{2.13}$$

2.2.3 Array Response Vector

We have obtained the wireless channel model for a single antenna. In this section, we will develop expressions for the antenna array response and proceed with a channel model incorporating array response vectors. From Figure 2.1, it is observed that the transmitted signal arrives at the base-station antenna array through several specular paths with different DOAs and different time delays. Processing a signal arriving from a single antenna cannot distinguish the different DOAs. Therefore, it is necessary to use multiple antennas to identify DOAs and further suppress multiple access interference. Previous antenna array response vector modelling can be found in [14] and [57].

As we mentioned in Section 2.2.2, the transmitted wave arrives at the base-station

antenna array from a dominant direction with some angle spread. The problem of the angle spread for antenna array CDMA systems is studied in [6]. In this thesis, we make the simplifying assumptions that the angle spread of each specular path is negligible and that the received signals are narrowband with respect to the array aperture so that the signal envelope does not change significantly during the propagation time through the antenna array. We assume that the mobile and the base-station antenna array are in the same plane and the mobile is in the far-field of the antenna array so that the propagating wave impinges on the antenna array as a plane rather than a spherical wave. We also assume that the antenna elements in the array are identical. In this case, the array response vector is parameterized by the angular carrier frequency ω_c and the relative time delays across the antenna array for a given array geometry. Taking the first antenna element as the reference point, we denote τ_m^a to be the propagation delay between the reference point and the mth element for a wavefront impinging from the direction θ. The array response vector for an M-element antenna array is then given by

$$\mathbf{a}(\theta) = \begin{bmatrix} 1 \\ e^{-j\omega_c \tau_2^a(\theta)} \\ \vdots \\ e^{-j\omega_c \tau_M^a(\theta)} \end{bmatrix} \tag{2.14}$$

At this point, we have introduced all the channel parameters. The vector channel impulse response is expressed as

$$\mathbf{g}(t) = \sum_{p=1}^{P} \sqrt{\mu_p S_p}\alpha_p(t)\mathbf{a}(\theta_p)\delta_p(t-\tau_p) \tag{2.15}$$

where the direction of arrival (DOA), θ_p for $p = 1, \cdots, P$, of each path is determined by the physical location of the dominant reflectors and relative time delay τ_p is due to the large distance separation between these reflectors.

In this thesis, we only consider fast fading and assume that $\sqrt{\mu_p S_p}$ is normalized to unity. The receiver algorithms derived in the following chapters are directly applicable to the channels including path loss and shadowing. It is also straightforward to extend the simulations in this thesis to include path loss and shadowing, as done in [12].

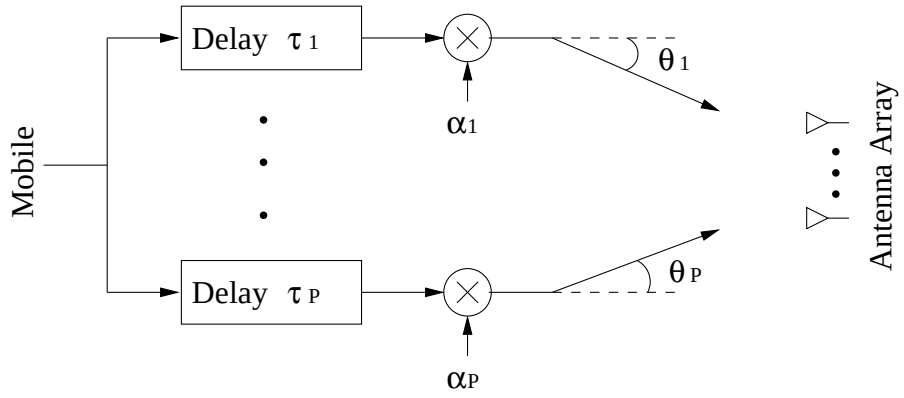

Figure 2.3: Multipath Vector Channel Model

Therefore, the channel impulse response vector used in this thesis is given by

$$\mathbf{g}(t) = \sum_{p=1}^{P} \alpha_p(t)\mathbf{a}(\theta_p)\delta_p(t-\tau_p) \tag{2.16}$$

Figure 2.3 illustrates the multipath vector channel model given by (2.16). Since the time delay difference between two paths is normally larger than one chip interval in CDMA systems with high chip rates, the resolvable multipath provides a means for diversity combining. Thus, a RAKE receiver structure [69] can be used to improve receiver performance.

2.3 Signal Model

In this section, we first analyze the spread spectrum signals found in DS-CDMA systems and then introduce the received continuous signal models which are used to derive receiver structures in the following chapters.

2.3.1 Spread Spectrum Signal

CDMA systems are interference-limited and suffer from the so-called *near-far* problem. As described in Chapter 1, the near-far effect arises due to unequal received powers from mobile users.. In commercial DS-CDMA systems, channel coding is used to improve communication system performance. An M-ary orthogonal Walsh

modulator combined with a long code of period $2^{42}-1$ has been adopted to suppress multiple access interference in second generation systems IS95. To overcome the near-far problem, precise power control is required to guarantee that the received signal powers from different mobile users are equal [70]. If no power control is used, the conventional single-user CDMA receiver is subject to the near-far problem [43]. Power control algorithms may cause additional overhead and increase transmitter/receiver complexity. More importantly, using power control cannot eliminate the bit error rate (BER) floor and the BER performance still suffers from the near-far problem.

The objective of this thesis is to investigate near-far resistant receiver structures using spatial-temporal signal processing techniques. It is not necessary to use precise power control to make the received powers be equal. In Multi-rate systems, precise power control is difficult. To this end, we consider a generic CDMA system to study the fundamental performance improvement achieved by the new receivers obtained in later chapters. Before transmission, the information symbols for each user are spread over a wider bandwidth using a spreading code which is also used to distinguish different users. We use short spreading codes to derive new receiver structures. However, it will be verified in the following chapters that the new receivers are also applicable to long codes which are currently utilized in IS95. A typical spreading process is illustrated in Figure 2.4. The transmitted signal waveform is determined by the spreading code and the signal bandwidth is spread.

For a system with K active users, the transmitted signal from the kth user is given by

$$s_k(t) = A_k \sum_{i=1}^{N} b_k(i) c_k(t - iT_b) \tag{2.17}$$

where A_k is the amplitude of the kth user, $b_k(i) \in \{+1, -1\}$ (BPSK) is the ith transmitted bit of the kth user with equal probability and $c_k(t)$ represents the spreading waveform of the kth user, which is given by

$$c_k(t) = \sum_{l=0}^{L-1} c_{kl} p(t - lT_c) \tag{2.18}$$

where $c_{kl} \in \{+1, -1\}$ $(l = 1 \cdots L-1)$ is the spreading code, $p(t)$ is the chip pulse, T_c

is the chip interval, T_b is the bit interval and processing gain is defined as

$$L = T_b/T_c \tag{2.19}$$

In this thesis, we assume that $p(t)$ is rectangular. Extension of the results obtained to other chip waveforms is straightforward. We assume that the information bits from K users are independent, the spreading code sequences for K users are independent and the spreading waveform has normalized energy, i.e.,

$$\int_0^{T_b} |c_k(t)|^2 = 1 \tag{2.20}$$

Under the normalized constraint, the chip waveform used in this thesis is illustrated in Figure 2.5.

2.3.2 Received Signal for Synchronous Single-Path Channel

The transmitted signal passes through the propagation channel and arrives at a base-station antenna array with M elements. For single-path synchronous channels, the impulse response vector of the channel from the kth transmitter to antenna array output is simplified as

$$\mathbf{g}_k(t) = \alpha_k(t)\mathbf{a}(\theta_k(t))\delta(t) \tag{2.21}$$

where $\alpha_k(t)$ and $\mathbf{a}(\theta_k(t))$ are the fading attenuation corresponding to user k's channel and the M-dimensional array response vector with direction-of-arrival (DOA) $\theta_k(t)$ from the kth user, respectively. The channel fading attenuations for K users are assumed to be mutually independent and also independent of information bit symbols.

The received composite signal at the base-station antenna array from K users is then given by

$$\mathbf{x}(t) = \sum_{k=1}^{K} \mathbf{x}_k(t) = \sum_{k=1}^{K} s_k(t) * \mathbf{g}_k(t) + \mathbf{n}(t) \tag{2.22}$$

where $\mathbf{n}(t)$ is the additive white Gaussian noise vector with zero mean and covariance matrix $\sigma^2\mathbf{I}_M$, where $\mathbf{I}_M$ is an $M \times M$ identity matrix. We assume that $\alpha_k(t)$ and

$\theta_k(t)$ remain unchanged over an N-bit duration. Therefore, we suppress the time-dependence from these quantities and denote them as α_k and θ_k, respectively. Then

$$s_k(t) * \mathbf{g}_k(t) = A_k \alpha_k \mathbf{a}(\theta_k) \sum_{i=1}^{N} b_k(i) c_k(t - iT_b) \tag{2.23}$$

We denote the channel array response vector for user k as

$$\mathbf{f}_k = A_k \alpha_k \mathbf{a}(\theta_k) \tag{2.24}$$

where the mth component of $\mathbf{f}_k$ is $f_k^m = A_k \alpha_k a^m(\theta_k)$ and $a^m(\theta_k)$ is the mth component of array response vector $\mathbf{a}(\theta_k)$. The received signal at the mth array element (for $m = 1, \cdots, M$) is given by

$$x^m(t) = \sum_{k=1}^{K} \sum_{i=1}^{N} f_k^m b_k(i) c_k(t - iT_b) + n^m(t) \tag{2.25}$$

where $n^m(t)$ is AWGN at the mth array element. The received signal vector at the base-station antenna array can be written as

$$\mathbf{x}(t) = \sum_{k=1}^{K} \sum_{i=1}^{N} \mathbf{f}_k b_k(i) c_k(t - iT_b) + \mathbf{n}(t) \tag{2.26}$$

2.3.3 Received Signal for Asynchronous Multipath Channel

For asynchronous multipath channels, the impulse response of the channel from transmitter to antenna array output for the kth user is given by

$$\mathbf{g}_k(t) = \sum_{p=1}^{P_k} \alpha_{k,p}(t) \mathbf{a}(\theta_{k,p}(t)) \delta(t - \tau_{k,p}) \tag{2.27}$$

where $\mathbf{a}(\theta_{k,p}(t))$ is the M-dimensional array response vector with direction-of-arrival (DOA) $\theta_{k,p}(t)$ for the pth path of the kth user, $\alpha_{k,p}(t)$ and $\tau_{k,p}$ represents channel attenuation and relative time delay for the kth user through the pth propagation path, respectively. P_k is the total number of the propagation paths for user k.

We assume $\tau_{k,p} \in [0, T_b)$ for $k \in \{1, \cdots, K\}$ and $p \in \{1, \cdots, P_k\}$, and $\tau_{k,p} < \tau_{k,q}$ for $p < q$. The channel fading attenuations $\alpha_{k,p}(t)$ for $k \in \{1, \cdots, K\}$ and $p \in \{1, \cdots, P_k\}$ are assumed to be mutually independent and also independent of information bit symbols.

Thus, we obtain the received composite signal at the base-station antenna array from K users

$$\mathbf{x}(t) = \sum_{k=1}^{K}\sum_{i=1}^{N}\mathbf{x}_k(t) = \sum_{k=1}^{K}\sum_{i=1}^{N} s_k(t) * \mathbf{g}_k(t) + \mathbf{n}(t) \tag{2.28}$$

where the additive white Gaussian noise vector $\mathbf{n}(t)$ is the same as that for the synchronous single-path case. Similar to Section 2.3.2, we also assume that $\alpha_{k,p}(t)$ and $\theta_{k,p}(t)$ remain unchanged over the N-bit duration and denote these quantities as $\alpha_{k,p}$ and $\theta_{k,p}$ respectively. From (2.17),

$$s_k(t) * \mathbf{g}_k(t) = A_k \sum_{i=1}^{N}\sum_{p=1}^{P_k} \alpha_{k,p}\mathbf{a}(\theta_{k,p})c_k(t - iT_b - \tau_{k,p})b_k(i) \tag{2.29}$$

We denote the channel array response vector through the pth path for the kth user as

$$\mathbf{f}_{k,p} = A_k\alpha_{k,p}\mathbf{a}(\theta_{k,p}) \tag{2.30}$$

where the mth component of $\mathbf{f}_{k,p}$ is $f_{k,p}^m = A_k\alpha_{k,p}a^m(\theta_{k,p})$ and $a^m(\theta_{k,p})$ is the mth component of array response vector $\mathbf{a}(\theta_{k,p})$. Then, the received signal at the mth array element (for $m = 1, \cdots, M$) from the kth user is expressed as

$$x_k^m(t) = \sum_{k=1}^{K}\sum_{i=1}^{N}\sum_{p=1}^{P_k} f_{k,p}^m c_k(t - iT_b - \tau_{k,p})b_k(i) + n^m(t) \tag{2.31}$$

where $n^m(t)$ is AWGN at the mth array element. Similar to the synchronous case, the received signal vector is given by

$$\mathbf{x}(t) = \sum_{k=1}^{K}\sum_{i=1}^{N}\sum_{p=1}^{P_k} \mathbf{f}_{k,p}c_k(t - iT_b - \tau_{k,p})b_k(i) + \mathbf{n}(t) \tag{2.32}$$

Multipath fading causes inter-symbol interference (ISI) and multi-access interference (MAI) arises due to the asynchronous channel. Figure 2.6 shows the example for a two-user system, where each user's signal propagates through two paths.

2.4 Problem Formulation

The objectives of this thesis are to detect information bit sequences and estimate channel array response vectors for all the users jointly and investigate performance improvement using advanced signal processing techniques.

Denote the bit vector, for $i = 1, \cdots, N$,

$$\mathbf{b}(i) = \left[\begin{array}{ccc} b_1(i) & \cdots & b_K(i) \end{array} \right]^T \tag{2.33}$$

Then, the unknown parameters are bit vectors $\mathbf{b}(i)$ for $i = 1, \cdots, N$ and channel array response vectors $\mathbf{f}_{k,p}$ for $k = 1, \cdots, K$ and $p = 1, \cdots, P_k$. We solve this problem by maximizing the likelihood function of the received signal conditioned on these unknown parameters

$$[\hat{\mathbf{b}}(i), \hat{\mathbf{f}}_{k,p}] = \max_{\mathbf{b}(i), \mathbf{f}_k} [\Omega(\mathbf{x}(t) | \mathbf{b}(i), \mathbf{f}_{k,p}, i = 1, \cdots, N, k = 1, \cdots, K, p = 1, \cdots, P_k)] \tag{2.34}$$

where $\Omega(\mathbf{x}(t) | \mathbf{b}(i), \mathbf{f}_{k,p}, i = 1, \cdots, N, k = 1, \cdots, K, p = 1, \cdots, P_k)$ is the likelihood function of the received signal $\mathbf{x}(t)$ conditioned on the unknown parameters $\mathbf{b}(i)$ for $i = 1, \cdots, N$ and $\mathbf{f}_{k,p}$ for $k = 1, \cdots, K$ and $p = 1, \cdots, P_k$.

The difficulty of this problem is that since the unknown parameters for different users are coupled together, the computational complexity of the exhaustive search of the optimum solution in (2.34) is prohibitive. This motivates us to investigate computationally efficient algorithms and corresponding performance measures. We will address these issues in the following chapters.

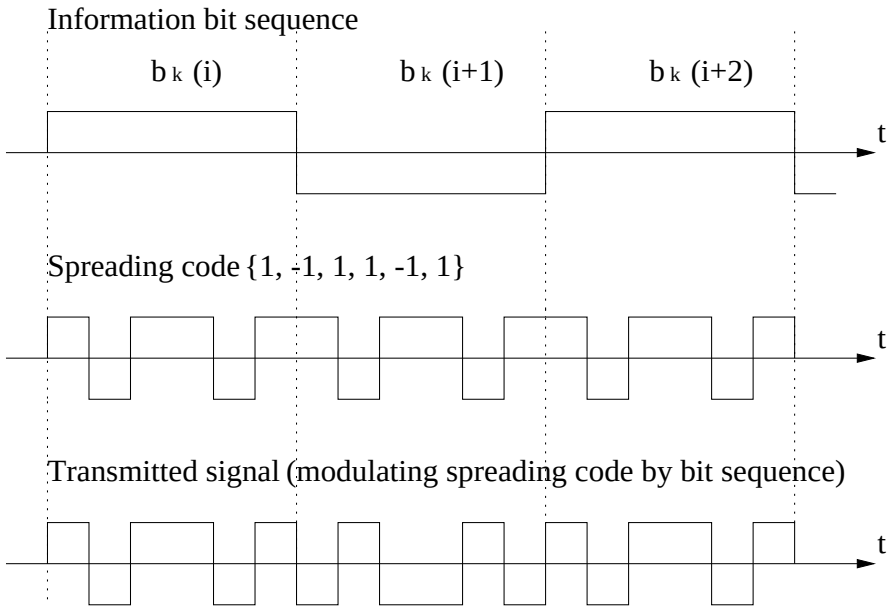

Figure 2.4: Information Symbol Spreading Process

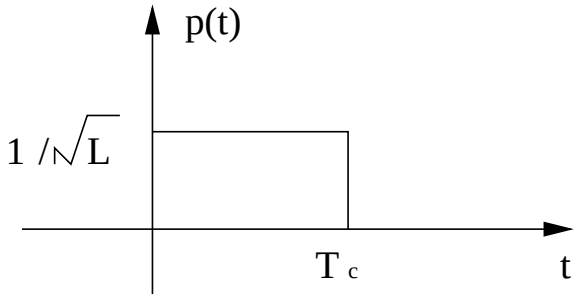

Figure 2.5: Chip Waveform Used in this Thesis for Single-Rate Systems

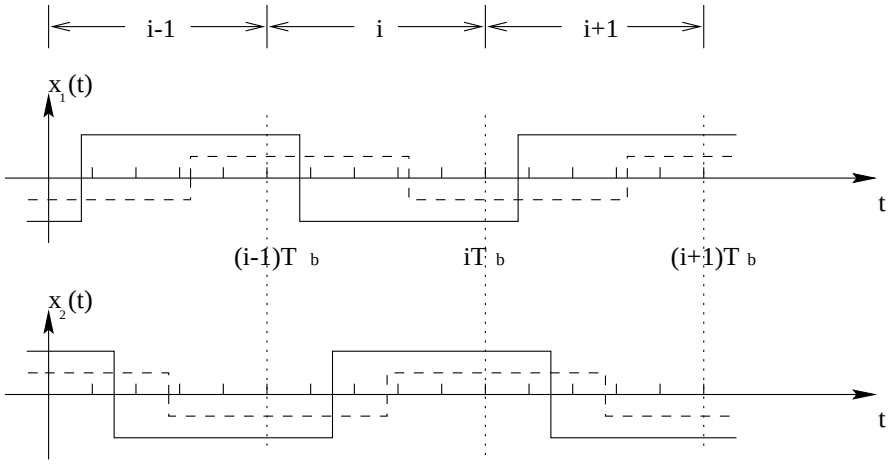

Figure 2.6: The Received Signal for a Two-User Two-Path System

Chapter 3

Spatial-Temporal Decorrelating Receiver for Synchronous Single-Path Channels

3.1 Introduction

The maximum-likelihood (ML) criterion is a well-principled approach to obtain practical estimators. However, computing the ML estimator may be difficult, or even make the problem be intractable, when the unknown parameters from different sources are combined together in the observation data such as in the case of the received composite signal in multi-user communication systems. A numerical solution is needed in this case. Newton-Raphson and scoring methods have been used to iteratively compute an ML estimate. However, these two approaches suffer from convergence problems [34]. A third iterative method, the expectation-maximization (EM) algorithm, provides guaranteed convergence to a local maximum under mild conditions [8] [23].

Feder and Weinstein apply the expectation-maximization (EM) algorithm to parameter estimation of superimposed signals [17]. Bit sequence detection with joint random parameter estimation using the EM algorithm is studied for single-user systems in [20]. Recently, applications of the EM algorithm to CDMA systems have been proposed for signal detection [60], channel estimation [16] [15] and joint channel estimation and signal detection [101]. The space-alternating generalized EM (SAGE)

algorithm can achieve better performance than the standard EM algorithm [19]. Applications of the SAGE algorithm in multi-user CDMA channels can be found in [7] [60] [78]. An iterative ML signal detector is proposed for known channels in [60] using the SAGE algorithm. Application of the SAGE algorithm for channel parameter estimation can be found in [7]. In [78], joint parameter estimation and signal detection is developed using the SAGE algorithm based on the discrete wavelet transform for a single antenna system.

In this chapter, we investigate the integration of spatial signal processing with multi-user signal detection for the synchronous CDMA systems with non-orthogonal spreading codes over a single dominant-path Rayleigh fading channel. The motivation to focus on synchronous systems is as follows: a K-user asynchronous system can be modelled as a synchronous system with $K \times N$ users, where N is the number of bits in each transmitted block [43]. Most importantly, the synchronous problem formulation simplifies the derivation and analysis of the new algorithm and the results obtained can be generalized to the case of higher complexity asynchronous multipath systems [11].

We first formulate a spatial-temporal decorrelator which we show to be near-far resistant. Then, we derive two new receivers for jointly estimating channel array response vectors and detecting information symbol sequences by applying the EM and SAGE algorithms, respectively. The analytical bit error probability and Cramér-Rao Lower Bound (CRLB) for the estimated channel are derived to measure performance of the new receivers.

This chapter is organized as follows. The discrete-time system model is developed in Section 3.2. In Section 3.3, we derive a spatial-temporal decorrelator using the maximum likelihood criteria and analyze its asymptotic efficiency. EM-based and SAGE-based spatial-temporal decorrelating receivers are obtained in Section 3.4 and Section 4.5, respectively. The receivers' performances are analyzed in Section 3.6. Section 3.7 presents simulation results.

3.2 Discrete-Time Formulation

We rewrite the received signal at the mth array element (for $m = 1, \cdots, M$) from (2.25)

$$x^m(t) = \sum_{k=1}^{K} f_k^m b_k(i) c_k(t - iT_b) + n^m(t) \tag{3.1}$$

The received signal at each element first passes through a filter matched to the chip waveform $p(t)$ given in (2.18), and is then sampled at the chip rate. The received discrete-time signal at the ith bit interval from the mth element can be obtained for sample $g \in \{0, 1, \cdots, L-1\}$ as

$$x^m(i, g) = \int_{t=gT_c}^{(g+1)T_c} x^m(t) p^*(t) dt \tag{3.2}$$

for the chip waveform $p(t)$. Finally, the gth sample of the ith bit for the mth antenna element is obtained in terms of the sampled chips c_{kg} by substituting (3.1) into (3.2) yielding

$$x^m(i, g) = \sum_{k=1}^{K} f_k^m c_{kg} b_k(i)/L + n^m(i, g) \tag{3.3}$$

where f_k^m, the mth component of the channel array response vector, is defined in (2.24) and where

$$n^m(i, g) = \int_{t=gT_c}^{(g+1)T_c} n^m(t) p^*(t) dt \tag{3.4}$$

is Gaussian distributed with zero mean and variance σ^2/L. We denote the code vector for the kth user as

$$\mathbf{c}_k = \frac{1}{L} \begin{bmatrix} c_{k0} & c_{k1} & \cdots c_{k(L-1)} \end{bmatrix}^T \tag{3.5}$$

The matched filter output at the mth element for $m \in \{1, \cdots, M\}$ can be written in vector form as

$$\mathbf{x}^m(i) = \sum_{k=1}^{K} f_k^m b_k(i) \mathbf{c}_k + \mathbf{n}^m(i) \tag{3.6}$$

where $\mathbf{n}^m(i) = [n^m(i, 0) \;\; n^m(i, 1) \;\; \cdots \;\; n^m(i, L-1)]^T$.

We define the total impulse response vector for user k, including fading channel, array response vector and spreading code vector defined above as

$$\mathbf{h}_k^m(i) = f_k^m \mathbf{c}_k \tag{3.7}$$

Equation (3.6) can be written in terms of (3.7) as

$$\mathbf{x}^m(i) = \sum_{k=1}^{K} \mathbf{h}_k^m b_k(i) + \mathbf{n}^m(i) \tag{3.8}$$

Denote

$$\mathbf{x}(i) = [(\mathbf{x}^1(i))^T \ \cdots \ (\mathbf{x}^M(i))^T]^T \tag{3.9}$$

$$\mathbf{h}_k = [(\mathbf{h}_k^1)^T \ \cdots \ (\mathbf{h}_k^M)^T]^T \tag{3.10}$$

and

$$\mathbf{n}(i) = [(\mathbf{n}^1(i))^T \ \cdots \ (\mathbf{n}^M(i))^T]^T$$

The received discrete-time signal from antenna array is given by

$$\mathbf{x}(i) = \sum_{k=1}^{K} \mathbf{x}_k(i) = \sum_{k=1}^{K} \mathbf{h}_k b_k(i) + \mathbf{n}(i) \tag{3.11}$$

where $\mathbf{x}_k(i)$ is the received signal from the kth user and $\mathbf{n}(i)$ is AWGN vector with zero vector mean and covariance matrix $\frac{\sigma^2}{L}\mathbf{I}_{ML}$, where $\mathbf{I}_{ML}$ is an $ML \times ML$ identity matrix.

Vector $\mathbf{h}_k$ contains the spatial and temporal channel characteristics of our system. The spatial-temporal channel vector $\mathbf{h}_k$ can also be decomposed as

$$\mathbf{h}_k = \begin{bmatrix} \mathbf{c}_k & \mathbf{0} & \cdots & \mathbf{0} \\ \mathbf{0} & \mathbf{c}_k & \ddots & \mathbf{0} \\ \vdots & \ddots & \ddots & \vdots \\ \mathbf{0} & \mathbf{0} & \cdots & \mathbf{c}_k \end{bmatrix} \begin{bmatrix} f_k^1 \\ f_k^2 \\ \vdots \\ f_k^M \end{bmatrix} = C_k \mathbf{f}_k \tag{3.12}$$

where C_k is an $ML \times M$ spreading code sequence matrix of the kth user, and $\mathbf{0}$ represents an L-dimensional zero column-vector.

Denoting

$$H = [\mathbf{h}_1 \ \cdots \ \mathbf{h}_K] \tag{3.13}$$

and

$$\mathbf{b}(i) = [b_1(i) \ \cdots \ b_K(i)]^T \tag{3.14}$$

the received composite signal is given by

$$\mathbf{x}(i) = H\mathbf{b}(i) + \mathbf{n}(i) \tag{3.15}$$

A necessary condition that K users are identifiable is that H is of full column rank, which requires

$$ML > K \tag{3.16}$$

3.3 Spatial-Temporal Decorrelator

In this section, we derive a spatial-temporal decorrelator based on the discrete-time system model using the maximum-likelihood criteria for known channel array response vectors, i.e., H is known at the receiver. Then we investigate the near-far resistance of the new detector and compare the near-far resistance with that of the conventional single-user detector.

3.3.1 Detector for Known Channel

The log-likelihood of the received signal $\mathbf{x}(i)$ conditioned on the bit vector $\mathbf{b}(i)$is given by (for the sake of simplicity, we omit the time index i in this section)

$$\Omega(\mathbf{b}) = -\frac{1}{\sigma^2/L}(\mathbf{x} - H\mathbf{b})^H(\mathbf{x} - H\mathbf{b}) \tag{3.17}$$

where the superscript H denotes conjugate transpose. The unknown parameters are the information bit vector $\mathbf{b}$.

If H is available, i.e., the channel and array response vectors are known, the bit vector decision variable $\hat{\mathbf{b}}_d$ can be obtained by maximizing the above log-likelihood function

$$\hat{\mathbf{b}}_d = \arg\max_{\mathbf{b}} \Omega(\mathbf{b}) \tag{3.18}$$

Taking the derivative of log-likelihood function (3.17) with respect to the bit vector $\mathbf{b}$, we obtain

$$\frac{\partial\Omega(\mathbf{b})}{\partial\mathbf{b}} = \frac{1}{\sigma_2/L}(H^H H\mathbf{b} - 2H^H\mathbf{x}) \tag{3.19}$$

Since the bit vector is discrete-valued, this is not a standard maximum-likelihood (ML) estimation problem. The approximate ML solution for the bit vector $\mathbf{b}$ can be

found by equating (3.19) to zero. For BPSK modulation, we have

$$\hat{\mathbf{b}} = \text{sign}\{[H^H H]^{-1} H^H \mathbf{x}\} \tag{3.20}$$

where

$$\text{sign}\{a\} = \begin{cases} 1, & \text{if} \quad a \geq 0 \\ -1, & \text{if} \quad a < 0 \end{cases}$$

We define the spatial-temporal cross-correlation matrix as

$$R \equiv H^H H \tag{3.21}$$

From (3.12) and (3.13), the kjth component of matrix R is given by

$$R_{kj} = \mathbf{h}_k^H \mathbf{h}_j = \mathbf{f}_k^H C_k^H C_j \mathbf{f}_j$$

Using the definition of C_k, we obtain

$$C_k^H C_j = \mathbf{c}_k^H \mathbf{c}_j \mathbf{I}_M$$

Thus, R_{kj} is given by

$$R_{kj} = \mathbf{c}_k^H \mathbf{c}_j \mathbf{f}_k^H \mathbf{f}_j \tag{3.22}$$

Define the spatial correlation between user k and user j as

$$f_{kj} = \mathbf{f}_k^H \mathbf{f}_j \tag{3.23}$$

and the temporal correlation between user k and user j as

$$\rho_{kj} = \mathbf{c}_k^H \mathbf{c}_j \begin{cases} \leq 1/L, & if \quad k \neq j \\ = 1/L, & if \quad k = j \end{cases} \tag{3.24}$$

The spatial-temporal correlation matrix can be written as

$$R = \begin{bmatrix} f_{11}\rho_{11} & f_{12}\rho_{12} & \cdots & f_{1K}\rho_{1K} \\ f_{21}\rho_{21} & f_{22}\rho_{22} & \cdots & f_{2K}\rho_{2K} \\ \vdots & \ddots & \ddots & \vdots \\ f_{K1}\rho_{K1} & f_{K2}\rho_{K2} & \cdots & f_{KK}\rho_{KK} \end{bmatrix} \tag{3.25}$$

If the spreading codes are orthogonal, the cross-correlation between two different codes is zero for a synchronous system, i.e., $\rho_{ij} = \mathbf{c}_i^H \mathbf{c}_j = 0$ (for $i \neq j$) for a synchronous system. In this case, R is diagonal and no multi-access interference exists. However, if the system is asynchronous, we cannot guarantee this zero cross-correlation. If the spreading codes are not orthogonal, even for synchronous systems, the cross-correlation between two different spreading codes will be nonzero. In this chapter, we analyze a synchronous system with non-orthogonal spreading codes.

We may interpret (3.20) as a maximum SNR beamformer computational structure using steering vector H^H followed by a decorrelator $[H^H H]^{-1}$. Using (3.20), (3.21), the detected bit vector can be written in the form

$$\hat{\mathbf{b}} = \text{sign}\{R^{-1}\mathbf{z}\} = \text{sign}\{R^{-1}F^H\mathbf{y}\} \tag{3.26}$$

where

$$\mathbf{z} = H^H\mathbf{x} = \begin{bmatrix} \mathbf{f}_1^H & \mathbf{0}^T & \cdots & \mathbf{0}^T \\ \mathbf{0}^T & \mathbf{f}_2^H & \ddots & \mathbf{0}^T \\ \vdots & \ddots & \ddots & \vdots \\ \mathbf{0}^T & \mathbf{0}^T & \cdots & \mathbf{f}_K^H \end{bmatrix} \begin{bmatrix} \mathbf{y}_1 \\ \mathbf{y}_2 \\ \vdots \\ \mathbf{y}_K \end{bmatrix} = F^H\mathbf{y} \tag{3.27}$$

and the kth components in vector $\mathbf{y}$ represents the despreading output for user k and is given by

$$\mathbf{y}_k = C_k^H\mathbf{x} \tag{3.28}$$

This detector structure is a conventional single-user detector with a maximum SNR beamformer followed by a decorrelator, see Figure 3.1. Matrix R includes both the temporal cross-correlation due to the non-orthogonal spreading codes and the instantaneous spatial correlation because of the spatial distribution of the active users in the system. This structure differs from that of [49] since the matched-filter (despreader) occurs prior to beamforming. For unknown channels, in order to compute the beamforming weight vector for each user, we have to estimate the corresponding channel array response vector. For CDMA systems, it is necessary to despread the received signal before estimating the related channel parameters. Therefore, the

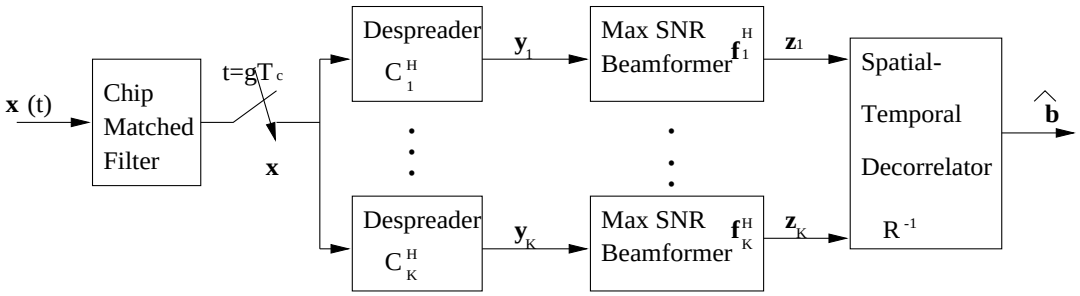

Figure 3.1: Spatial-Temporal Decorrelator Structure for Synchronous Single-path Channels

detector structure obtained in this thesis is more practical than the one proposed in [49].

Substituting (3.15) into (3.20) and using definition of R (c.f. (3.21)), the spatial-temporal decorrelator output can be simplified to

$$\hat{\mathbf{b}} = \text{sign}\{\mathbf{b} + R^{-1}H^H\mathbf{n}\} = \text{sign}\{\mathbf{b} + \mathbf{w}\} \tag{3.29}$$

where $\mathbf{w}$ is the spatial-temporal decorrelator output AWGN vector with zero mean and variance

$$Var[\mathbf{w}] = E[|R^{-1}H^H\mathbf{n}|^2] = \frac{\sigma^2}{L}R^{-1}$$

If there is no base-station antenna array, the spatial-temporal decorrelator reduces to the classic decorrelating detector proposed in [43], which we refer to from here on as temporal decorrelator.

3.3.2 Near-far Resistance

The asymptotic efficiency is a performance measure for multi-user signal detection in the limit as the background noise goes to zero. The kth user's asymptotic efficiency is defined as [96]

$$\eta_k = \lim_{\sigma\to 0}\frac{e_k(\sigma)}{w_k} = \sup\{0 \le r \le 1 : \lim_{\sigma\to 0} P_k(\sigma)/Q(\frac{\sqrt{rw_k}}{\sigma}) < +\infty\} \tag{3.30}$$

where $e_k(\sigma)$ is the kth user's effective energy required to achieve the same error probability in the absence of interferers, w_k is the received energy for user k, $P_k(\sigma)$ represents bit-error-rate (BER) of the kth user when the variance of the background thermal noise modelled by AWGN is σ^2 and

$$Q(x) = \int_x^\infty \frac{\exp(-y^2/2)}{\sqrt{2\pi}} dy$$

is the error function.

Because the asymptotic efficiency of the temporal decorrelator in a single-path Rayleigh fading channel is the same as that of an additive white Gaussian channel [114], we only consider the AWGN channel here. In this case,

$$\mathbf{f}_k = \begin{bmatrix} f_k^1 \\ \vdots \\ f_k^M \end{bmatrix} = A_k \mathbf{a}_k(\theta_k)$$

The kth user error probability for the spatial-temporal decorrelator can be obtained as

$$P_k^d = Q\left(\frac{1}{\frac{\sigma}{\sqrt{L}}\sqrt{(R^{-1})_{kk}}}\right) \tag{3.31}$$

where $(R^{-1})_{kk}$ represents the kth diagonal element of matrix R^{-1} [107]. Similar to the case of single antenna systems [42], the asymptotic efficiency of the spatial-temporal decorrelator for the kth user is given by

$$\eta_k^d = max^2\left\{0, \frac{1}{\sqrt{R_{kk}(R^{-1})_{kk}}}\right\} = \frac{1}{R_{kk}(R^{-1})_{kk}} \tag{3.32}$$

The kth user's bit error probability for the conventional single-user detector (c.f. (3.26)) is given by

$$P_k^c = p[z_k > 0 | b_k = -1] = 2^{1-K} \sum_{b_i \in \{+1,-1\}} Q\left(\frac{R_{kk} - \sum_{i \neq k} R_{ik} b_i}{\frac{\sigma}{\sqrt{L}}\sqrt{R_{kk}}}\right) \tag{3.33}$$

where the second equation is due to the usual assumption of equally probable transmitted information symbols. When the background noise variance σ^2 tends to zero,

(3.33) is dominated by the event corresponding to $b_i = -1$, $i \neq k$, i. e.,

$$2^{1-K} \sum_{b_i \in \{+1,-1\}} Q\left(\frac{R_{kk} - \sum_{i \neq k} |R_{ik}|}{\frac{\sigma}{\sqrt{L}} \sqrt{R_{kk}}} \right) \tag{3.34}$$

Thus, the kth user's asymptotic efficiency of the conventional single-user detector, η_k^c, can be obtained by substituting (3.34) into (3.33) and (3.30)

$$\eta_k^c = max^2 \left\{ 0, \frac{\sqrt{R_{kk}} - \sum_{i \neq k} |R_{ik}| / \sqrt{R_{kk}}}{\sqrt{R_{kk}}} \right\} = max^2 \left\{ 0, 1 - \sum_{i \neq k} \frac{|R_{ik}|}{R_{kk}} \right\} \tag{3.35}$$

The kth user's near-far resistance is defined as its worst case asymptotic efficiency over all possible energies of the interferers and given by [43]

$$\bar{\eta}_k = \inf_{w_i \geq 0, i \neq k} \eta_k \tag{3.36}$$

If $\bar{\eta}_k$ is nonzero, the performance level of the corresponding detector is guaranteed no matter how powerful the multi-access interference. The detector with nonzero $\bar{\eta}_k$ is said to be *near-far resistant.*

Example: To numerically compare the asymptotic efficiency for the spatial-temporal decorrelator and the conventional single-user detector, we consider a four-user system based on a set of spreading codes from Gold sequences of length seven. The corresponding cross-correlation matrix of the spreading codes is given by [9]

$$R_c = \frac{1}{7} \begin{bmatrix} 7 & -1 & 3 & 3 \\ -1 & 7 & -1 & 3 \\ 3 & -1 & 7 & -1 \\ 3 & 3 & -1 & 7 \end{bmatrix}$$

We assume a uniform linear array (ULA) with half-wavelength spacing at the base-station, see Figure 3.2. The kth user antenna array response with the first element as the reference point is given by

$$\mathbf{a}(\theta_k) = [1 \;\; e^{-j2\pi d \sin\theta_k/\lambda} \;\; \cdots \;\; e^{-j2(M-1)\pi d \sin\theta_k/\lambda}]^T \tag{3.37}$$

where $d = \lambda/2$ in our case and λ is the propagation wavelength. For this antenna array, R_{ik} is given by

$$R_{ik} = \begin{cases} \rho_{ik} A_i A_k \mathbf{a}_i^H \mathbf{a}_k, & if \quad i \neq k \\ M A_k^2 / L, & if \quad i = k \end{cases} \tag{3.38}$$

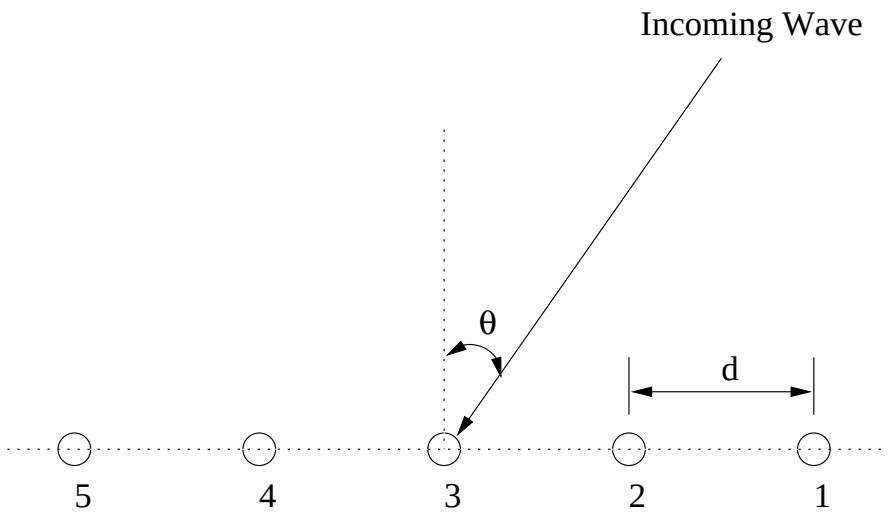

Figure 3.2: Uniform Linear Array

To evaluate the effect of the base-station antenna array on detector performance, we consider two cases: a single antenna and a three-element antenna array. The direction-of-arrivals (DOAs) for four active users are $[25°, 5°, -15°, -35°]$ with respect to the array boresight. We refer the first user as the desired user and define the power ratio as A_k^2/A_1^2, for $k = 2, \cdots, K$. In this example, we assume that all interferers have equal transmitted power.

Figure 3.3 compares the asymptotic efficiencies for the spatial-temporal decorrelator and the conventional single-user detector with and without an antenna array. Conventional single-user detector with antenna arrays can be generalized from Figure 1.1 by incorporating a beamformer into detector structure between the despreading matched filter and the decision rule for each user. Note that the asymptotic efficiencies of the spatial-temporal decorrelator for both single-antenna and antenna-array cases are constant. This means that performance of the spatial-temporal decorrelator is independent of the received energies from interferers provided that the array response vectors of the active users are perfectly known or estimated at the receiver. Therefore, the spatial-temporal decorrelator is near-far resistant. Also note that the asymptotic efficiencies for both conventional single-user detectors tend to zero as the interferers become stronger. Note that the conventional single-user detector is not

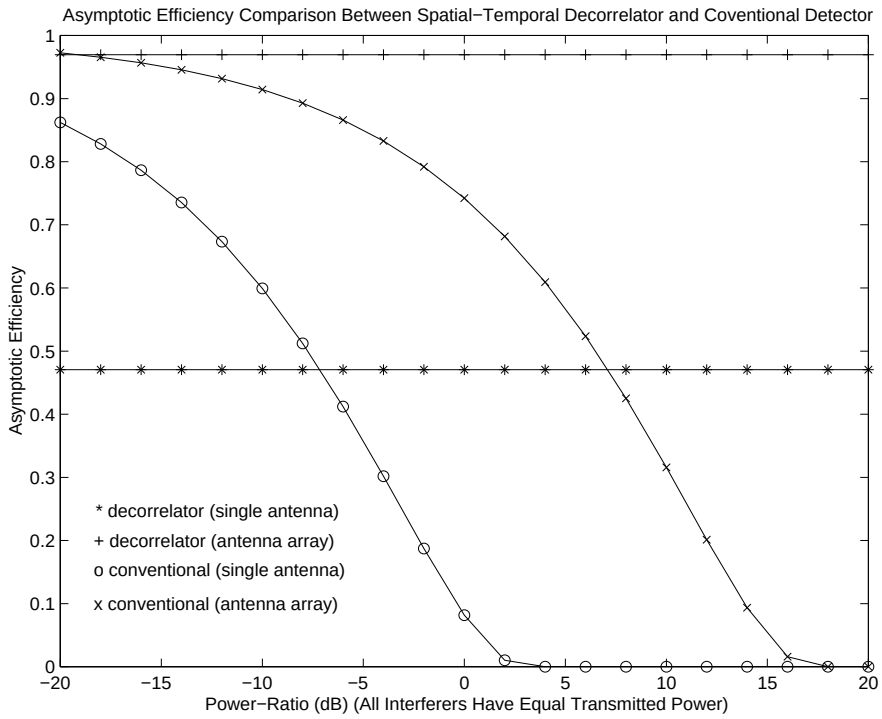

Figure 3.3: Asymptotic Efficiencies for Single Antenna and a Three-Element Antenna Array

near-far resistant when an antenna array is used . However, from Figure 3.3, it can be observed that using an antenna array can significantly increase the asymptotic efficiency for either the spatial-temporal decorrelator or the conventional single-user detector.

Properties of the spatial-temporal decorrelator are summarized as follows:

1. The spatial-temporal decorrelator is near-far resistant.

2. Performance of the spatial-temporal decorrelator is independent of energies of interferers.

3. Using antenna arrays can improve the asymptotic efficiency of the spatial-temporal decorrelator.

The above analysis is based on the assumption that matrix R is available, implying that the channel array response vectors, $\mathbf{f}_k$ (for $k = 1, \cdots, K$), are known at the receiver. This is not the case in a practical application. We now investigate the problem of joint channel estimation and signal detection. In the following two sections, we address the key implementation issues of the proposed spatial-temporal decorrelator. From here on, we refer to the joint parameter estimation and spatial-temporal signal decorrelation as the spatial-temporal decorrelating receiver.

3.4 EM-Based Decorrelating Receiver

In this section, we first briefly introduce the expectation-maximization (EM) algorithm, then apply the EM algorithm to derive an iterative receiver structure. The available observed data at the receiver is a data vector set $\{\mathbf{x}(i); 1, \cdots, N\}$.

3.4.1 EM algorithm

The EM algorithm is an iterative method to solve the maximum-likelihood (ML) estimation problem given the observed data when direct maximization of likelihood is not practical [8]. The EM algorithm is based on the notion of two data sets, the incomplete data $\mathbf{r}$ and the complete data $\mathbf{x}$. Incomplete data $\mathbf{r}$ (usually the observed data) is available at the receiver, while the unavailable complete data forms a many-to-one mapping $\mathbf{x} \rightarrow \mathbf{r}$. The EM algorithm includes a two-step iteration consisting of the E-step (expectation step) and the M-step (maximization step). In the E-step, the conditional expectation of complete data $\mathbf{x}$ is computed given incomplete observed data $\mathbf{r}$ and the current estimate of parameters $\hat{\theta}^j$ at jth iteration:

$$U(\theta|\hat{\theta}^j) = E[\log f(\mathbf{x}|\theta)|\mathbf{r}, \hat{\theta}^j] \tag{3.39}$$

In the M-step, the likelihood function is maximized to obtain the parameter estimate at the next iteration

$$\hat{\theta}^{j+1} = \arg\max_{\theta} U(\theta|\hat{\theta}^j) \tag{3.40}$$

Each iteration of the EM algorithm increases the likelihood function $U(\theta|\hat{\theta}^j)$ until a point of maximum is reached. However, there is no guarantee that the convergence will be to a global maximum. For likelihood functions with multiple maxima, the EM algorithm may converge to a local maximum which depends on the initial estimate $\hat{\theta}^0$. Using multiple starting points, the EM algorithm could achieve better performance at the expense of increased complexity. A more detained presentation of the EM algorithm can be found in [54].

3.4.2 Iterative Parallel Receiver

We first rewrite equation (3.11) for times $i = 1, \cdots, N$ as

$$\mathbf{x}(i) = \sum_{k=1}^{K} \mathbf{x}_k(i) = \sum_{k=1}^{K} \mathbf{h}_k b_k(i) + \mathbf{n}(i) \tag{3.41}$$

and choose the complete data set as in [17]

$$\mathbf{x}^C(i) = \left[\begin{array}{cccc} \mathbf{x}_1^T(i) & \mathbf{x}_2^T(i) & \cdots & \mathbf{x}_K^T(i) \end{array} \right]^T \tag{3.42}$$

where superscript c denotes complete data and $\mathbf{x}_k(i)$ (for $k = 1, \cdots, K$) represents the received signal from the kth user and is given by

$$\mathbf{x}_k(i) = \mathbf{h}_k b_k(i) + \mathbf{n}_k(i) \tag{3.43}$$

where $\mathbf{n}_k(i)$ is the decoupled background noise vector for user k with zero mean and covariance matrix $\frac{\sigma^2}{LK}\mathbf{I}_{ML}$. Discarding the terms which are independent of the bit vector $\mathbf{b}(i)$ and using the notation in (3.13) for matrix H, the log-likelihood function of the complete data can be expressed in simplified notation as

$$\Omega(\mathbf{x}^C|\mathbf{b}(i), H) = -\frac{1}{\sigma^2/KL} \sum_{i=1}^{N} \sum_{k=1}^{K} (\mathbf{x}_k - \mathbf{h}_k b_k(i))^H (\mathbf{x}_k - \mathbf{h}_k b_k(i)) \tag{3.44}$$

From (3.44), it is clear that the coupled K-user optimization problem in (3.41) has been transformed to K parallel single-user optimization problems.

The expectation step (E-step) of the EM algorithm is to compute the conditional expectation of the log-likelihood in (3.44) conditioned on $\mathbf{h}_k$ and $b_k(i)$ (for

$k = 1, \cdots, K$ and $i = 1, \cdots, N$) given the maximum-likelihood estimates from the previous iteration stage. For our decoupled problem, the E-step obtains the conditional expectation of the complete data set which is calculated using standard properties of conditional multivariate Gaussian distributions [17] [68] (for $k = 1, \cdots, K$ and $i = 1, \cdots, N$)

$$\hat{\mathbf{x}}_k^{j+1}(i) = E[\mathbf{x}_k(i)|\mathbf{x}(i), \hat{\mathbf{h}}_k^j, \hat{b}_k^j(i)] = \hat{\mathbf{h}}_k^j \hat{b}_k^j(i) + \frac{1}{K}(\mathbf{x}(i) - \sum_{k=1}^{K} \hat{\mathbf{h}}_k^j \hat{b}_k^j(i)) \tag{3.45}$$

where the superscript j denotes the jth iteration.

The maximization step (M-step) of the algorithm is to obtain maximum likelihood estimates of $\mathbf{h}_k$ (for $k = 1, \cdots, K$)and $b_k(i)$ (for $k = 1, \cdots, K$ and $i = 1, \cdots, N$) for the next iteration by maximizing (3.44) given the conditional expectation of the complete data

$$[\hat{\mathbf{h}}_k^{j+1}, \hat{b}_k^{j+1}(i)] = \arg \max_{\mathbf{h}_k, b_k(i)} \{-\sum_{i=1}^{N} (\hat{\mathbf{x}}_k^{j+1}(i) - \mathbf{h}_k b_k(i))^H (\hat{\mathbf{x}}_k^{j+1}(i) - \mathbf{h}_k b_k(i))\} \tag{3.46}$$

Given the bit sequence detection results at the jth iteration, $\hat{b}_k^j(i)$ for $k = 1, \cdots, K$ and $i = 1, \cdots, N$, $\hat{\mathbf{h}}_k^{j+1}$ for $k = 1, \cdots, K$ can be obtained by equating the derivative of (3.46) with respect to $\mathbf{h}_k$ to zero yielding

$$\hat{\mathbf{h}}_k^{j+1} = \frac{1}{N} \sum_{i=1}^{N} \hat{\mathbf{x}}_k^{j+1}(i) \hat{b}_k^j(i)$$

Then, for a given channel array response vector estimate at the $(j+1)$st iteration, $\hat{\mathbf{h}}_k^{j+1}$ for $k = 1, \cdots, K$, we obtain the bit sequences at the $(j+1)$st iteration, for $k = 1, \cdots, K$ and $i = 1, \cdots, N$ as

$$\hat{b}_k^{j+1}(i) = (\hat{\mathbf{h}}_k^{j+1})^H \hat{\mathbf{x}}_k^{j+1}(i)$$

Rewriting (3.45) as

$$\hat{\mathbf{x}}_k^{j+1}(i) = \frac{K-1}{K} \hat{\mathbf{h}}_k^j \hat{b}_k^j(i) + \frac{1}{K} \left(\mathbf{x}(i) - \sum_{k_1=1, k_1 \neq k}^{K} \hat{\mathbf{h}}_{k_1}^j \hat{b}_{k_1}^j(i) \right) \tag{3.47}$$

the EM-Based decorrelating receiver to jointly estimate channel array response vectors and detect information symbols is summarized as follows:

E-step: compute the conditional expectation of interference

plus noise, for $k = 1, \cdots, K$ and $i = 1, \cdots, N$

$$\hat{\mathbf{u}}_k^{j+1}(i) = \mathbf{x}(i) - \sum_{k_1=1, k_1 \neq k}^{K} \hat{\mathbf{h}}_{k_1}^{j} \hat{b}_{k_1}^{j}(i) \tag{3.48}$$

M-step: obtain the decoupled ML estimates, for $k = 1, \cdots, K$ and $i = 1, \cdots, N$

$$\hat{\mathbf{h}}_k^{j+1} = \frac{1}{N} \sum_{i=1}^{N} (\frac{K-1}{K} \hat{\mathbf{h}}_k^{j} \hat{b}_k^{j}(i) + \frac{1}{K} \hat{\mathbf{u}}_k^{j+1}(i)) \hat{b}_k^{j}(i) \tag{3.49}$$

$$\hat{b}_k^{j+1}(i) = \text{sign}\{(\hat{\mathbf{h}}_k^{j+1})^H (\frac{K-1}{K} \hat{\mathbf{h}}_k^{j+1} \hat{b}_k^{j}(i) + \frac{1}{K} \hat{\mathbf{u}}_k^{j+1}(i))\} \tag{3.50}$$

The above signal detection/estimation approach is actually K parallel conventional single-user detectors at each iteration, as shown in Figure 3.4. The remarkable advantage of the EM-based spatial-temporal decorrelating receiver is that the K-dimensional optimization problem is decoupled to K parallel single dimensional optimization problems, and hence, reduces computational complexity.

This section derives an iterative parallel multi-user receiver structure based on the EM algorithm. Because the desired parameters are channel attenuations and bit sequences for each user, we decompose the received signal (observed data) into its signal components from all active users and choose the decomposed signals to form the complete data set. After decomposition, the channel estimation and bit detection problems have been transformed those of single-user receivers. The advantage of this choice is that it is easy to derive joint channel estimation and bit detection algorithms for each user.

There exists a tradeoff between the choice of the complete data set and the computational complexity. Different choices of the complete data set will result in different receiver structures. An alternate choice of complete data set for multi-user signal detection can be found in [60] for known channels. In [60], the interference users's bits are treated as missing data for each desired user. The missing data and received incomplete data form the complete data set. At the E-step, the conditional expectation of the complete data is computed using the *a priori* distribution of the missing data. This choice results in improved convergence and increased complexity in terms of the number of users.

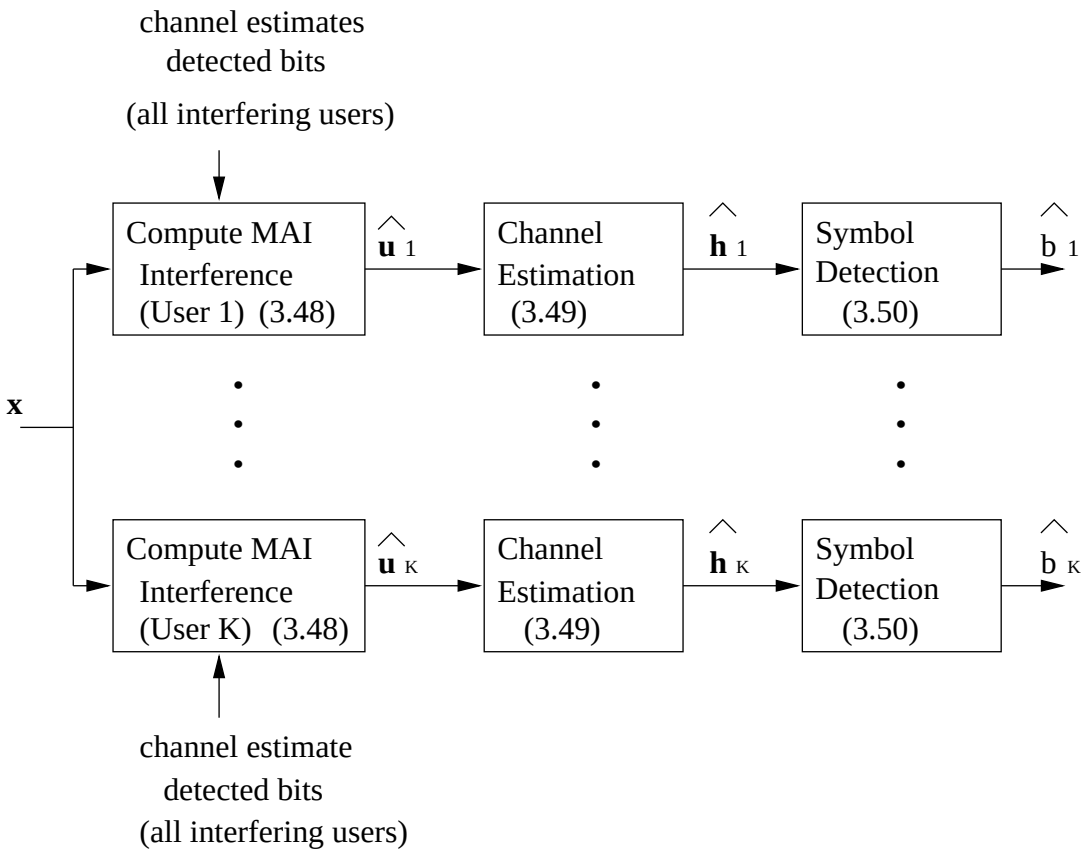

Figure 3.4: EM-Based Spatial-Temporal Receiver Structure at Each Iteration Cycle

3.5 SAGE-based Decorrelating Receiver

The M-step in the EM algorithm simultaneously maximizes the conditional expectation of the complete-data likelihood. The simultaneous maximization necessitates an overly informative complete-data and hence results in slow convergence. Investigation to improving the convergence rate of the EM algorithm leads to the space alternating generalized expectation-maximization (SAGE) algorithm [19], which will be addressed next.

3.5.1 SAGE Algorithm

Because less-informative complete-data lead to improved asymptotic convergence rates which implies that the distance between successive iterations and the limit

point of the EM algorithm tends to zero monotonically [22] with large step sizes and greater likelihood increases in the early iterations [18] [22], minimizing the information of the complete-data set could achieve improved performance for the EM algorithm. However, since the EM algorithm employs the simultaneous updates, a less informative complete-data can result in an intractable problem formulation [8] [18]. To overcome this problem, the SAGE algorithm maximizes a small group of the unknown parameters sequentially by choosing a small hidden-data, or complete-data set. Convergence of the SAGE algorithm has been established in [19].

The first step of the SAGE algorithm is to choose an index set. For a problem of K unknown parameter sets, a set S is defined to be an index set if it is nonempty, is a subset of the set $\{1, \cdots, K\}$ and has no repeated entries [19]. Based on the index set S, identifying an admissible hidden-data space $\mathbf{x}^S$ which must be a complete-data set in the sense of the standard EM algorithm in [8].

The SAGE algorithm iterates the following steps:

Starting with an initial parameter vector estimate at iteration $j = 0$.

1. Choose a new index set $S = S^j$, a subset of the parameters, which defines an admissible hidden-data space $\mathbf{x}^{S^j}$

2. Compute the following conditional expectation of $\mathbf{x}^{S^j}$ given observed data $\mathbf{x}$ and the previous estimate of parameter vector $\hat{\theta}^j$

$$\Omega(\theta_{S^j}|\hat{\theta}^j) = E[\ln f(\mathbf{x}_{S^j}|\hat{\theta}_{\bar{S}^j})|\mathbf{x}, \hat{\theta}^j] \tag{3.51}$$

3. Obtain the next estimate by maximizing over the chosen subset while keeping the other parameters fixed

$$\begin{aligned} \hat{\theta}_{S^j}^{j+1} &= \arg\max_{\theta_{S^j}} \Omega(\theta_{S^{j+1}}|\hat{\theta}^j) \\ \hat{\theta}_{\bar{S}^j}^{j+1} &= \hat{\theta}_{\bar{S}^j}^{j} \end{aligned} \tag{3.52}$$

where the index set $\bar{S}^j$ is the complement of S^j

4. Increment j and go to step 1.

3.5.2 Iterative Sequential Receiver

For the CDMA system model considered, we would like to estimate each user's channel parameter and detect the information symbol individually. In step 1, we choose user index k as the index set. Thus, the admissible hidden-data space for index k for $k = 1, \cdots, K$ and $i = 1, \cdots, N$ is given by (c.f. 3.11)

$$\mathbf{x}_k^S(i) \sim \mathcal{N}(\mathbf{h}_k b_k(i), \frac{\sigma^2}{L}\mathbf{I}_{ML}) \tag{3.53}$$

where superscript S represents the hidden-data space and $\mathcal{N}$ denotes the multivariate Gaussian distribution.

The log-likelihood function after removing the terms independent of $\mathbf{h}_k$ and $b_k(i)$ is straightforwardly computed as

$$\Omega(\mathbf{x}_k^S(1), \cdots, \mathbf{x}_k^S(N)) = -\frac{1}{\sigma^2/L}\sum_{i=1}^{N}(\mathbf{x}_k^S(i) - \mathbf{h}_k b_k(i))^H(\mathbf{x}_k^S(i) - \mathbf{h}_k b_k(i)) \tag{3.54}$$

Given the estimation results at the jth iteration, the conditional expectation of $\mathbf{x}_k^S(i)$ (for $k = 1, \cdots, K$ and $i = 1, \cdots, N$) in Step 2 is given by

$$\hat{\mathbf{x}}_k^{S^{j+1}}(i) = \hat{\mathbf{h}}_k^j \hat{b}_k^j(i) + (\mathbf{x}(i) - \sum_{i=1}^{K}\hat{\mathbf{h}}_i^j \hat{b}_i^j(i)) = \mathbf{x}(i) - \sum_{k_1=1, k_1\neq k}^{K}\hat{\mathbf{h}}_{k_1}^j \hat{b}_{k_1}^j(i) \tag{3.55}$$

where $\sum_{k_1\neq k}\hat{\mathbf{h}}_{k_1}^j \hat{b}_{k_1}^j(i)$ is the sum of the received signals from all interfering users. Substituting (3.55) into equation (3.54), we obtain the conditional expectation of the log-likelihood function of $\mathbf{x}_k^S(i)$. The maximization results at Step 3 are obtained as

$$[\hat{\mathbf{h}}_k^{j+1}, \hat{b}_k^{j+1}(i)] = \arg\max_{\mathbf{h}_k, b_k(i)}\{-\sum_{i=1}^{N}(\hat{\mathbf{x}}_k^{S^{j+1}}(i) - \mathbf{h}_k b_k(i))^H(\hat{\mathbf{x}}_k^{S^{j+1}}(i) - \mathbf{h}_k b_k(i))\} \tag{3.56}$$

Equation (3.56) is similar to (3.46) except that the complete data estimate $\hat{\mathbf{x}}_k^{j+1}(i)$ is replaced by the hidden-data space estimate $\hat{\mathbf{x}}_k^{Sj+1}(i)$ for $k = 1, \cdots, K$ and $i = 1, \cdots, N$.

Thus, SAGE-based receiver for joint channel array response vector estimation and information symbol detection is obtained as

for $j = 1, 2, \ldots$

$k = (j \text{ modulo } K)$

E-step: compute the conditional expectation of hidden-data

for $i = 1, \cdots, N$

$$\hat{\mathbf{x}}_k^{S^{j+1}}(i) = \mathbf{x}(i) - \sum_{i=1, \neq k}^{K} \hat{\mathbf{h}}_i^j \hat{b}_i^j(i) \tag{3.57}$$

M-step: obtain the maximum-likelihood estimates $\hat{\mathbf{h}}_k$ and $\hat{b}_k(i)$

for $i = 1, \cdots, N$

$$\hat{\mathbf{h}}_k^{j+1} = \frac{1}{N} \sum_{i=1}^{N} \hat{\mathbf{x}}_k^{S^{j+1}}(i) \hat{b}_k^j(i) \tag{3.58}$$

$$\hat{b}_k^{j+1}(i) = \text{sign}\{(\hat{\mathbf{h}}_k^{j+1})^H \hat{\mathbf{x}}_k^{S^{j+1}}(i)\} \tag{3.59}$$

for all $k_1 \in \{1, \cdots, k-1, k+1, \cdots, K\}$

$$\hat{\mathbf{h}}_{k_1}^{j+1} = \hat{\mathbf{h}}_{k_1}^j$$

$$\hat{b}_{k_1}^{j+1}(i) = \hat{b}_{k_1}^j(i)$$

The above steps can be interpreted as follows: substituting (3.57) into (3.59), we obtain

$$\hat{b}_k^{j+1}(i) = \text{sign}\{((\hat{\mathbf{h}}_k^{j+1})^H \hat{\mathbf{x}}_k(i) - \sum_{k_1=1, k_1 \neq k}^{K} \hat{f}_{kk_1}^{j+1} \rho_{kk_1} \hat{b}_{k_1}^j(i))\} \tag{3.60}$$

where $\hat{f}_{kk_1}^{j+1} = (\hat{\mathbf{f}}_k^{j+1})^H \hat{\mathbf{f}}_{k_1}^j$ is the estimated instantaneous spatial correlation defined in (3.23) at the *(j+1)*st iteration and ρ_{kk_1} is the cross-correlation defined in equation (3.24). Equation (3.60) implies that the information symbol detection at each iteration involves explicit interference cancellation given the current channel estimation and the previous bit detection results. Therefore, the SAGE-based receiver has a sequential interference cancellation structure. We define the required K updating steps for all K active users as one iteration cycle of the SAGE-based receiver. The receiver structure for a single iteration cycle for a K-user system is illustrated in Figure 4.5. We observe that the optimization results from the previous users are used to estimate channel array response vectors and detect bit sequences for the latter ones. Therefore, in contrast to the parallel structure of the EM-based receiver in Figure 3.4,

a. Receiver Structure

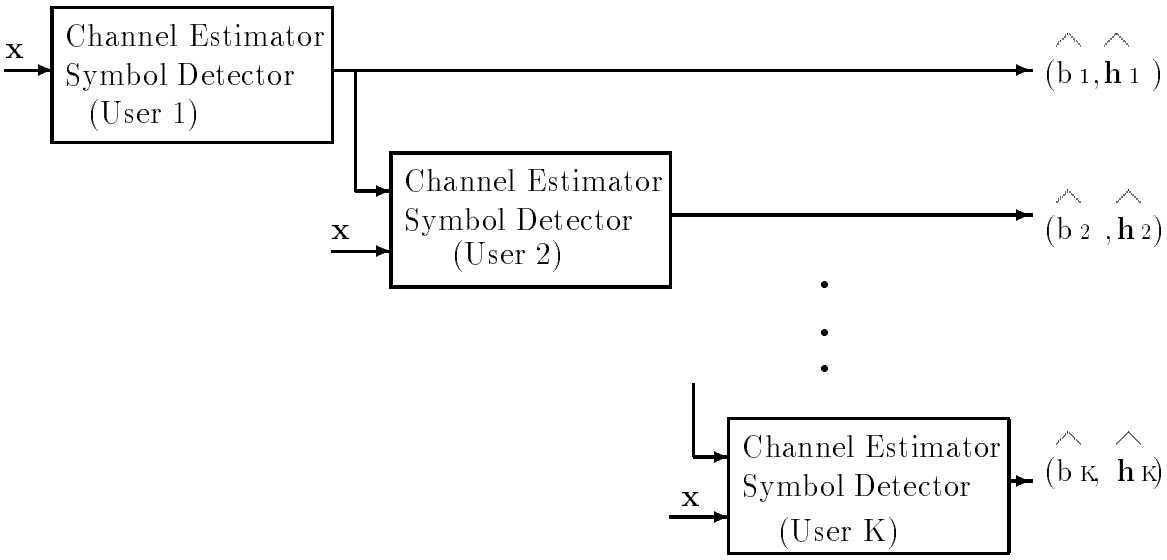

b. Channel Estimator and Symbol Detector for User k

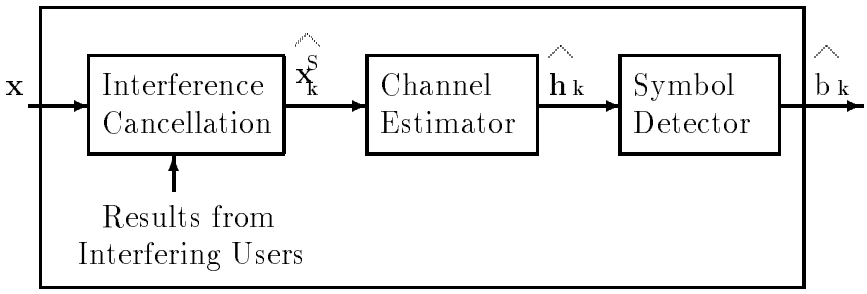

Figure 3.5: SAGE-Based Spatial-Temporal Receiver Structure at Each Iteration Cycle

the SAGE-based spatial-temporal decorrelating receiver has a sequential structure at each iteration cycle.

When there is only one active user in the system, the EM-based receiver and the SAGE-based receiver are identical, and both receivers reduce to the joint fading channel estimator and signal detector for a single-user system as proposed in [20]. It can be observed from (3.48) and (3.49) that interference cancellation capability of the EM-based receiver reduces as the number of the active users becomes large. When the number of the active users in the system gets large so that $\frac{K-1}{K} \approx 1$ and $\frac{1}{K} \approx 0$, the EM-based receiver reduces to the conventional single-user receiver. However, this is not true for the SAGE-based receiver. As the number of active users in the system increases, possible degradation of the SAGE-based receiver would be caused by less accurate channel array response vector estimates and BER performance degradation from interfering users. Therefore, the SAGE-based receiver would be expected to have superior BER and channel estimates, in addition to the observed improved convergence over that of the EM-based receiver.

REMARK 1: The algorithms derived in Sections 3.4 and 4.5 are applicable to long code receivers as well as short code receivers. Because the multi-user signals have been decoupled before bit detection, we do not need to compute the inversion of the spreading code cross-correlation matrix, R^{-1}. However, all users' spreading codes must be known at the base-station receiver.

REMARK 2: It is straightforward to extend the results in Sections 3.4 and 4.5 for BPSK modulation to other modulation schemes by modifying (3.50) and (3.59) for the EM and SAGE algorithms, respectively.

3.6 Receiver Performance

In this section, we assess the performance of the proposed spatial-temporal decorrelating receiver. Since we propose to iteratively estimate the channel array response vectors and detect the transmitted information symbols, we analyze the convergence

of the receivers and determine the bit-error rate (BER) for symbol detection and the Cramer-Rao lower bound (CRLB) for channel estimation. Finally. we calculate the computational complexity of the iterative spatial-temporal decorrelating receivers.

3.6.1 Convergence

From (3.17), it can be easily verified that the log-likelihood function is continuous and differentiable with respect to the unknown parameters. Since the likelihood function increases monotonically with each iteration [8], it is bounded above and the proposed receivers converge to fixed stationary points or local/global maxima depending on the initial guess of the unknown parameters [106].

For a given maximum-likelihood estimate $\hat{\theta}$, the convergence parameter is defined as

$$\mu = \min_{j \leq 1 : j \in \mathcal{Z}} \frac{\hat{\theta}^{j+1} - \hat{\theta}}{\hat{\theta}^{j} - \hat{\theta}} \tag{3.61}$$

where $\hat{\theta}^{j}$ and $\hat{\theta}^{j+1}$ are the estimates at the jth and $(j+1)$st iterations, respectively. From (3.61), the smaller the convergence parameter, the faster the algorithm converges. The convergence rate is therefore proportional to $1/\mu$. Since μ is the smallest one among the convergence parameters for all iteration steps, $1/\mu$ reflects the best iteration step in which the most significant convergence occurs. In the simulation results provided in Section 3.7, $1/\mu$ is corresponding to the largest convergence step (c. f. Figures 3.11, 3.12, 3.13 and 3.14).

The convergence parameter of the EM-type algorithms can be shown to be bounded below by the largest eigenvalue of the matrix [8] [23]

$$[\mathbf{I} - F_{\mathbf{x}}(F_{\mathbf{x}^C})^{-1}]$$

where $F_{\mathbf{x}^C}$ and $F_{\mathbf{x}}$ are Fisher information matrices of the complete data and observed data, respectively. Here, we would like to investigate the effect of using an antenna array on receiver convergence. For simplicity and without loss of generality, we assume that the channel array response vectors are given.

Given the log-likelihood function $\Omega(\theta)$ of the observed signal with respect to the unknown parameter vector θ, the corresponding Fisher information matrix is defined as [34]

$$I_\theta = -E[\frac{\partial^2 \Omega(\theta)}{\partial \theta^2}] \tag{3.62}$$

The Fisher information matrix of the incomplete data (observed data) is obtained by taking the derivative of (3.17) with respect to $\mathbf{b}$,

$$F_{\mathbf{x}} = \frac{4L}{\sigma^2} R \tag{3.63}$$

Taking the derivatives of (3.44) and (3.54) with respect to b_k, respectively, we can obtain the required Fisher information matrix of the complete data used in the EM-based receiver as

$$F_{\mathbf{x}_k^C} = \frac{4KL}{\sigma^2} R^C \tag{3.64}$$

and the Fisher information matrix of the hidden-data space used in the SAGE-based receiver as

$$F_{\mathbf{x}_k^S} = \frac{4L}{\sigma^2} R_{kk} \tag{3.65}$$

where R_{kk} is the kth diagonal component of R and $R^C = \text{diag}\{R_{kk}\}$. The convergence parameters for the EM-based and SAGE-based receiver are obtained as

$$\mu_{EM} = \max \text{eigenvalue}\{\mathbf{I}_K - \frac{1}{K} R_{kk}^{-1} R\} \tag{3.66}$$

and

$$\mu_{SAGE} = \max \text{eigenvalue}\{\mathbf{I}_K - R_{kk}^{-1} R\} \tag{3.67}$$

From the definition of R, it can be verified that μ_{EM} and μ_{SAGE} are the functions of the spatial correlation which is a function of the users' positions as well as the cross-correlation between the users' spreading codes.

Example: We again consider a system with a uniform linear array at the base-station over an AWGN channel. The inter-element spacing of antenna array is half-wavelength and the DOAs of the active users are uniformly distributed in $[-60°, 60°]$. The Gold sequences of length 31 from [52] are assigned to mobile users. All active

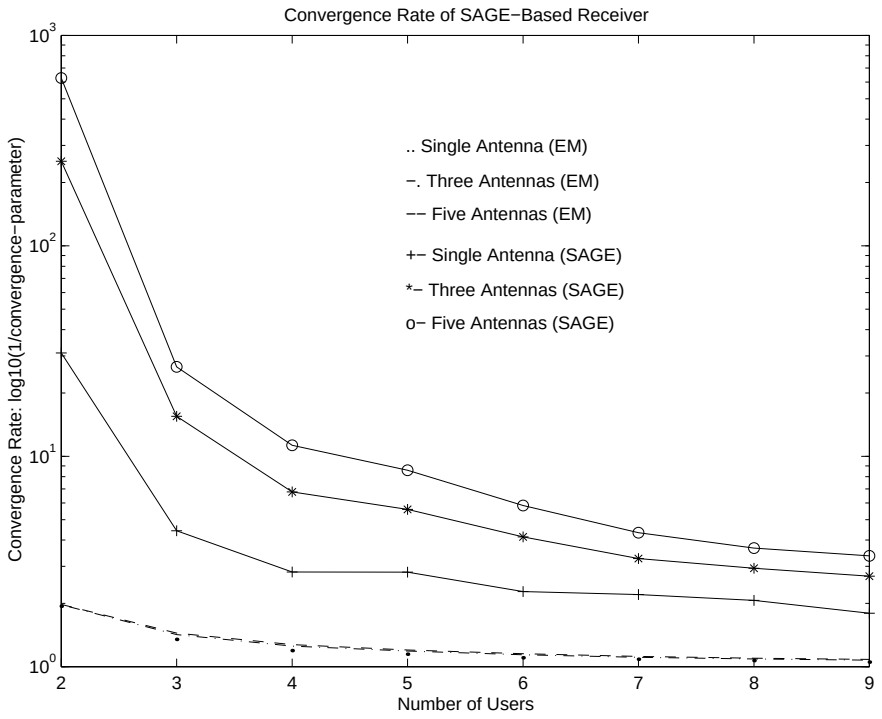

Figure 3.6: Convergence Rate Upper Bounds on the Proposed Receivers Defined as $1/\mu$

users have equal transmitted power. The convergence rate curves are plotted in terms of the number of users and number of antennas and averaged over 5,000 trials. From Figure 3.6, it can be observed that the convergence becomes slower as the number of active users increases in the system. An interesting remark is that using a base-station antenna array can accelerate the convergence rate of the iterative receivers. We also observe that the SAGE-based receiver converges much faster than the EM-based receiver and that the benefit in using base-station antenna arrays combined with the SAGE-based receiver is more striking than that of the antenna-array EM-based receiver. In Section 3.7, simulation results show that the SAGE-based receiver does converge faster than the EM-based receiver.

Since we have assumed that channels remain unchanged during each block transmission, larger bit block sizes result in more accurate channel estimates [16]. Therefore, it is expected that large bit block size improve convergence of the proposed

iterative receivers.

3.6.2 Bit Error Rate (BER)

Similar to the case of decorrelating detector for single-antenna single-path systems [42] [107], the proposed spatial-temporal decorrelator with known channels completely eliminates multi-access interference at the expense of increase of background noise. Therefore, we will focus on computing the average SNR for the desired user. Then, the analytical BER of the spatial-temporal decorrelator directly follows the standard BER expression for corresponding single-user detector.

From (3.29), it is observed that the bit decision vector is an unbiased estimator containing a zero-mean noise vector $\mathbf{w}$ whose covariance matrix is $\frac{\sigma^2}{L}R^{-1}$. Without loss of generality, we assume that the first user is the desired user. The (1, 1) entry of R^{-1} is given by

$$[R^{-1}]_{11} = \frac{1}{|R|}\begin{vmatrix} R_{22} & \cdots & R_{2K} \\ \vdots & \ddots & \vdots \\ R_{K2} & \cdots & R_{KK} \end{vmatrix}$$

Denoting

$$\xi_{ij} = A_i A_j \mathbf{a}_i^H \mathbf{a}_j \rho_{ij} \tag{3.68}$$

the ijth entry of R is given by

$$R_{ij} = \alpha_i^* \alpha_j \xi_{ij} \tag{3.69}$$

Since R and its submatrix (without the first row and the first column) are Hermitian symmetric, it can be easily shown that

$$\begin{vmatrix} R_{22} & \cdots & R_{2K} \\ \vdots & \ddots & \vdots \\ R_{K2} & \cdots & R_{KK} \end{vmatrix} = |\alpha_2|^2 \cdots |\alpha_K|^2 \begin{vmatrix} \xi_{22} & \cdots & \xi_{2K} \\ \vdots & \ddots & \vdots \\ \xi_{K2} & \cdots & \xi_{KK} \end{vmatrix}$$

and

$$|R| = |\alpha_1|^2 \cdots |\alpha_K|^2 \begin{vmatrix} \xi_{11} & \cdots & \xi_{1K} \\ \vdots & \ddots & \vdots \\ \xi_{K1} & \cdots & \xi_{KK} \end{vmatrix}$$

where $|\alpha_k|^2 = \alpha_k^* \alpha_k$. We denote

$$d_1 = \begin{vmatrix} \xi_{11} & \cdots & \xi_{1K} \\ \vdots & \ddots & \vdots \\ \xi_{K1} & \cdots & \xi_{KK} \end{vmatrix}$$

and

$$d_2 = \begin{vmatrix} \xi_{22} & \cdots & \xi_{2K} \\ \vdots & \ddots & \vdots \\ \xi_{K2} & \cdots & \xi_{KK} \end{vmatrix}$$

Then $[R^{-1}]_{11}$ is obtained as

$$[R^{-1}]_{11} = \frac{d_2}{d_1 |\alpha_1|^2} \tag{3.70}$$

The received SNR γ_1 for the desired user assuming a fixed fading attenuation α_1 is $\gamma_1 = \frac{d_1 L}{d_2 \sigma^2} |\alpha_1|^2$. Thus, the average SNR is given by

$$\bar{\gamma}_1 = \frac{d_1 L}{d_2 \sigma^2} E[|\alpha_1|^2] \tag{3.71}$$

where $E[.]$ represents expectation. Finally, the bit error probability for the first user is obtained as [69]

$$P_1 = \frac{1}{2} \left(1 - \sqrt{\frac{\bar{\gamma}_1}{1 + \bar{\gamma}_1}} \right) \tag{3.72}$$

3.6.3 Cramér-Rao Lower Bound (CRLB)

To measure channel array response vector estimation performance, we derive the Cramér-Rao lower bound. We collect the unknown parameters into the column vector

$$\mathbf{a} = \begin{bmatrix} \mathbf{a}_1^T & \cdots & \mathbf{a}_K^T \end{bmatrix}^T \tag{3.73}$$

where $\mathbf{a}_k = \alpha_k \mathbf{a}(\theta_k)$ is the channel array response vector for the kth user.

For an M-element antenna array, we define the $M \times M$ matrix for the ith bit of the kth user, $k = 1, \cdots, K$, as

$$B_k(i) = \text{diag}[b_k(i), \ \cdots, \ b_k(i)]$$

The CRLB matrix for parameter vector $\mathbf{a}$ is given by

$$\mathbf{CRLB}(\mathbf{a}) = \frac{1}{L}[\sum_{i=1}^{N} G(i)]^{-1} \tag{3.74}$$

where

$$G(i) = \begin{bmatrix} \gamma_1\rho_{11}I_M & \sqrt{\gamma_1\gamma_2}\rho_{12}\mathbf{B}_{12}(i) & \cdots & \sqrt{\gamma_1\gamma_K}\rho_{1K}\mathbf{B}_{1K}(i) \\ \sqrt{\gamma_1\gamma_2}\rho_{12}\mathbf{B}_{12}(i) & \gamma_2\rho_{22}I_M & \ddots & \vdots \\ \vdots & \ddots & \ddots & \vdots \\ \sqrt{\gamma_1\gamma_K}\rho_{1K}\mathbf{B}_{1K}(i) & \cdots & \cdots & \gamma_K\rho_{KK}I_M \end{bmatrix} \tag{3.75}$$

for $i = 1, \cdots, N$, $j = 1, \cdots, N$

$$\mathbf{B}_{kj}(i) = B_k^H(i)B_j(i) = \begin{cases} \mathbf{I}_M, & \text{if} \quad b_k(i) = b_j(i) \\ -\mathbf{I}_M, & \text{if} \quad b_k(i) = -b_j(i) \end{cases}$$

and $\gamma_k = A_k^2/\sigma^2$ is the signal-to-noise ratio (SNR) corresponding to the kth user and ρ_{ij} is the spreading code cross-correlation defined in (3.24). For a detailed derivation of the CRLB, see Appendix A.

Clearly, the Fisher information matrix, $\sum_{i=1}^{N} G(i)$, is a function of SNR at the ith bit and the cross-correlation between the spreading codes. The channel array response estimates satisfy

$$E[(\hat{\mathbf{a}} - \mathbf{a})(\hat{\mathbf{a}} - \mathbf{a})^H] \geq \mathbf{CRLB}(\mathbf{a}) \tag{3.76}$$

3.6.4 Computational Complexity

The additional computational complexity induced by the EM-based and SAGE-based receivers at each iteration over the conventional single-user receiver is caused by multi-user signal decoupling. After decoupling, the complexity for the channel estimation and bit sequence detection is comparable to that for the conventional single-user receiver. Since using digital signal processors (DSPs) makes it possible to complete a multiplication within the time equivalent to perform an addition, we calculate the computational burden for both multiplication and addition. We consider the complexity for each user at each iteration cycle.

		Decoupling	Channel Estimation	Bit Detection
Multiplications	EM	ML(K-1)	MLN	2ML
	SAGE	ML(K-1)	MLN	ML
Additions	EM	(ML-1)(K-1)	MLN(N-1)	2(ML-1)
	SAGE	(ML-1)(K-1)	ML(N-1)	ML-1

Table 3.1: Computational Complexity for the EM-Based and SAGE-Based Receivers

We first consider the computational complexity of the EM-based receiver. From (3.48), to obtain the conditional expectation of interference plus noise for each bit of each user requires $ML(K-1)$ multiplications and $(ML-1)(K-1)$ additions. From (3.49) and (3.50), it needs MLN multiplications and $MLN(N-1)$ additions to estimate channel array response vector for each user and $2ML$ multiplications and $2(ML-1)$ additions to detect each bit for each user.

For the SAGE-based receiver, from (3.57), computing the conditional expectation of hidden data corresponding to each user at each bit interval requires $ML(K-1)$ multiplications and $(ML-1)(K-1)$ additions. And from (3.58) and (3.59), it requires MLN multiplications and $ML(N-1)$ additions to obtain the channel array response vector estimate for each user and ML multiplications and $(ML-1)$ additions to detect each bit for each user.

The computational complexity comparison is summarized in Table 3.1. We observe that the computational complexity of both iterative receivers increases linearly with the number of users in the systems. The channel estimation of the EM-based receiver needs more additions than that of the SAGE-based receiver. The EM-based receiver requires twice computational complexity than the SAGE-based receiver for bit detection.

3.7 Simulation Results

In this section, we present performance results for the proposed receivers. A randomly generated Gold sequence of length 31 is assigned to each user in our CDMA system [69]. In [16], it is shown that a bit block length larger than 20 is required to achieve desired BER performance for Gauss-Seidel iterative receiver. Therefore, in the simulations, we choose to transmit a 100-bit information sequence from each user and assume the channels remain unchanged during the data-block transmission. The bit sequences are randomly generated for each user with different seeds. We insert one training bit in the first bit position in each sequence. The DOAs are uniformly distributed in $[-60°, 60°]$. The initial guesses of the channel and array response vectors are obtained using the training bits. More training bits can result in better initial channel estimates. However, this will reduce information transmission efficiency. Then using (3.27), we obtain the initial detected information bit vectors. The simulation results are computed from 10,000-200,000 trials, depending on the signal-to-noise ratio, so that the BER is calculated to within $\pm 5\%$ with a 95% confidence for BER to 10^{-4}. [12].

Because of the computational complexity, we simulate only up to five users in the system to demonstrate the multi-access interference suppression capability for proposed receivers. A five-user system is not realistic for practical applications. To predict system capacity, large numbers of users should be simulated. However, system capacity estimation via exhausive simulation is computationally prohibitive. A possible approach for capacity prediction is to analyze the residual interference statistics after the final iteration step.

Although the results are obtained by simulating small number of users, it is expected that with a large number of users a similar performance improvement would also hold for the SAGE-based receiver, as has been explained in Section 3.5.2.

A. Performance Comparison

This example is used to compare performance of the proposed receivers. There are five

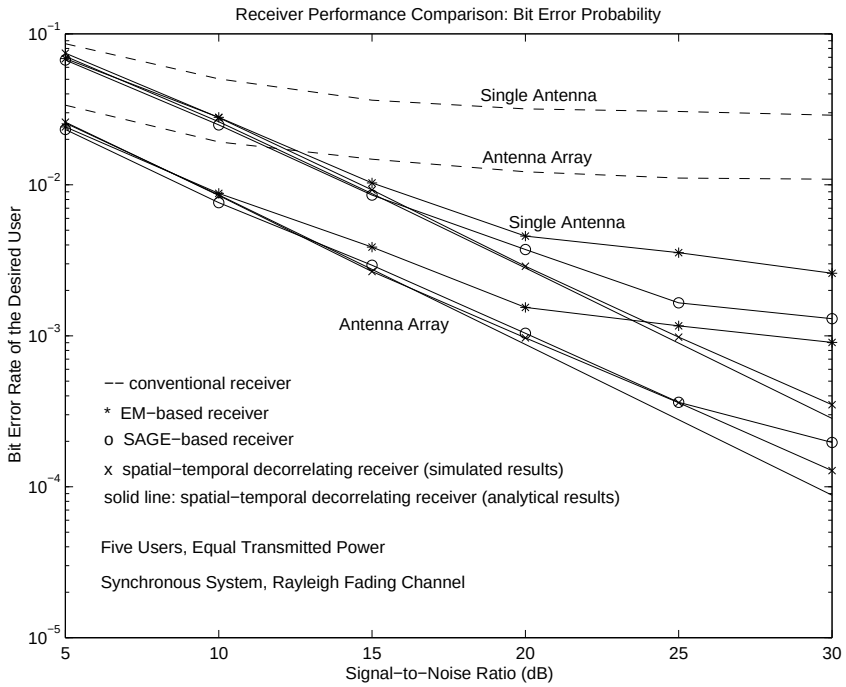

Figure 3.7: Bit Error Rate of the Proposed Receivers for Single Antenna and a Three-Element Antenna Array

active users in the system and either a single antenna or a three-element base-station antenna array. For simplicity of analysis, all users have equal transmitted power. Both the SAGE-based and EM-based decorrelating receivers use eight iterations. From Figure 3.7, we can observe that both the EM-based and SAGE-based decorrelating receivers significantly outperform the conventional single-user receiver. When a single antenna is used, both EM and SAGE-based decorrelating receivers do not converge to the spatial-temporal decorrelating receiver with perfect knowledge of channel and array response vectors. However, the performance of the SAGE-based receiver is greatly improved by using an antenna array. This is mainly due to the antenna array's improved channel estimates, as shown in Figure 3.8. When the SNR is larger than 20dB, the channel estimates of the SAGE-based receiver do not reach the CRLB. However, the loss in channel estimation performance at such a high SNR does not have strong effect on symbol detection. At a BER of 10^{-2}, the three-element antenna array can achieve about 6 dB gain over a single antenna.

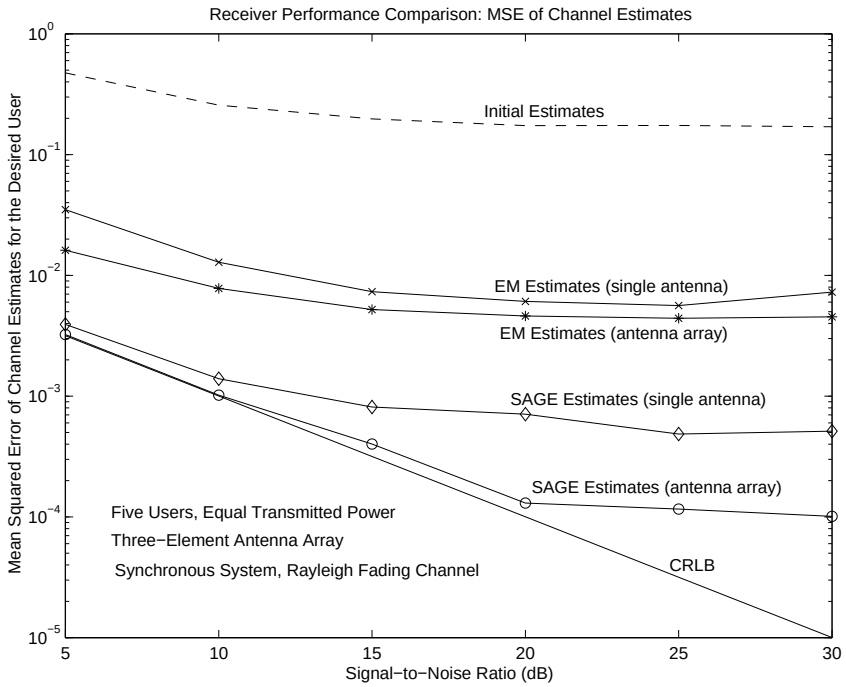

Figure 3.8: Mean Squared Error of Channel Estimates of the Proposed Receivers for Single Antenna and a Three-Element Antenna Array

B. Near-Far Resistance

To address the near-far resistance of the proposed receivers, we consider five active users and a two-element base-station antenna array. We assume that the first user is the desired user with 20 dB SNR and fixed transmitted power. Again, all other interferers are assumed to have equal and time-varying transmitted power. At the power-ratio of 20 dB, the transmitted powers of the interferers are all 100 times stronger than that of the desired user. This represents an extreme near-far environment. Figure 3.9 shows that the SAGE-base decorrelating receiver converges to the spatial-temporal decorrelating receiver with perfect knowledge of channel and array response vectors and is therefore near-far resistant. Although the EM-based decorrelating receiver is an improvement over the conventional single-user receiver, neither receiver is near-far resistant as shown in Figure 3.9. From Figure 3.10, it is observed that channel estimates the SAGE-based receiver has improved near-far

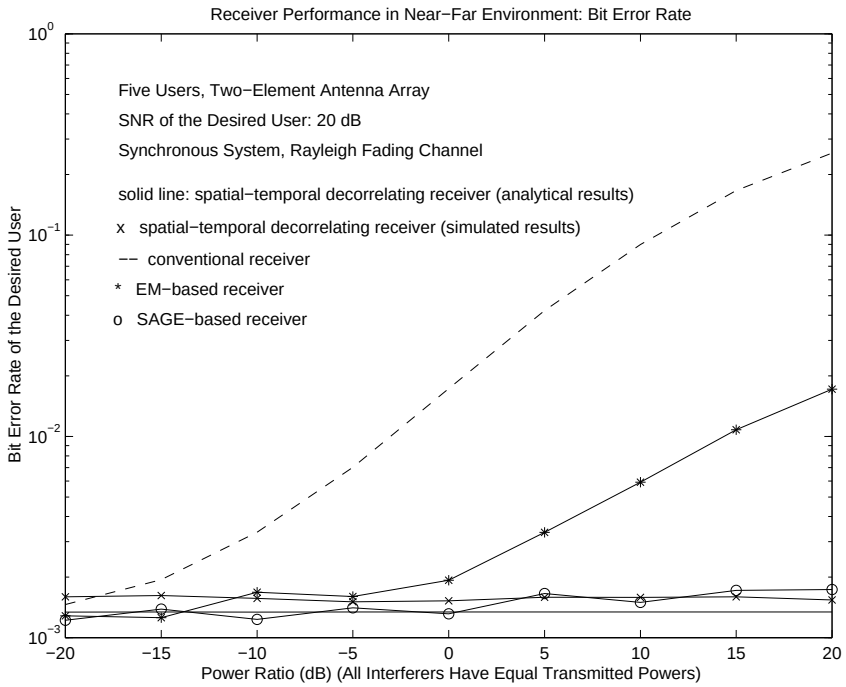

Figure 3.9: Bit Error Rate of the Proposed Receivers for a Two-Element Antenna Array in Near-Far Environment

resistance compared to that of the EM-based receiver.

C. Convergence

Two more examples are used to illustrate the convergence of the proposed iterative receivers. In the first example, five users with equal transmitted power are considered in the system containing a three-element base-station antenna-array. Figures 3.11 and 3.12 show convergence and BER performance of the SAGE-based and EM-based decorrelating receivers, respectively. The SAGE-based decorrelating receiver converges faster than the EM-based decorrelating receiver. The former also achieves better BER performance at the last stage than the latter. A final example is used to compare the convergence of the two iterative receivers in near-far environment for a five-user system with a two-element base-station antenna array. Again, the SAGE-based receiver seems to converge faster than the EM-based receiver even when strong interfering users exist, as shown in Figures 3.13 and 3.14. From Figure

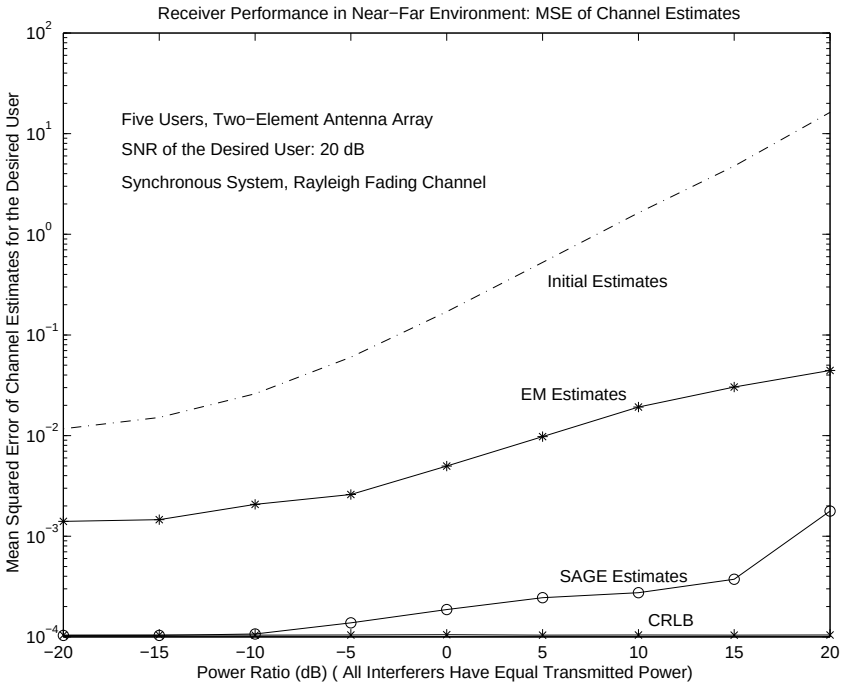

Figure 3.10: Mean Squared Error of Channel Estimates of the Proposed Receivers for a Two-Element Antenna Array in Near-Far Environment

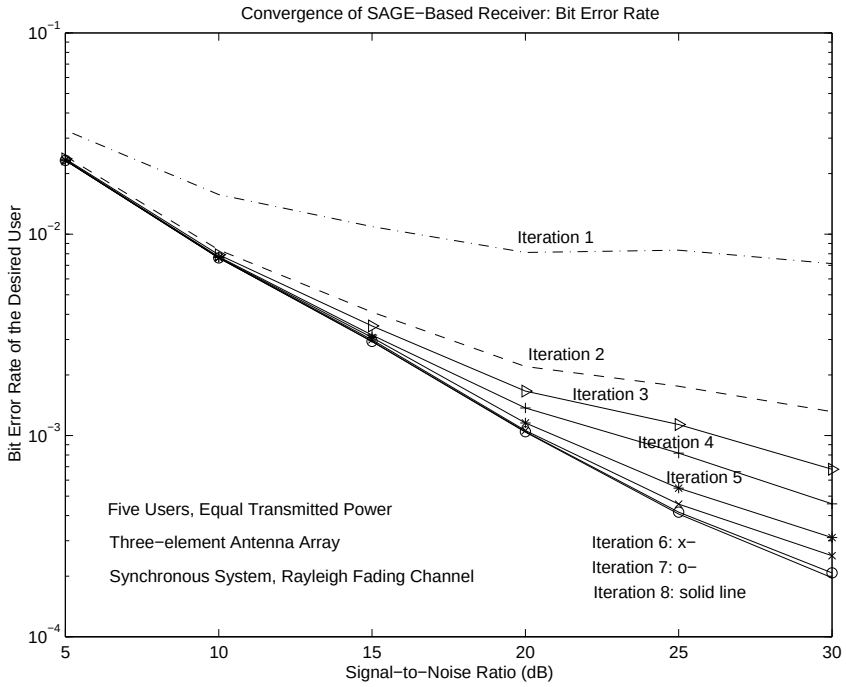

Figure 3.11: Convergence of SAGE-Based Receiver for a Three-Element Antenna Array

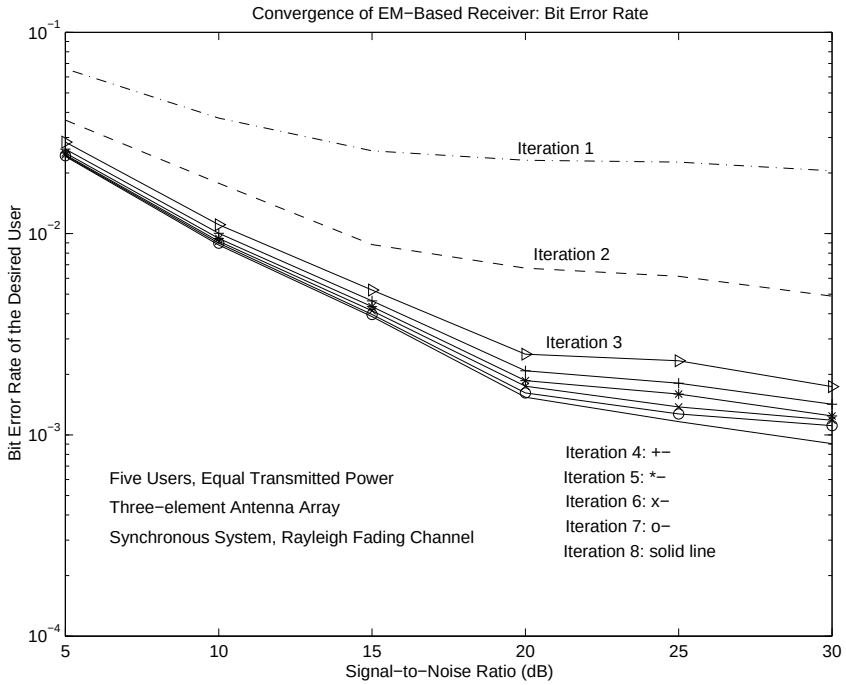

Figure 3.12: Convergence of EM-Based Receiver for a Three-Element Antenna Array

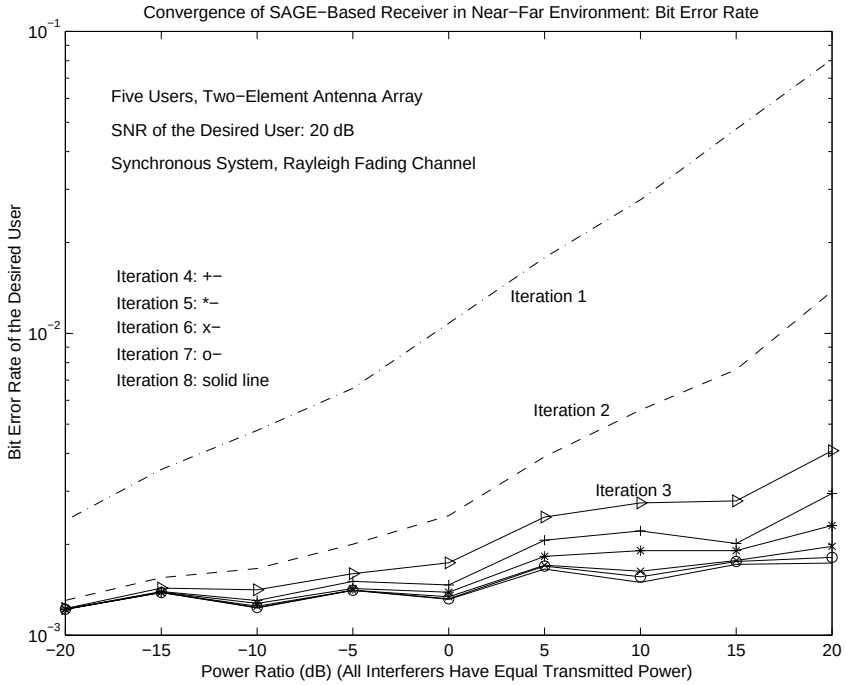

Figure 3.13: Convergence of SAGE-Based Receiver for a Two-Element Antenna Array in Near-Far Environment

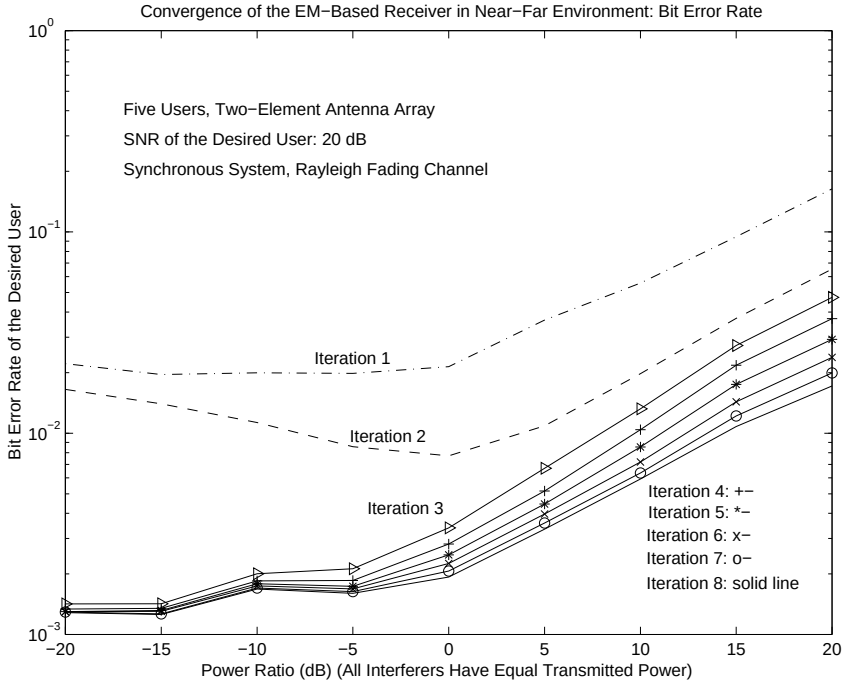

Figure 3.14: Convergence of EM-Based Receiver for a Two-Element Antenna Array in Near-Far Environment

3.14, we observe that iteration two achieves very little performance gain in low power ratio region. This may be explained as follows: with the starting points, the likelihood function slope from iteration two to iteration three is much steeper than that from iteration one to iteration two. These results are consistent with the analytical prediction developed in Section 3.5. Overall, the SAGE-based receiver has more multiple access interference suppression capability than the EM-based receiver for CDMA systems.

Although Gold codes are used to simulate the proposed receivers, similar results are also obtained using randomly generated PN (pseudo-noise) chip squences for proposed spatial-temporal decorrelating receivers. Both the EM-based and SAGE-based receivers show good convergence to fixed points even with random assigned initial guesses and outperform conventional receiver. Similar result is also found in [16] for channel estimation using the EM algorithm.

REMARK 3: Because the receivers converge very quickly in the low SNR region: for a required BER, three iterations can achieve acceptable performance.

3.8 Conclusions

We have derived a spatial-temporal decorrelator based on a new discrete-time signal model as well as employing the maximum likelihood criteria for the CDMA uplink with a base-station antenna array with Rayleigh fading. The spatial-temporal decorrelator is near-far resistant. Numerical results show that the incorporation of the base-station antenna array results in significant performance improvement. Two receiver structures are obtained by applying the EM and SAGE algorithms to implement the spatial-temporal decorrelating receiver iteratively. Since the EM-based and SAGE-based receivers have explicit interference cancellation capability, we also call the new receivers as the EM-based and SAGE-based interference cancelling receivers, respectively. It is shown that while the base-station antenna arrays can accelerate

the convergence rate of the SAGE-based receiver, arrays have little effect on the EM-based receiver's convergence. The bit error probability and CRLB are derived for the proposed receiver. Simulation results show that both the EM-based and SAGE-based decorrelating receivers can achieve significant performance gain over the conventional single-user receiver. Out of the two receiver structures obtained, the SAGE-based receiver outperforms the EM-based receiver while having similar computational complexity and converges to the BER performance of the spatial-temporal decorrelating receiver with known channels. The channel estimates of the SAGE-based receiver are closer to the CRLB than those of the EM-based receiver. The simulated BER results for the spatial-temporal decorrelating receiver agree closely with analytical results.

Chapter 4

Spatial-Temporal Decorrelating Receiver for Asynchronous Multipath Fading Channels

4.1 Introduction

In CDMA systems, the time delay difference of different multipath channels for each user is normally significantly larger than a spreading chip interval, and the wider the bandwidth of the spread signal, the more resolvable the individual path components are in time. Therefore, we can use this natural time diversity to combine the different multipath components so as to reduce the received signal strength fluctuation due to fading attenuations [84].

Since the results in the last chapter have demonstrated that the SAGE-based receiver outperforms the EM-based receiver, we only consider the SAGE algorithm in this chapter. We extend the spatial-temporal decorrelating receiver obtained in Chapter 3 in several ways. First, we incorporate a maximal-ratio combiner into the receiver structure. Utilization of the RAKE structure in multipath channels can improve the receiver performance [32] [58]. Second, in addition to multi-user signal decomposition, refer to Section 3.5.2, we estimate the channel array response vectors by decoupling the multipath signals. Thus, we introduce a double decoupling for

multi-user multipath channel estimation. Finally, we derive a BER lower bound for asynchronous multipath CDMA systems with base-station antenna arrays.

In this chapter, we first develop a synchronous equivalent discrete-time model in Section 4.2 and then formulate a spatial-temporal decorrelator for known channel parameters in Section 4.3. In Section 4.4, we apply the SAGE algorithm to the synchronous equivalent discrete-time system model and obtain an iterative receiver structure for joint channel array response vector estimation and information symbol detection for known time delays. A bit-error-rate (BER) lower bound is derived for maximal-ratio diversity combining in Section 4.5. Simulation results are provided in Section 4.6.

4.2 Synchronous Equivalent Discrete-Time Model

4.2.1 Discrete-Time Formulation

The synchronous equivalent discrete-time model is proposed for single-antenna single-path additive white Gaussian noise (AWGN) channels in [44]. Here we extend the synchronous equivalent model to multipath multi-antenna fading channels. Since we have assumed time delays $\tau_{k,p} \in [0, T_b)$ for $k \in \{1, \cdots, K\}$ and $p \in \{1, \cdots, P_k\}$ in Section 2.3.3, one complete bit of each transmission falls in a time interval of length $2T_b$, as shown in Figure 2.6. Therefore, we choose $2T_b$ to be the observation interval to collect samples for each bit. To express the chip-waveform matched filter output in a compact form, we denote

$$\tau_{k,p} = (u_{k,p} + v_{k,p})T_c \tag{4.1}$$

where $u_{k,p} \in \{0, \cdots, L-1\}$ is an integer and $v_{k,p} \in [0, 1)$ for $k \in \{1, \cdots, K\}$ and $p \in \{1, \cdots, P_k\}$. Let us denote a $2L$-dimensional column spreading code vector by appending L zeros

$$\mathbf{c}_k = \frac{1}{L}[c_{k0}\ c_{k1}\ \cdots\ c_{k(L-1)}\ 0\ \cdots\ 0]^T \tag{4.2}$$

From Figure 2.6, we observe that three consecutive bits contribute to each observation interval. The received signal at each antenna element first passes through a filter matched to the chip waveform, and is then sampled at the chip rate. The received discrete-time signal at the ith observation interval from the mth element can be obtained as

$$x^m(i,g) = \int_{t=gT_c}^{(g+1)T_c} x^m(t)p^*(t)dt \tag{4.3}$$

Using the notation in [44], the $2L$ sample vector for the ith observation interval from the mth element can be written as

$$\mathbf{x}^m(i) = \sum_{k=1}^{K}\sum_{p=1}^{P_k}[\mathbf{h}_{k,p}^{-1,m}b_k(i-1) + \mathbf{h}_{k,p}^{0,m}b_k(i) + \mathbf{h}_{k,p}^{1,m}b_k(i+1)] + \mathbf{n}^m(i) \tag{4.4}$$

where

$$\mathbf{h}_{k,p}^{-1,m} = f_{k,p}^m[(1-v_{k,p})\mathbf{T}_L^{L-u_{k,p}}\mathbf{c}_k + v_{k,p}\mathbf{T}_L^{L-u_{k,p}-1}\mathbf{c}_k] = f_{k,p}^m\mathbf{c}_{k,p}^{-1} \tag{4.5}$$

$$\mathbf{h}_{k,p}^{0,m} = f_{k,p}^m[(1-v_{k,p})\mathbf{T}_R^{u_{k,p}}\mathbf{c}_k + v_{k,p}\mathbf{T}_R^{u_{k,p}+1}\mathbf{c}_k] = f_{k,p}^m\mathbf{c}_{k,p}^{0} \tag{4.6}$$

$$\mathbf{h}_{k,p}^{1,m} = f_{k,p}^m[(1-v_{k,p})\mathbf{T}_R^{L+u_{k,p}}\mathbf{c}_k + v_{k,p}\mathbf{T}_R^{L+u_{k,p}+1}\mathbf{c}_k] = f_{k,p}^m\mathbf{c}_{k,p}^{1} \tag{4.7}$$

and $\mathbf{T}_L$ and $\mathbf{T}_R$ are the acyclic left shift operator and right shift operator, respectively. For example,

$$\mathbf{T}_L^3\mathbf{c}_k = \frac{1}{L}\begin{bmatrix} c_{k3} & c_{k4} & \cdots & c_{k(L-1)} & 0 & \cdots & 0 \end{bmatrix}^T$$

and

$$\mathbf{T}_R^3\mathbf{c}_k = \frac{1}{L}\begin{bmatrix} 0 & 0 & 0 & c_{k0} & c_{k1} & \cdots & c_{k(L-1)} & 0 & \cdots & 0 \end{bmatrix}^T$$

Denoting

$$\mathbf{x}(i) = \begin{bmatrix} (\mathbf{x}^1(i))^T & \cdots & (\mathbf{x}^M(i))^T \end{bmatrix}^T \tag{4.8}$$

$$\mathbf{h}_{k,p}^{-1} = \begin{bmatrix} (\mathbf{h}_{k,p}^{-1,1})^T & \cdots & (\mathbf{h}_{k,p}^{-1,M})^T \end{bmatrix}^T$$

$$\mathbf{h}_{k,p}^{0} = \begin{bmatrix} (\mathbf{h}_{k,p}^{0,1})^T & \cdots & (\mathbf{h}_{k,p}^{0,M})^T \end{bmatrix}^T$$

$$\mathbf{h}_{k,p}^{1} = \begin{bmatrix} (\mathbf{h}_{k,p}^{1,1})^T & \cdots & (\mathbf{h}_{k,p}^{1,M})^T \end{bmatrix}^T$$

and

$$\mathbf{n}(i) = \begin{bmatrix} (\mathbf{n}^1(i))^T & \cdots & (\mathbf{n}^M(i))^T \end{bmatrix}^T$$

The received discrete-time signal from the antenna array can now be expressed as

$$\mathbf{x}(i) = \sum_{k=1}^{K} \sum_{p=1}^{P_k} H_{k,p} \mathbf{b}_k^w(i) + \mathbf{n}(i) \tag{4.9}$$

where

$$H_{k,p} = \left[\begin{array}{ccc} \mathbf{h}_{k,p}^{-1} & \vdots & \mathbf{h}_{k,p}^{0} \quad \vdots \quad \mathbf{h}_{k,p}^{1} \end{array} \right] \tag{4.10}$$

$$\mathbf{b}_k^w(i) = \left[\begin{array}{ccc} b_k(i-1) & b_k(i) & b_k(i+1) \end{array} \right]^T$$

and $\mathbf{n}(i)$ is an AWGN vector with zero-mean and covariance matrix $\frac{\sigma^2}{L}\mathbf{I}_{2ML}$, where $\mathbf{I}_{2ML}$ is a $2ML \times 2ML$ identity matrix. The superscript w in $\mathbf{b}_k^w(i)$ denotes a three-bit sliding window for each desired bit located in the center of the small window. Without loss of generality, we assume that the number of the propagation channels for each user is the same, i.e., $P_k = P$ for $k = 1, \cdots, K$. Actually, for the case of unequal P_k's, we can let $P = \max\{P_1, \cdots, P_K\}$ and append $P - P_k$ zeros for $k = 1, \cdots, K$. Letting

$$H_k = \sum_{p=1}^{P} H_{k,p} \tag{4.11}$$

the $2ML$ received signal vector at the ith observation interval is given by

$$\mathbf{x}(i) = \sum_{k=1}^{K} H_k \mathbf{b}_k^w(i) + \mathbf{n}(i) \tag{4.12}$$

Define a $2ML \times 3K$ matrix

$$\mathcal{H} = \left[\begin{array}{ccccc} H_1 & \vdots & \cdots & \vdots & H_K \end{array} \right] \tag{4.13}$$

and a $3K$ dimensional column vector

$$\mathbf{b}^w(i) = \left[\begin{array}{ccc} \mathbf{b}_1^w(i)^T & \cdots & \mathbf{b}_K^w(i)^T \end{array} \right]^T \tag{4.14}$$

the synchronous equivalent discrete-time model is given by

$$\mathbf{x}(i) = \mathcal{H}\mathbf{b}^w(i) + \mathbf{n}(i) \tag{4.15}$$

4.2.2 Spatial-Temporal Channel Matrix

In (4.11), matrix H_k incorporates both spatial and temporal channel characteristics of our system. Denote, for $k \in \{1, \cdots, K\}$, $p \in \{1, \cdots, P\}$ and $n \in \{-1, 0, 1\}$,

$$\mathbf{h}_{k,p}^n = \begin{bmatrix} f_{k,p}^1 \mathbf{c}_{k,p}^n \\ \vdots \\ f_{k,p}^M \mathbf{c}_{k,p}^n \end{bmatrix} = \begin{bmatrix} \mathbf{c}_{k,p}^n & \cdots & \mathbf{0} \\ \vdots & \ddots & \vdots \\ \mathbf{0} & \cdots & \mathbf{c}_{k,p}^n \end{bmatrix} \begin{bmatrix} f_{k,p}^1 \\ \vdots \\ f_{k,p}^M \end{bmatrix} = C_{k,p}^n \mathbf{f}_{k,p} \tag{4.16}$$

From (4.10), we obtain

$$H_{k,p} = [C_{k,p}^{-1} \vdots C_{k,p}^0 \vdots C_{k,p}^1] \begin{bmatrix} \mathbf{f}_{k,p} & \mathbf{0} & \mathbf{0} \\ \mathbf{0} & \mathbf{f}_{k,p} & \mathbf{0} \\ \mathbf{0} & \mathbf{0} & \mathbf{f}_{k,p} \end{bmatrix} = C_{k,p} F_{k,p} \tag{4.17}$$

The spatial-temporal channel matrix for the kth user is then given by (c.f. (4.11))

$$H_k = \sum_{p=1}^{P} C_{k,p} F_{k,p} \tag{4.18}$$

where the $3M \times 3$ matrix $F_{k,p}$ represents the spatial channel characteristic due to antenna array and multipath fading attenuation and $2ML \times 3M$ matrix $C_{k,p}$ represents the temporal channel characteristic, including spreading code and relative time delays, corresponding to the pth path for the kth user.

A necessary condition that K users are identifiable is that H be of full column rank. Based on the discrete-time system model developed in this section, a necessary condition is

$$2ML > 3K \tag{4.19}$$

4.3 Signal Detection for Known Channels

In this section, we derive a spatial-temporal decorrelator based on the synchronous equivalent discrete-time system model using the maximum-likelihood criterion for known channels. For the sake of notational simplicity, we omit the time index i in this section.

4.3.1 Spatial-Temporal Decorrelator

For a known spatial-temporal channel matrix H, the log-likelihood of the received signal $\mathbf{x}$ conditioned on the bit vector $\mathbf{b}$ is given by

$$\Omega(\mathbf{b}) = -\frac{1}{\sigma^2/L}(\mathbf{x} - \mathcal{H}\mathbf{b}^w)^H(\mathbf{x} - \mathcal{H}\mathbf{b}^w) \tag{4.20}$$

where the superscript H denotes conjugate transpose, $\mathbf{b} = [b_1 \ \cdots \ b_K]^T$. Vector $\mathbf{b}$ can be obtained from $\mathbf{b}^w$.

The bit vector decision variable $\hat{\mathbf{b}}$ can be obtained by maximizing the above log-likelihood function

$$\hat{\mathbf{b}}_d^w = \arg\max_{\mathbf{b}} \Omega(\mathbf{b}) \tag{4.21}$$

Taking the derivative of log-likelihood function (4.20) with respect to the sliding window bit vector $\mathbf{b}^w$ defined in (4.14) and equating the result to zero, we obtain

$$\hat{\mathbf{b}}^w = \text{sign}\{[\mathcal{H}^H\mathcal{H}]^{-1}\mathcal{H}^H\mathbf{x}\} \tag{4.22}$$

where sign$\{a\} = 1$ if $a \geq 0$ or -1 if $a < 0$.

We define the spatial-temporal cross-correlation matrix as

$$\mathcal{R} = \mathcal{H}^H\mathcal{H} = [H_1 \ \cdots \ H_K]^H[H_1 \ \cdots \ H_K] \tag{4.23}$$

The detector in (4.22) is a spatial-temporal decorrelating detector. The (k,j)th sub-matrix in $\mathcal{R}$, $\mathcal{R}_{kj}$ is given by

$$\mathcal{R}_{kj} = H_k^H H_j = \sum_{p=1}^{P} F_{k,p}^H C_{k,p}^H \sum_{q=1}^{P} C_{j,q} F_{j,q}$$

Using definition in (4.16) and (4.17), we obtain

$$C_{k,p}^H C_{j,q} = \begin{bmatrix} \mathbf{c}_{k,p}^{-1H}\mathbf{c}_{j,q}^{-1}\mathbf{I}_M & \mathbf{c}_{k,p}^{0H}\mathbf{c}_{j,q}^{-1}\mathbf{I}_M & \mathbf{0} \\ \mathbf{c}_{k,p}^{-1H}\mathbf{c}_{j,q}^{0}\mathbf{I}_M & \mathbf{c}_{k,p}^{0H}\mathbf{c}_{j,q}^{0}\mathbf{I}_M & \mathbf{c}_{k,p}^{1H}\mathbf{c}_{j,q}^{0}\mathbf{I}_M \\ \mathbf{0} & \mathbf{c}_{k,p}^{0H}\mathbf{c}_{j,q}^{1}\mathbf{I}_M & \mathbf{c}_{k,p}^{1H}\mathbf{c}_{j,q}^{1}\mathbf{I}_M \end{bmatrix} \tag{4.24}$$

Define the spatial correlation coefficient

$$f_{kj,pq} = \mathbf{f}_{k,p}^H \mathbf{f}_{j,q} \tag{4.25}$$

and the temporal correlation coefficient

$$\rho_{kj,pq}^{m,n} = \mathbf{c}_{k,p}^{mH} \mathbf{c}_{j,q}^{n} \tag{4.26}$$

where $m \in \{-1, 0, 1\}$ and $n \in \{-1, 0, 1\}$. From (4.5), (4.6) and (4.7), we obtain

$$\rho_{kj,pq}^{-1,1} = 0$$

and

$$\rho_{kj,pq}^{m,n} = \rho_{kj,pq}^{n,m}$$

We define the spatial-temporal correlation coefficient as

$$\phi_{kj}^{m,n} = \sum_{p=1}^{P} \sum_{q=1}^{P} f_{kj,pq} \rho_{kj,pq}^{m,n} \tag{4.27}$$

where P is the number of propagation paths. Using (4.17), $\mathcal{R}_{kj}$ is obtained as

$$\mathcal{R}_{kj} = \begin{bmatrix} \phi_{kj}^{-1,-1} & \phi_{kj}^{0,-1} & 0 \\ \phi_{kj}^{0,-1} & \phi_{kj}^{0,0} & \phi_{kj}^{0,1} \\ 0 & \phi_{kj}^{0,1} & \phi_{kj}^{1,1} \end{bmatrix} \tag{4.28}$$

To derive the detector structure, we write the spatial-temporal channel matrix H_k for $k = 1, \cdots, K$ as

$$H_k = \sum_{p=1}^{P} C_{k,p} \mathbf{A}_{k,p} \alpha_{k,p} \tag{4.29}$$

where

$$\mathbf{A}_{k,p} = A_k \begin{bmatrix} \mathbf{a}(\theta_{k,p}) & \mathbf{0} & \mathbf{0} \\ \mathbf{0} & \mathbf{a}(\theta_{k,p}) & \mathbf{0} \\ \mathbf{0} & \mathbf{0} & \mathbf{a}(\theta_{k,p}) \end{bmatrix}$$

Thus, we obtain

$$\mathbf{z} = \mathcal{H}^H \mathbf{x} = \begin{bmatrix} \sum_{p=1}^{P} \alpha_{1,p}^{*} \mathbf{A}_{1,p}^{H} C_{1,p}^{H} \mathbf{x} \\ \vdots \\ \sum_{p=1}^{P} \alpha_{K,p}^{*} \mathbf{A}_{K,p}^{H} C_{K,p}^{H} \mathbf{x} \end{bmatrix} \tag{4.30}$$

The detector structure is illustrated in Figure 4.1. After sampling the chip-waveform matched filter output, the received signal is first synchronized and despread. The despread outputs for all K users are then beamformed by maximum-SNR beamforming.

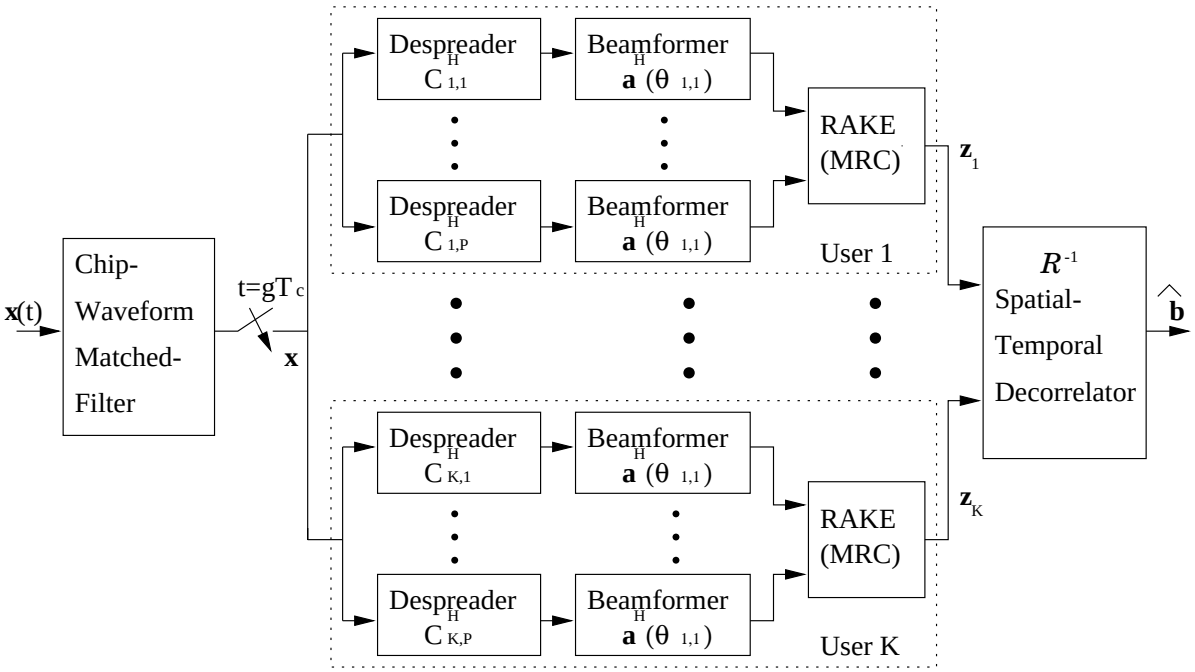

Figure 4.1: Spatial-Temporal Decorrelating Detector for Known Channel Parameters

The signals from different paths are then linearly combined using a maximal ratio combiner (MRC). Finally, the decision variable is obtained by a spatial-temporal decorrelator. Note that the decorrelator, $\mathcal{R}^{-1}$, decorrelates a combination of inter-symbol interference caused by multipath propagation and multi-access interference (MAI).

Substituting (4.15) into (4.22), the spatial-temporal decorrelating detector output can be simplified to

$$\hat{\mathbf{b}}^{w} = \text{sign}\{\mathbf{b}^{w} + \mathcal{R}^{-1}\mathcal{H}^{H}\mathbf{n}\} = \text{sign}\{\mathbf{b}^{w} + \mathbf{w}\} \tag{4.31}$$

where $\mathbf{w}$ is spatial-temporal decorrelating detector output AWGN vector with zero mean and variance $\frac{\sigma^2}{L}\mathcal{R}^{-1}$.

4.3.2 Asymptotic Efficiency

The asymptotic efficiency of the spatial-temporal decorrelator for the kth user is obtained by a similar method as in Chapter 3:

$$\eta_k^d = \max^2 \left\{ 0, \frac{1}{\sqrt{\mathcal{R}_{(k-1)3+2}(\mathcal{R}^{-1})_{(k-1)3+2}}} \right\} = \frac{1}{\mathcal{R}_{(k-1)3+2}(\mathcal{R}^{-1})_{(k-1)3+2}} \tag{4.32}$$

where $\mathcal{R}_{(k-1)3+2}$ is the $(k-1)3+2$-th component of matrix $\mathcal{R}$ and $(\mathcal{R}^{-1})_{(k-1)3+2}$ is the $(k-1)3+2$-th component of matrix $\mathcal{R}$ inverse. From (4.26) and (4.27), $\mathcal{R}_{(k-1)3+2}$ is given by

$$\mathcal{R}_{(k-1)3+2} = \phi_{kk}^{0,0}$$

The kth user's asymptotic efficiency of the conventional single-user detector is given by

$$\eta_k^c = \max^2 \left\{ 0, 1 - \sum_{i=1, i\neq k}^{K} \frac{|\mathcal{R}_{(i-1)3+2,(k-1)3+2}|}{\mathcal{R}_{(k-1)3+2}} \right\} \tag{4.33}$$

where $\mathcal{R}_{(i-1)3+2,(k-1)3+2}$ is given by

$$\mathcal{R}_{(i-1)3+2,(k-1)3+2} = \phi_{ik}^{0,0}$$

Figure 4.2 and Figure 4.3 illustrate two numerical examples for the asymptotic efficiency. In these examples, we consider a five-user system and the Gold sequences of length 31 from [52] are assigned to five users. We assume a uniform linear array with half-wavelength spacing at the base-station and the DOAs for five users are uniformly distributed in $[-60°, 60°]$ with respect to the array boresight. The relative time delays are assumed to be uniformly distributed in $[0, T_b)$. The results are averaged over 2,000 trials for randomly generated Rayleigh fading attenuations, DOAs and time delays. Figure 4.2 shows the results for a single antenna system. The asymptotic efficiencies of the spatial-temporal decorrelator and the conventional single-user detector are plotted for single dominant path channels and three-path channels. We observe that although multipath diversity slightly improves the asymptotic efficiency of the spatial-temporal decorrelator, the asymptotic efficiency of the conventional single-user detector becomes worse for the multipath systems. This is because multipath

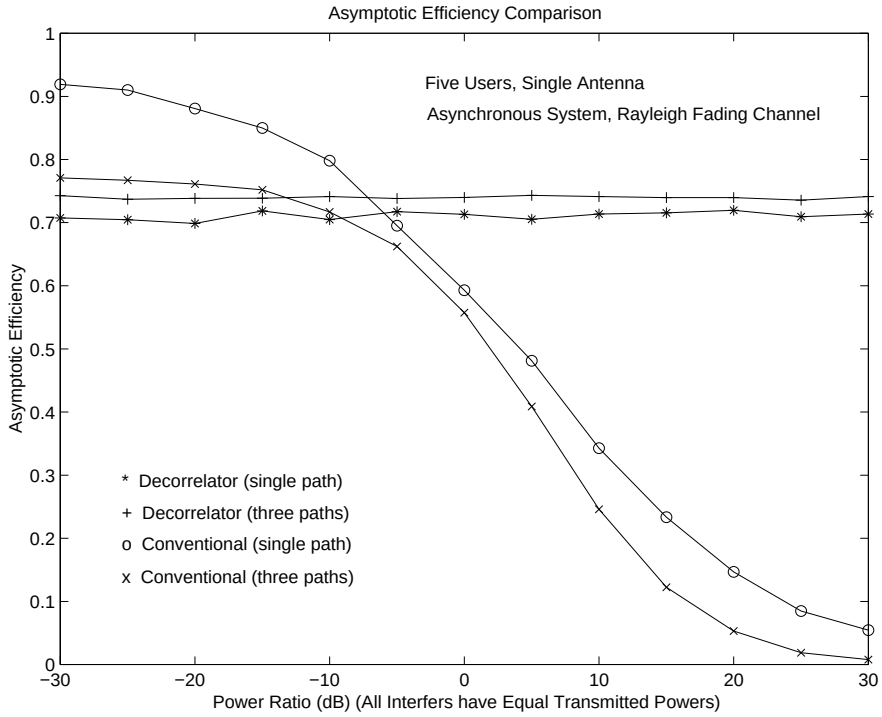

Figure 4.2: Asymptotic Efficiency for a Single Antenna System

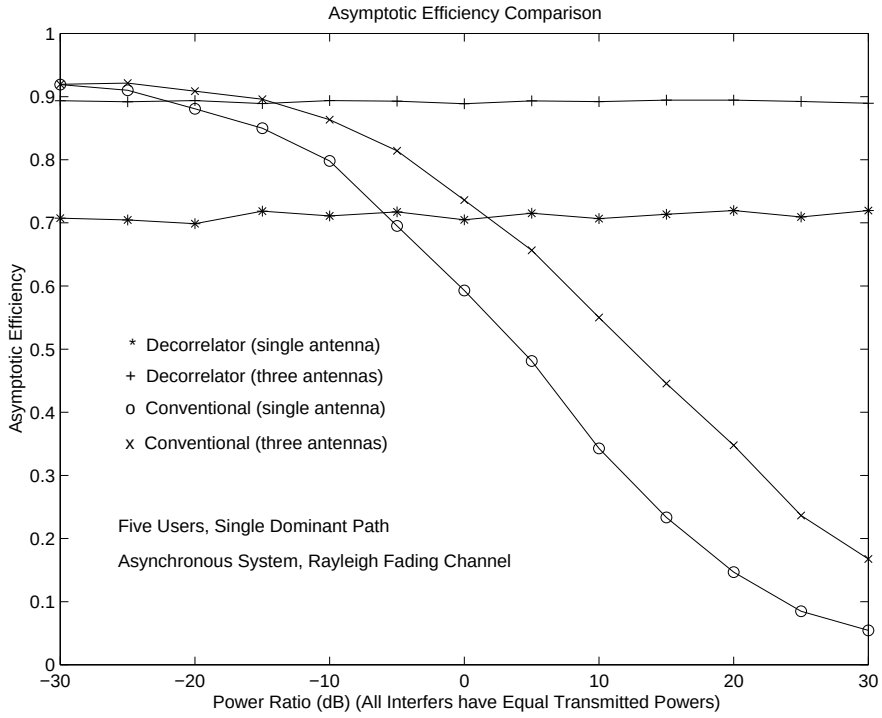

Figure 4.3: Asymptotic Efficiency for Single Dominant-Path Channels

induces more interference with respect to the desired user for a system with three or more users. The asymptotic efficiencies of the spatial-temporal decorrelator and the conventional single-user detector are provided in Figure 4.3 for single dominant path channels. The results in this example show that using a base-station antenna array improves the asymptotic efficiencies for both the spatial-temporal decorrelator and the conventional single-user detector. From these numerical results, we find that multipath diversity has little influence on asymptotic efficiency and the base-station antenna array can be used to improve this performance. Also observed is that similar to the synchronous single-path case, the asymptotic efficiency of the spatial-temporal detector is invariant to the received signal energies from the interfering users, and therefore, the spatial-temporal decorrelator is near-far resistant. However, performance of the conventional single-user detector degrades when the interference becomes stronger. As long as the cross-correlations between the spreading codes over relative time delays are nonzero, i.e., $\mathcal{R}_{(i-1)3+2,(k-1)3+2}$ is nonzero for $i \neq k$, the asymptotic efficiency of the conventional single-user detector will tend to zero with an increase of the interfering users' energies.

4.4 Joint Signal Detection and Channel Estimation

The results in Section 4.3 are based on the assumption that the relative time delays, $\tau_{k,p}$, and channel array response vectors, $\mathbf{f}_{k,p}$ (for $k = 1, \cdots, K$ and $p = 1, \cdots, P$), are known at the receiver. However, in practical applications, we have to estimate these channel parameters. In this section, we investigate the problem of joint signal detection and channel array response vector estimation assuming that we know the time delays at the receiver. We apply the space alternating generalized expectation-maximization (SAGE) algorithm [19] to derive a sequential receiver structure which jointly estimates the channel array response vectors and detects the information symbol sequences for all active users in the system.

We assume that the relative time delays for all the users are known at the receiver. The timing error effects on multi-user signal detection are analyzed in [3] [5] [63] [111] and it is found that the timing error is much more serious to multi-user signal detector's BER performance than any other channel parameter error. We will study the time error effects on the iterative receiver developed in this section using simulations.

4.4.1 SAGE-Based Receiver

The available observed incomplete data is a data vector set $\{\mathbf{x}(i); i = 1, \cdots, N\}$, where N is the number of bits at each block. Similar to the approach in Chapter 3, we choose user index k as the index set to detect the information bit sequences, thus the admissible hidden-data space, complete data, for index k and $i = 1, \cdots, N$ is given by

$$\mathbf{x}_k^S(i) = H_k \mathbf{b}_k^w(i) + \mathbf{n}(t) = \sum_{p=1}^{P} H_{k,p} \mathbf{b}_k^w + \mathbf{n}(t) \tag{4.34}$$

where $H_{k,p} = C_{k,p} F_{k,p}$. Given the spatial channel estimation results at the jth iteration, $\hat{F}_{k,p}^j$, for $k = 1, \cdots, K$ and $p = 1, \cdots, P$, and symbol detection results, $\hat{\mathbf{b}}_k^{wj}$, at the jth iteration, the conditional expectation of $\mathbf{x}_k^S(i)$, for $k = 1, \cdots, K$ and $i = 1, \cdots, N$, is obtained as

$$\hat{\mathbf{x}}_k^S(i) = \mathbf{x}(i) - \sum_{k_1=1, k_1 \neq k}^{K} \sum_{p=1}^{P} \hat{H}_{k_1,p}^j \hat{\mathbf{b}}_{k_1}^{wj}(i) \tag{4.35}$$

where we have denoted $\hat{H}_{k,p}^j = C_{k,p} \hat{F}_{k,p}^j$ for $k = 1, \cdots, K$ and $p = 1, \cdots, P$. Thus, the log-likelihood function of $\hat{\mathbf{x}}_k^S(i)$, for $k = 1, \cdots, K$, after discarding the terms independent of $F_{k,p}$ and $\mathbf{b}_k^w(i)$, for $k = 1, \cdots, K$ and $p = 1, \cdots, P$, is given by

$$\Omega(\hat{\mathbf{x}}_k^S(1), \cdots, \hat{\mathbf{x}}_k^{Sj}(N)) = -\frac{1}{\sigma^2/L} \sum_{i=1}^{N} \left(\hat{\mathbf{x}}_k^{Sj}(i) - \sum_{p=1}^{P} H_{k,p} \mathbf{b}_k^w(i) \right)^H \left(\hat{\mathbf{x}}_k^{Sj}(i) - \sum_{p=1}^{P} H_{k,p} \mathbf{b}_k^w(i) \right) \tag{4.36}$$

The maximization results at the next iteration are given by

$$[\hat{F}_k^{j+1}, \hat{\mathbf{b}}_k^{w^{j+1}}] = \arg \max_{H_k, \mathbf{b}_k^w(i)} \Omega(\hat{\mathbf{x}}_k^{Sj}(1), \cdots, \hat{\mathbf{x}}_k^{Sj}(N))$$

Equating the derivative of (4.36) with respect to $\mathbf{b}_k^m(i)$ to zero, for $i = 1, \cdots, N$, and using the channel parameter estimation results, the symbol sequence detection results are given by

$$\hat{\mathbf{b}}_k^{w^{j+1}} = \text{sign}[(\hat{\mathcal{R}}_{kk}^{j+1})^{-1} \hat{H}_k^{j+1^H} \hat{\mathbf{x}}_k^{Sj}(i)]$$

where

$$\hat{\mathcal{R}}_{kk}^{j+1} = \hat{H}_k^{j+1^H} \hat{H}_k^{j+1}$$

and

$$\hat{H}_k^{j+1} = \sum_{p=1}^{P} C_{k,p} \hat{F}_{k,p}^{j+1}$$

To obtain the estimation results of $F_{k,p}$, for $k = 1, \cdots, K$ and $p = 1, \cdots, P$, we further decouple the complete data $\mathbf{x}_k^S(i)$ by choosing path index p as the index subset, the corresponding admissible hidden-data set for user index k and path index p is given by

$$\mathbf{x}_{k,p}^S(i) = H_{k,p}\mathbf{b}_k^w + \mathbf{n}(t) \tag{4.37}$$

where $i = 1, \cdots, N$. The conditional expectation of $\mathbf{x}_{k,p}^S(i)$, for $k = 1, \cdots, K$, $p = 1, \cdots, P$ and $i = 1, \cdots, N$, is obtained as

$$\hat{\mathbf{x}}_{k,p}^S(i) = \hat{\mathbf{x}}_k^S(i) - \sum_{p_1=1, p_1 \neq p}^{P} \hat{H}_{k,p_1}\mathbf{b}_k^w = \mathbf{x}(i) - \sum_{p_1=1, p_1 \neq p}^{P} \hat{H}_{k,p_1}\mathbf{b}_k^w - \sum_{k_1=1, k_1 \neq k}^{K} \sum_{p=1}^{P} \hat{H}_{k_1,p}^j \hat{\mathbf{b}}_{k_1}^{wj}(i) \tag{4.38}$$

The log-likelihood function of $\hat{\mathbf{x}}_{k,p}^S(i)$, for $k = 1, \cdots, K$ and $p = 1, \cdots, P$, is obtained as

$$\Omega(\hat{\mathbf{x}}_{k,p}^S(1), \cdots, \hat{\mathbf{x}}_{k,p}^{Sj}(N)) = -\frac{1}{\sigma^2/L} \sum_{i=1}^{N} (\hat{\mathbf{x}}_{k,p}^{Sj}(i) - H_{k,p}\mathbf{b}_k^w(i))^H (\hat{\mathbf{x}}_{k,p}^{Sj}(i) - H_{k,p}\mathbf{b}_k^w(i)) \tag{4.39}$$

By maximizing the likelihood, we obtain the estimate of the spatial-temporal channel matrix, $\hat{H}_{k,p}$, for $k = 1, \cdots, K$ and $p = 1, \cdots, P$, (see Appendix B for a detailed derivation)

$$\hat{H}_{k,p} = [\sum_{i=1}^{N} \hat{\mathbf{x}}_{k,p}^{Sj}(i) \hat{\mathbf{b}}_k^{wjH}(i)][\sum_{i=1}^{N} \hat{\mathbf{b}}_k^{wj}(i) \hat{\mathbf{b}}_k^{wjH}(i)]^{-1} \tag{4.40}$$

Since $\hat{H}_{k,p} = C_{k,p}F_{k,p}$ with known $C_{k,p}$, we will use a least squares (LS) criterion [34] to obtain the unknown matrix $F_{k,p}$. The LS estimate can be found by minimizing

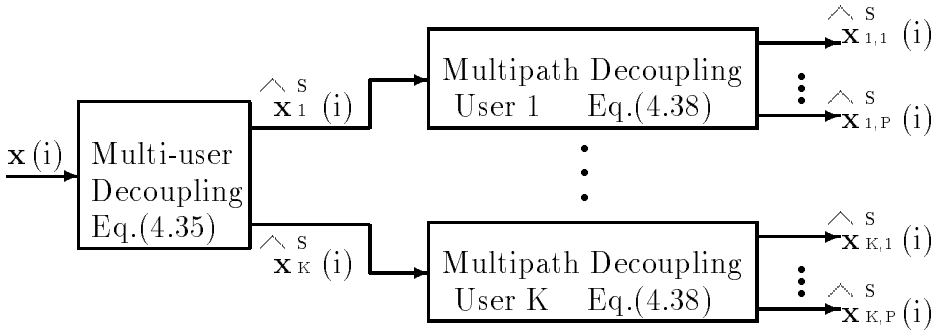

Figure 4.4: The Received Signal Decoupling Process

the following squared error

$$J(\theta) = (\hat{H}_{k,p} - C_{k,p}F_{k,p})^H(\hat{H}_{k,p} - C_{k,p}F_{k,p}) \tag{4.41}$$

Equation (4.39) can be further written as

$$J(\theta) = \hat{H}_{k,p}^H\hat{H}_{k,p} - 2\hat{H}_{k,p}^H C_{k,p}F_{k,p} + F_{k,p}^H C_{k,p}^H C_{k,p}F_{k,p}$$

Taking the derivative of $J(\theta)$ with respect to $F_{k,p}$, we have

$$\frac{\partial J(\theta)}{\partial F_{k,p}} = -2C_{k,p}^H\hat{H}_{k,p} + 2C_{k,p}^H C_{k,p}F_{k,p}$$

From (4.16) and (4.17), if the time delays are non-zero, the columns of $C_{k,p}$ are linearly independent, then $C_{k,p}$ is full rank and the spatial channel matrix is obtained as a least squares solution for a given $C_{k,p}$, for $k = 1, \cdots, K$ and $p = 1, \cdots, P$,

$$\hat{F}_{k,p} = (C_{k,p}^H C_{k,p})^{-1}C_{k,p}^H\hat{H}_{k,p} \tag{4.42}$$

The key in this receiver algorithm is to decouple the received signal, as illustrated in Figure 4.4. The first step is used to obtain the multi-user signals. The multipath signals for each user are further decoupled at the second step. The final decoupled signals are used to estimate the channel array response vector for each path of each user by maximum likelihood criteria. The estimates of the channel array response vectors are then used to detect the information sequence for each user.

The SAGE-based receiver for joint channel estimation and symbol detection is summarized as follows:

for $j = 1, 2, \cdots$

$k = (j \ \text{modulo} \ K)$

E-step: compute the conditional expectation of the hidden-data

for $i = 1, \cdots, N$

$$\hat{\mathbf{x}}_k^{Sj}(i) = \mathbf{x}(i) - \sum_{k_1=1, k_1 \neq k}^{K} \sum_{p=1}^{P} C_{k_1,p} \hat{F}_{k_1,p}^{j} \hat{\mathbf{b}}_{k_1}^{wj}(i) \tag{4.43}$$

for $p = 1, \cdots, P$

$$\hat{\mathbf{x}}_{k,p}^{Sj}(i) = \hat{\mathbf{x}}_k^{Sj}(i) - \sum_{p_1=1, p_1 \neq p}^{P} C_{k,p_1} \hat{F}_{k,p_1}^{j} \mathbf{b}_k^{w} \tag{4.44}$$

M-step: obtain the maximum-likelihood estimates $\hat{\mathbf{f}}_k$ for

$p = 1, \cdots, P$ and $\hat{b}_k(i)$ for $i = 1, \cdots, N$

$$\hat{F}_{k,p} = (C_{k,p}^H C_{k,p})^{-1} C_{k,p}^H [\sum_{i=1}^{N} \hat{\mathbf{x}}_{k,p}^{Sj}(i) \hat{\mathbf{b}}_k^{wH}(i)] [\sum_{i=1}^{N} \hat{\mathbf{b}}_k^{wj}(i) \hat{\mathbf{b}}_k^{wjH}(i)]^{-1} \tag{4.45}$$

$$\hat{\mathbf{b}}_k^{wj+1} = \text{sign}[(\hat{\mathcal{R}}_{kk}^{j+1})^{-1} \hat{H}_k^{j+1^H} \hat{\mathbf{x}}_k^{Sj}(i)] \tag{4.46}$$

$$\begin{aligned} \hat{F}_{k',p}^{j+1} &= \hat{F}_{k',p}^{j}, \qquad k' \neq k \\ \hat{\mathbf{b}}_{k'}^{wj+1}(i) &= \hat{\mathbf{b}}_{k'}^{wj}(i), \quad k' \neq k \end{aligned}$$

The basic receiver structure is the same as Figure 3.5 for the case of synchronous systems. For each decoupled user, the structure for each iteration is shown in Figure 4.5.

Since the SAGE algorithm guarantees that the likelihood function increases monotonically with each iteration, the proposed iterative spatial-temporal decorrelating receiver converges to a fixed stationary point or local/global maxima depending on the initial guess of the unknown parameters. In Chapter 3, we have shown that using a base-station antenna array accelerates receiver's BER convergence to that of perfectly known channel parameters.

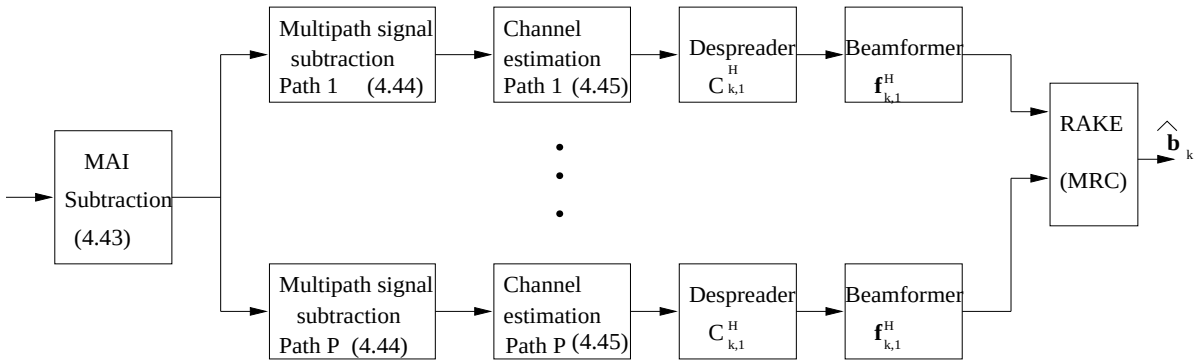

Figure 4.5: SAGE-Based Receiver Structure for Each User at Each Iteration Cycle

4.4.2 Computational Complexity

We consider the computational complexity of the SAGE-based iterative receiver for joint channel estimation and bit detection at each iteration cycle for each user. From (4.43), (4.16) and (4.17), we obtain that the number of multiplications needed to decouple the multi-user signals is $(3MLP+6ML)(K-1) = 3ML(P+2)(K-1)$ and the number of additions is $6ML(P+1)(K-1)$. From (4.44), it requires $3ML(P-1)+6ML = 3ML(P+1)$ multiplications and $6MLP$ additions to decouple the multipath signals for each user.

It will be shown in Section 5.3.2 that the multipath interference decorrelator is not needed for wideband CDMA systems containing resolvable paths. If we do not include the bit detection complexity from the multipath interference decorrelator, from (4.46), detecting one bit for each user requires $3MLP + 6ML = 3ML(P+2)$ multiplications and $6ML(P+1)$ additions.

Much computational complexity arises from the spatial channel matrix estimate in (4.45). The number of multiplications required is $6M^2L + 3ML + 6MLN + 9N$ plus the complexity of a $3M \times 3M$ matrix inverse and a 3×3 matrix inverse. Note that the computational complexity increases linearly with the number of the users in the system. From (4.24), we observe that $3M \times 3M$ matrix $C_{k,p}^H C_{k,p}$ is block diagonal and this property can be used to reduce the computational complexity to invert this matrix. However, the total complexity of the channel estimation due to antenna array

is still of the order M^2.

4.5 BER Lower Bound

In this section, we derive a lower bound of the bit-error-rate (BER) for the proposed iterative multi-user receiver for asynchronous multipath case assuming that the multi-user interference has been completely eliminated. The derivation of the analytical BER in this chapter is more difficult to obtain than the synchronous single-path case considered in Chapter 3. In the following, we assume that the channel array response vector for each user is known as well as the bit sequences of all interfering users. Therefore, the BER expression derived in this section provides an upper bound on the performance of a system with imperfect interference cancellation.

From (4.43) and (4.46), we obtain the decision variable for the kth user

$$\hat{\mathbf{y}}_k^{j+1} = (\hat{\mathcal{R}}_{kk}^{j+1})^{-1} \hat{H}_k^{j+1^H} [\mathbf{x}(i) - \sum_{k_1=1, k_1 \neq k}^{K} \hat{H}_{k_1}^j \hat{\mathbf{b}}_{k_1}^{wj}(i)] \tag{4.47}$$

From (4.47), it is observed that the multi-access interference is subtracted explicitly at each iteration. To obtain a BER lower bound for the kth user, we assume that the interference has been completely eliminated at the final iteration in the receiver algorithm and the multipath channel array response vectors of user k are perfectly known at the receiver. Thus, the decision variable of the kth user is given by

$$\mathbf{y}_k = \mathcal{R}_{kk}^{-1} H_k^H [H_k \mathbf{b}_k^w(i) + \mathbf{n}(i)] = \mathbf{b}_k^w + \mathbf{w}_k(i) \tag{4.48}$$

where $\mathbf{w}(i)$ is a zero mean AWGN vector with covariance matrix $\frac{\sigma^2}{L}\mathcal{R}_{kk}^{-1}$. To compute the BER of the desired bit $b_k(i)$ which is the second component in vector $\mathbf{b}_k^w(i) = [b_k(i-1) \;\; b_k(i) \;\; b_k(i+1)]$, we first derive the corresponding average SNR

$$\bar{\gamma}_k = \frac{1}{\frac{\sigma_2}{L} E[(\mathcal{R}_{kk}^{-1})_2]} \tag{4.49}$$

where $(\mathcal{R}_{kk}^{-1})_2$ is the second diagonal component of matrix $\mathcal{R}_{kk}^{-1}$ and $E[\cdot]$ represents the expectation over the Rayleigh-distributed channel attenuations. Since $\rho_{kk,pq}^{0,0} \leq 1/L$,

and $\rho_{kk,pq}^{-1,0}$ and $\rho_{kk,pq}^{1,1}$ are much smaller than $\rho_{kk,pq}^{0,0}$, we make the following approximation to (4.28)

$$\mathcal{R}_{kk} \approx \begin{bmatrix} \phi_{kk}^{-1,-1} & 0 & 0 \\ 0 & \phi_{kk}^{0,0} & 0 \\ 0 & 0 & \phi_{kk}^{1,1} \end{bmatrix} \tag{4.50}$$

In Section 4.6, it is shown by simulation that the approximation (4.50) is a reasonably good one. $(\mathcal{R}_{kk}^{-1})_2$ is then obtained as

$$(\mathcal{R}_{kk}^{-1})_2 = \frac{1}{\sum_{p=1}^{P}\sum_{q=1}^{P}\alpha_{k,p}^{*}\alpha_{k,q}\mathbf{a}(\theta_{k,p})\mathbf{a}(\theta_{k,q})\rho_{kk,pq}^{0,0}}$$

Since we have assumed that the channel attenuations are mutually independent, we have

$$E[(\mathcal{R}_{kk}^{-1})_2] = \frac{1}{MA_k^2\sum_{p=1}^{P}E[\alpha_{k,p}^2]\rho_{kk,pp}^{0,0}}$$

where $\alpha_{k,p}^2 = \alpha_{k,p}^{*}\alpha_{k,p}$. Because $\rho_{kk,pp}^{0,0}$, for $p = 1, \cdots, P$, are statistically identical, the average SNR for user k is obtained as

$$\bar{\gamma}_k = \frac{MLA_k^2\rho_{kk,11}^{0,0}}{\sigma^2}\sum_{p=1}^{P}E[\alpha_{k,p}^2] \tag{4.51}$$

Assuming that $E[\alpha_{k,p}^2]$ are identical for all P paths of user k, the BER lower bound for the kth user can be obtained [69](p. 781)

$$P_k = [(1-\mu)/2]^P\sum_{p=0}^{P-1}\begin{pmatrix} P-1+p \\ p \end{pmatrix}[(1+\mu)/2]^p \tag{4.52}$$

where

$$\mu = \sqrt{\frac{\bar{\gamma}_c}{(1+\bar{\gamma}_c)}}$$

and

$$\bar{\gamma}_c = \frac{MLA_k^2\rho_{kk,11}^{0,0}}{\sigma^2}E[\alpha_{k,p}^2]$$

4.6 Simulations

In this section, we present performance results for the proposed receivers. Gold sequences of length 31 from [52] are assigned to mobile users. In the simulations,

we transmit a 100-bit information sequence, i.e., a hundred-bit block, from each user and assume that the channel attenuations and DOAs remain unchanged during the data-block transmission. We insert one training bit in the first bit position in each sequence to obtain the initial channel array response vector estimates. A uniform linear array with half-wavelength spacing is used at the base-station and the DOAs are assumed to be uniformly distributed in $[-60°, 60°]$. The time delay of the first path for each active user is uniformly distributed in $(0,\ T_b/2)$ and the time delay of the second path for each user is uniformly distributed in $(T_b/2, T_b)$. Multipath channels are assumed to be Rayleigh distributed with same covariance for all paths. The channel array response vectors are assumed to be known for the spatial-temporal decorrelating receiver and the conventional single-user receiver. In all the simulations, we consider a CDMA system with base-station antenna arrays.

Figure 4.6 compares the BER performance among the proposed SAGE-based receiver (with unknown channel array response vectors), the spatial-temporal decorrelating receiver and the conventional single-user receiver. A three-element antenna array is used at the base-station. All users have equal transmitted power. It is observed that using RAKE combining, a two-path system can achieve significant BER performance gain over a single path system. Although the BER performance of the conventional single-user receiver for two-path channels outperforms that for single path channels, both show a BER floor which is caused by multi-access interference. The SAGE-based receiver for joint channel array response vector estimation and bit sequence detection achieves much better BER performance over the conventional single-user receiver and converges to the spatial-temporal decorrelating receiver. From Figure 4.6, we observe that the simulated BER performance of the spatial-temporal decorrelating receiver for multi-user systems is close to the BER lower bound. Figure 4.7 illustrates the corresponding channel estimates for the same system settings. The CRLB is taken from the previous chapter and provides a loose lower bound. The channel estimation performance for two-path systems is better than that for single path systems at 5 dB, 10 dB and 15 dB SNR points and slightly worse at SNR = 20

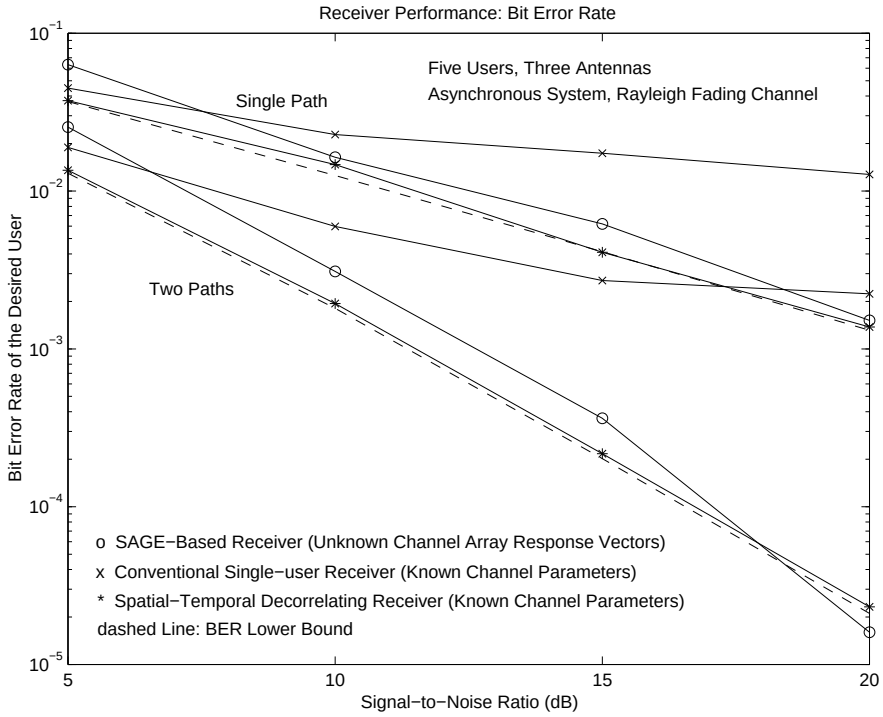

Figure 4.6: BER of the Proposed Receiver

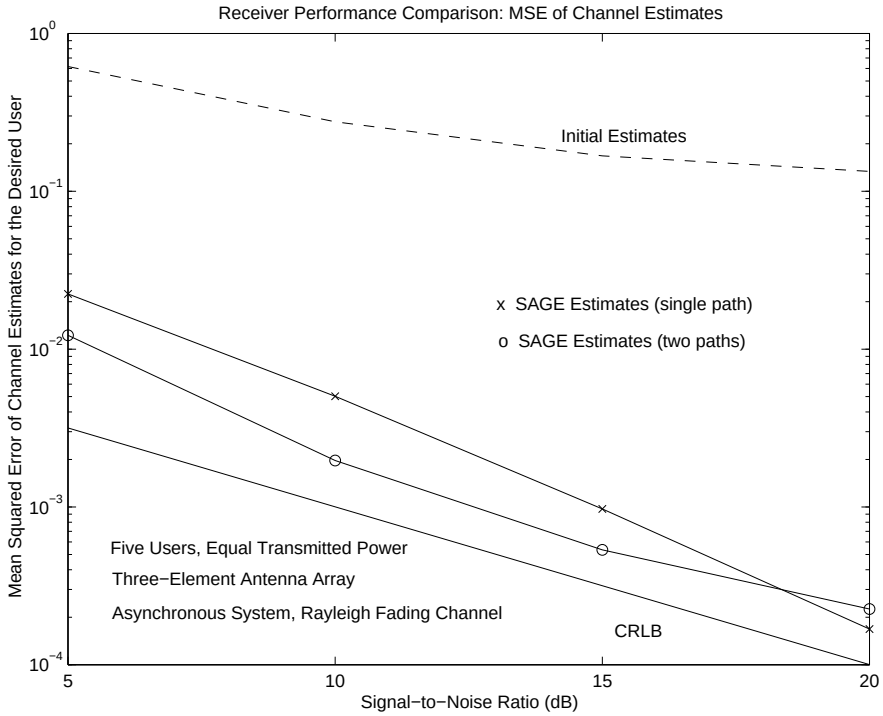

Figure 4.7: Mean Squared Error of Channel Estimates of the SAGE-based Receiver

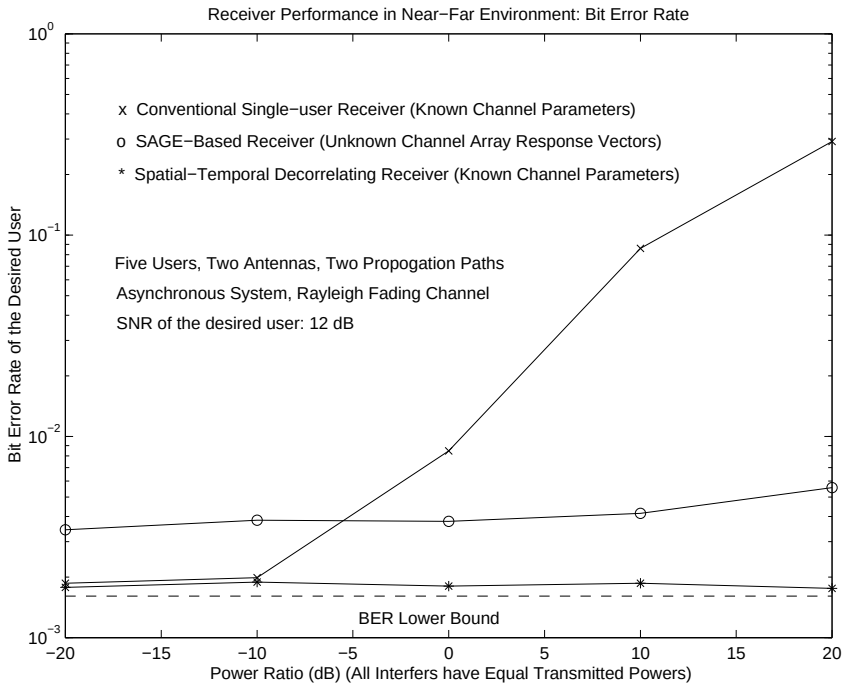

Figure 4.8: Near-Far Resistance of the Proposed Receiver

dB.

To verify the near-far resistance of the SAGE-based receiver, we consider a system with a two-element antenna array over two-path fading channels. The SNR of the desired user is 12 dB. All the interfering users have equal transmitted power and the power ratio changes from -20 dB to 20 dB. From Figure 4.8, it is observed that the BER of the conventional single-user receiver increases dramatically when the interfering users' signals becomes stronger. Thus, the conventional single-user receiver is not near-far resistant. However, the BER performance of the SAGE-based receiver is almost independent of the interfering user's energies. Therefore, the SAGE-based receiver is near-far resistant. Figure 4.9 illustrates the mean squared error of the channel array response vector estimates by the SAGE-based receiver. The channel estimation is near-far resistant and close to the CRLB obtained for the synchronous system in Appendix A. From Figures 4.6 and 4.8, we observe that the simulated BER results for the spatial-temporal decorrelating receiver with known channels are close to the BER lower bound. This indicates that the approximation in (4.50) may be

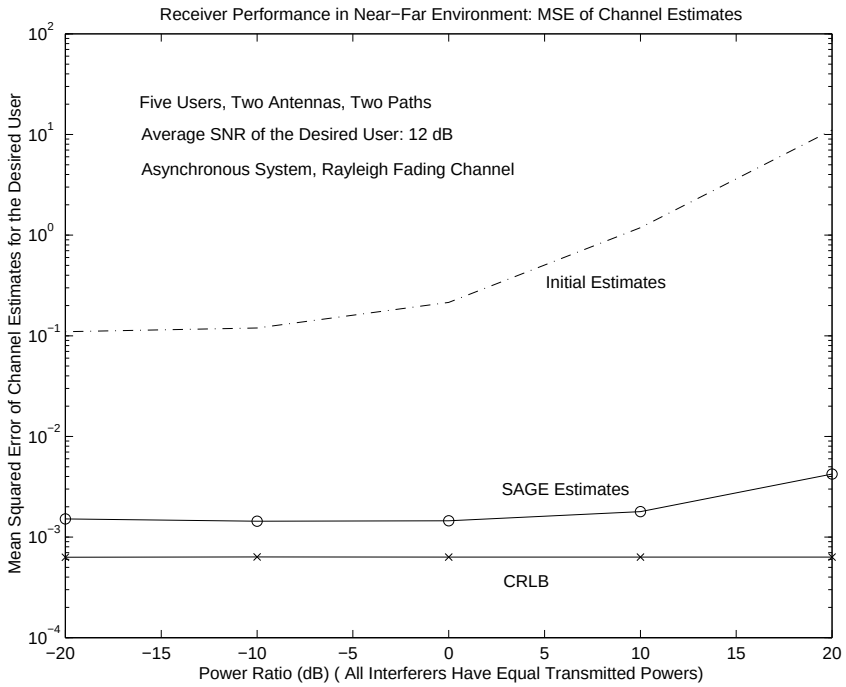

Figure 4.9: Mean Squared Error of Channel Estimates of the SAGE-based Receiver in Near-far Environment

reasonable.

BER convergence examples of the SAGE-based receiver are provided in Figure 4.10 for equal transmitted power and in Figure 4.11 for unequal transmitted power, respectively. In Figure 4.10, we consider a system with a three-element antenna array over two dominant path channels. The convergence of the receiver is very fast. After three iterations, we can obtain an acceptable BER level. Figure 4.11 illustrates the simulation results for a system with a two-element antenna array over two-path fading channels. We observe that when the multi-access interference becomes stronger, the convergence is slower.

In the previous examples, we assume that the relative time delays are known at the receiver. The final two examples are used to study imperfect time delay estimation effects on the SAGE-based receiver. We consider a four-user system with a two-element base-station antenna array over two-path Rayleigh fading channels. The timing errors are assumed to be uniformly distributed in $[-T_c/d, T_c/d]$, where

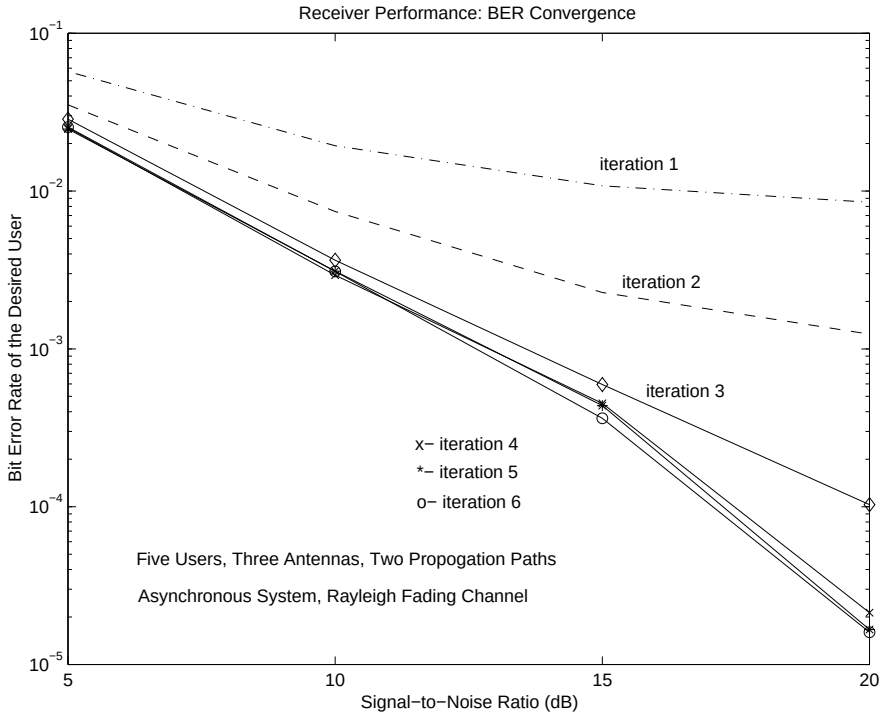

Figure 4.10: BER Convergence of the Proposed Receiver

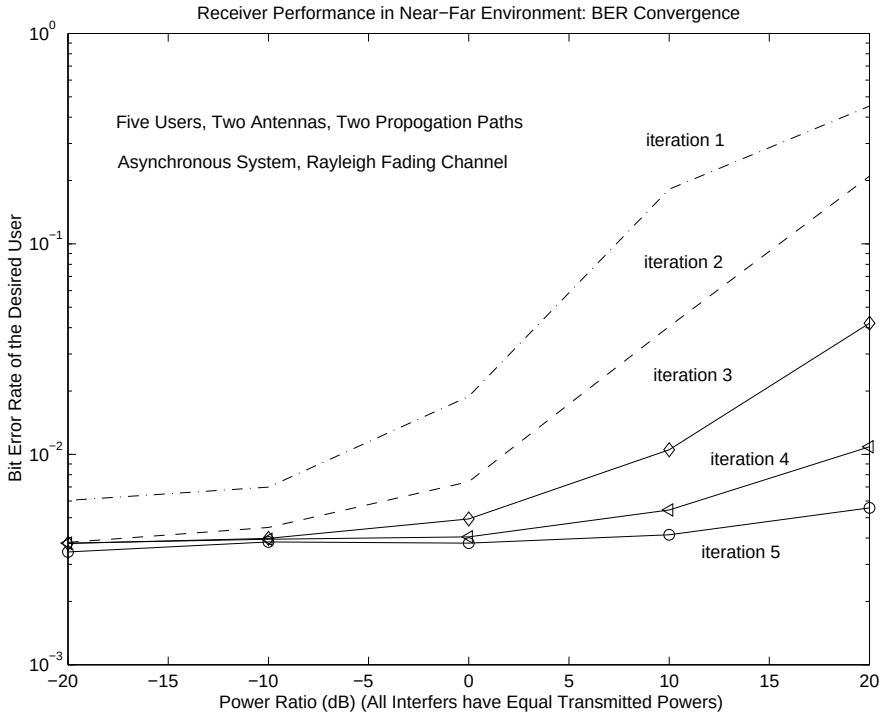

Figure 4.11: BER Convergence of the Proposed Receiver in Near-Far Environment

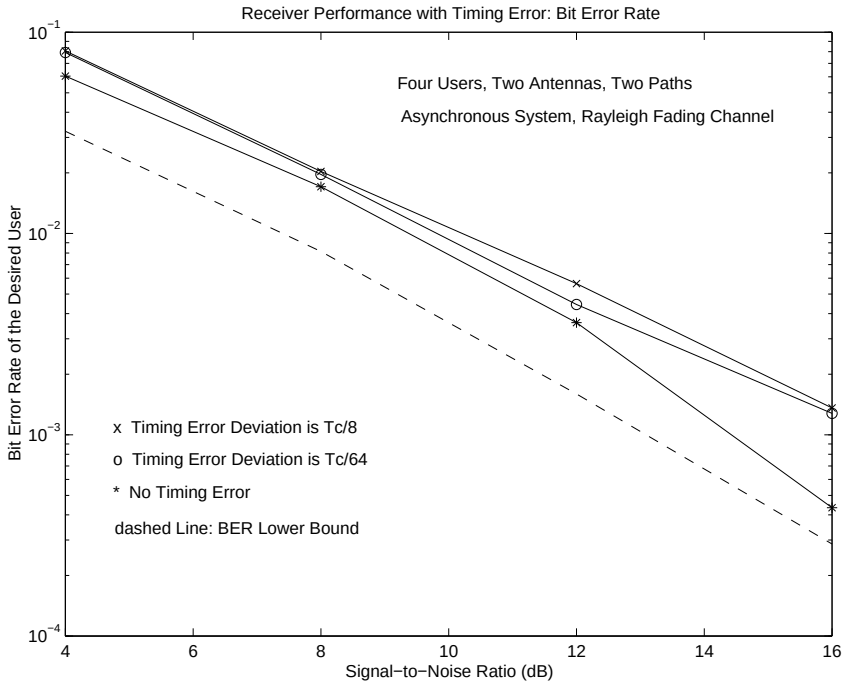

Figure 4.12: Timing Error Effect on BER Performance for the SAGE-Based Receiver

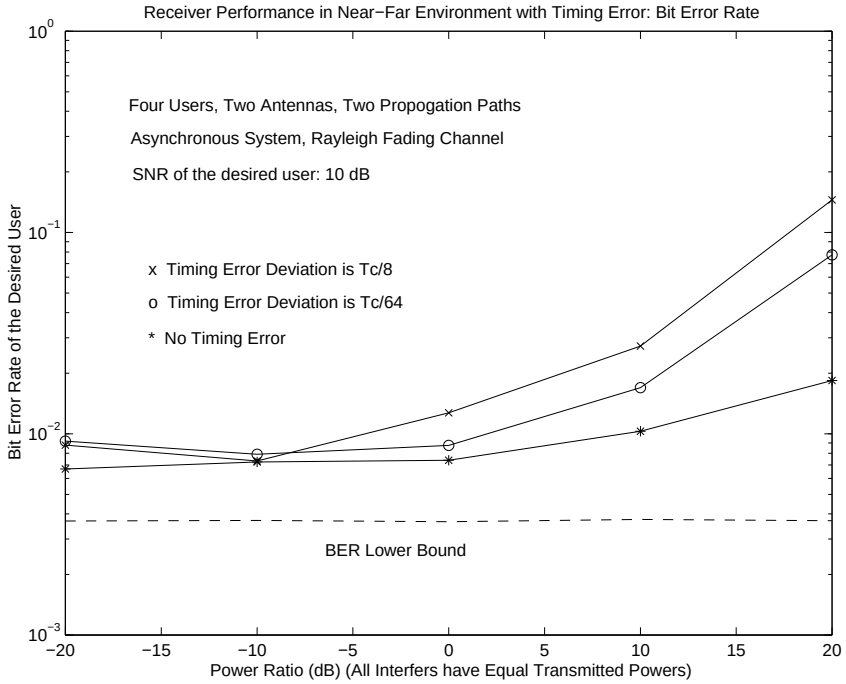

Figure 4.13: Timing Error Effect on BER Performance for the SAGE-Based Receiver in Near-Far Environment

T_c/d denotes the maximum timing error deviation. We use four and five iterations to obtain the results in Figures 4.12 and 4.13, respectively. Figure 4.12 shows the timing error effect on a system where all users have equal transmitted power. We observe that the BER performance degradation in low SNR regions due to timing errors is not significant. However, in near-far environments, BER performance becomes worse due to timing errors when the transmitted powers of the interferers get very large, as shown in Figure 4.13. Therefore, accurate time delay estimation methods are needed to make the SAGE-based receiver maintain near-far resistance. In [15], the root mean squared error (RMSE) of timing estimates is reported to be less than $0.01T_c$ using the EM algorithm for CDMA systems without a base-station antenna array. Incorporating time delay estimation into the receiver developed in Section 4.4 is a subject of future work which is discussed in Chapter 6.

4.7 Conclusions

In this chapter, we developed a synchronous equivalent discrete-time system model for asynchronous multipath CDMA systems with base-station antenna arrays. The spatial and temporal channel matrices are identified. Based on this model, we incorporated a maximal-ratio multipath combiner into the spatial-temporal decorrelator for known channels. Asymptotic efficiency is analyzed and the numerical results show that unlike base-station antenna arrays, multipath diversity does not improve a detector's asymptotic efficiency. The SAGE algorithm is applied to the synchronous equivalent model to derive an iterative receiver for joint channel array response vector estimation and bit sequence detection assuming that the relative time delays are known perfectly. A BER lower bound is derived to measure the receiver's performance. Simulation results show that the SAGE-based receiver is near-far resistant, its BER performance converges to the spatial-temporal decorrelating receiver (when all channel parameters are known) and the simulated BER is close to the derived lower bound. The mean squared error of the channel estimates used by the SAGE-based

receiver is close to the CRLB. Timing error effects on the SAGE-based receiver are studied by simulation. It is observed that the BER performance degradation due to timing error is not significant in the low SNR region when the transmitted powers for all users are equivalent. However, the near-far resistance of the SAGE-based receiver does suffer from timing errors.

Chapter 5

Iterative Multi-User Receiver for Multi-Rate Systems

5.1 Introduction

Future wireless communications systems aim at offering multi-rate transmission services such as voice, data and video. The proposed next generation CDMA standard, CDMA2000, will support the combination of voice and packet data transmission [87]. To provide integrated multi-rate communications, several multi-rate multi-access strategies have been studied [25] [50] [72]

1. Multi-code access

2. Fixed chip rate, variable processing gain

3. Fixed processing gain, variable chip rate

The multi-code access method multiplexes the high-rate user's transmitted bit sequences onto multiple low rate spreading codes. As a result, the bits from a high rate user are transmitted in parallel at the same rate as that of the low rate users. In the multi-code access strategy, all users have the same processing gain and each high-rate user can virtually be viewed as r low-rate users, where r is the ratio between transmission rates for high rate users and low rate users.

In fixed chip-rate, variable processing-gain access systems, all users have the same chip rate. Thus, the processing gain for higher-rate users is smaller than that for the lower-rate users. In contrast, in fixed processing gain, variable chip rate access systems, the processing gain for all users is constant and the chip rate for high rate users is higher than that for low rate users.

In [50], it is shown that multi-access strategy 2 can achieve better bit detection performance in terms of asymptotic efficiencyfor high-rate users for realistic spreading code cross-correlation values than strategy 1 using m-sequences and equi-correlated PN codes. Performance for low-rate users is comparable in these two multi-access systems. For access strategy 3, the receiver has to be synchronized to different rates and the system needs additional frequency planning due to the unequal bandwidth spreading of different rate users. It has been shown that access strategy 2 is more efficient than access method 3 [73]. Therefore, we will only consider access method 2 - fixed chip rate, variable processing gain.

Multi-user signal detection approaches for multi-rate systems have been proposed in [50] [72] [73] [74] for synchronous AWGN channels. A multi-user multi-rate decorrelator is proposed in [75] for asynchronous AWGN channels with known parameters and single antenna case. In this chapter, we investigate joint bit sequence detection and channel array response vector estimation for dual rate systems with base-station antenna arrays over asynchronous multipath fading channels. We extend multi-user decoupling techniques developed in the previous chapters to multi-rate systems.

We first formulate a synchronous-equivalent discrete-time model for dual rate asynchronous systems in Section 5.2 based on the technique in the previous chapter. A joint bit sequence detection and channel estimation receiver is derived in Section 5.3 by applying the SAGE algorithm to the synchronous equivalent discrete-time system model. Simulation results are provided in Section 5.4.

5.2 Discrete-Time Dual-Rate System Formulation

5.2.1 Received Dual Rate Signal

We consider a dual-rate transmission system with an M-element base-station antenna array over asynchronous multipath fading channels. The K users are grouped into K_h high rate users and K_l low rate users, where $K = K_h + K_l$. We assume that the chip rates are the same for the two groups of users, i.e., both groups of users have the same chip duration T_c. From here on, the subscripts h and l denote parameters for high rate and low rate users, respectively.

From (2.17), an N_h-bit transmitted signal from the k_h-th high rate user is given by

$$s_{k_h}(t) = A_{k_h} \sum_{i_h=1}^{N_h} b_{k_h}(i_h) c_{k_h}(t - i_h T_h) \tag{5.1}$$

where A_{k_h} is the amplitude of the k_h-th high rate user, $b_{k_h}(i_h) \in \{-1, 1\}$ is the i_h-th transmitted bit of the k_h-th user with equal probability and $c_{k_h}(t)$ has normalized energy $\int_0^{T_h} |c_{k_h}(t)|^2 dt = 1$, and represents the spreading waveform of the k_h-th high rate user, which is given by

$$c_{k_h}(t) = \sum_{l_h=0}^{L_h-1} c_{k_h l_h} p_h(t - l_h T_c) \tag{5.2}$$

where $c_{k_h l_h} \in \{+1, -1\}$ $(l_h = 0 \cdots L_h - 1)$ is the spreading code corresponding to the k_h-th high rate user, T_h is the high rate user's bit interval and the processing gain L_h of the high rate users is $L_h = T_h/T_c$

Similarly, the transmitted signal from the k_l-th low rate user is expressed as

$$s_{k_l}(t) = A_{k_l} \sum_{i_l=1}^{N_l} b_{k_l}(i_l) c_{k_l}(t - i_l T_l) \tag{5.3}$$

where A_{k_l}, $b_{k_l}(i_l) \in \{-1, 1\}$ and $c_{k_l}(t)$ are the k_l-th low rate user's transmitted amplitude, the i_l-th transmitted bit with equal probability and the corresponding spreading waveform with normalized energy, respectively. $c_{k_l}(t)$ is given by

$$c_{k_l}(t) = \sum_{l_l=0}^{L_l-1} c_{k_l l_l} p_l(t - l_l T_c) \tag{5.4}$$

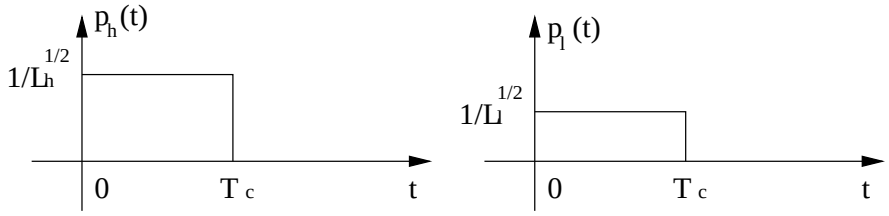

Figure 5.1: Chip Waveforms for High Rate Users and Low Rate Users

where $c_{k_l l_l} \in \{+1, -1\}$ $(l_l = 0 \cdots L_l - 1)$ is the spreading code. The processing gain L_l of low rate users is $L_l = T_l/T_c$, where T_l is the low rate user's bit interval. Since we assume that the spreading waveforms have normalized energy for both high rate and low rate users, the chip waveforms, $p_h(t)$ and $p_l(t)$, for high rate and low rate users have different amplitude, as illustrated in Figure 5.1. The average SNRs per bit for high rate and low rate users are therefore identical.

The total number of active users in the system is $K = K_h + K_l$. We assume that the information bits from all K users are independent and the spreading code sequences for all K users are mutually independent. The transmission rate of the low rate users is $1/T_l$, and the transmission rate of the high rate user is $1/T_h$. Define the rate-ratio to be

$$r = \frac{T_l}{T_h} \tag{5.5}$$

In the following, we assume that the rate-ratio r is an integer.

We assume that the propagation fading channels are asynchronous and contain multipath, and the channel parameters remain unchanged during the N_l-bit transmission. The received composite signal vector at the base-station antenna array is expressed as

$$\mathbf{x}(t) = \mathbf{x}_h(t) + \mathbf{x}_l(t) + \mathbf{n}(t) \tag{5.6}$$

where $\mathbf{x}_h(t)$ is the received signal from K_h high rate users (refer to Section 2.3.3)

$$\mathbf{x}_h(t) = \sum_{k_h=1}^{K_h} \mathbf{x}_{k_h}(t) = \sum_{k_h=1}^{K_h} \sum_{i_h=1}^{N_h} \sum_{p=1}^{P} \mathbf{f}_{k_h,p} c_{k_h}(t - i_h T_h - \tau_{k_h,p}) b_{k_h}(i_h) \tag{5.7}$$

and $\mathbf{x}_l(t)$ is the received signal from K_l low rate users

$$\mathbf{x}_l(t) = \sum_{k_l=1}^{K_l} \mathbf{x}_{k_l}(t) = \sum_{k_l=1}^{K_l} \sum_{i_l=1}^{N_l} \sum_{p=1}^{P} \mathbf{f}_{k_l,p} c_{k_l}(t - i_l T_l - \tau_{k_l,p}) b_{k_l}(i_l) \tag{5.8}$$

where $\tau_{k_h,p}$ is the time delay of the k_h-th high rate user through the pth propagation path, $\mathbf{f}_{k_h,p}$ is the corresponding channel array response vector with channel fading attenuation $\alpha_{k_h,p}$ and direction-of-arrival (DOA) $\theta_{k_h,p}$

$$\mathbf{f}_{k_h,p} = A_{k_h} \alpha_{k_h,p} \mathbf{a}(\theta_{k_h,p}) \tag{5.9}$$

$\tau_{k_l,p}$ and $\mathbf{f}_{k_l,p}$ are the counterparts for the low rate users and $\mathbf{f}_{k_l,p}$ is given by

$$\mathbf{f}_{k_l,p} = A_{k_l} \alpha_{k_l,p} \mathbf{a}(\theta_{k_l,p}) \tag{5.10}$$

$\mathbf{n}(t)$ is the complex additive white Gaussian noise vector with zero mean and covariance matrix $\sigma^2 \mathbf{I}_M$, where $\mathbf{I}_M$ is an $M \times M$ identity matrix.

5.2.2 Synchronous-Equivalent Discrete-Time Formulation

In this section, we extend the results in Section 4.2 for single-rate systems to dual-rate systems and formulate a synchronous-equivalent discrete-time system model for dual-rate multipath CDMA systems. For simplicity and without loss of generality, we assume $\tau_{k_h,p}, \tau_{k_l,p} \in [0, T_h)$ for $k_h \in \{1, \cdots, K_h\}$ and $k_l \in \{1, \cdots, K_l\}$ and $p \in \{1, \cdots, P\}$. Figure 5.2 illustrates an example of asynchronous received bits for a dual rate system with rate-ratio 4. In this case, one complete bit of each transmission falls in a time interval of length $T_h + T_l$ for low rate users. Therefore, we can choose $T_h + T_l$ to be the observation interval to collect samples of each bit for low rate users. In this observation interval, we obtain samples of r complete bits for high rate users. We sample the received signal at the chip rate after a filter matched to the chip waveform of the low rate users, $p_l(t)$. Then, for $m = 1, \cdots, M$ and $i = 1, \cdots, N$, we obtain the sample at the gth chip interval

$$x^m(i,g) = \int_{t=gT_c}^{(g+1)T_c} x^m(t) p_l^*(t) dt \tag{5.11}$$

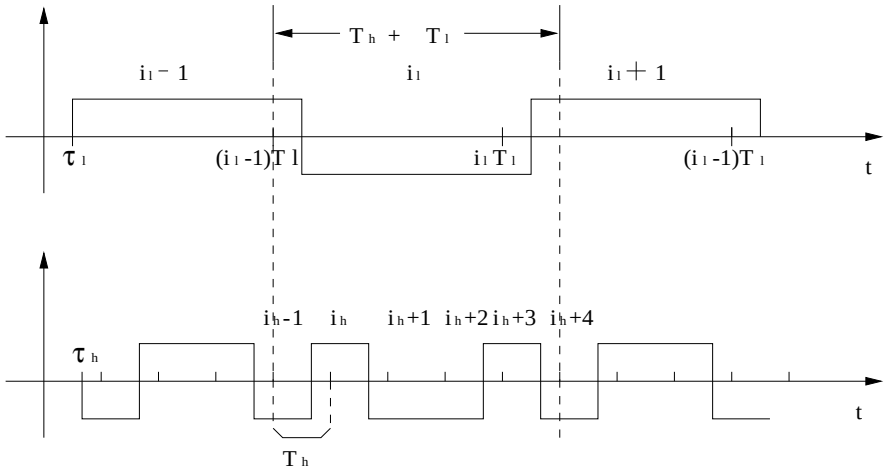

Figure 5.2: Received bits for a dual rate system

Then, for each observation interval, we obtain $L_h + L_l$ samples from each antenna element. For notational simplicity, we denote $L_d = L_h + L_l$.

We denote

$$\tau_{k_h,p} = (u_{k_h,p} + v_{k_h,p})T_c \tag{5.12}$$

and

$$\tau_{k_l,p} = (u_{k_l,p} + v_{k_l,p})T_c \tag{5.13}$$

where $u_{k_h,p}$ and $u_{k_l,p}$ are integers that take on values from $\{0, \cdots, L_h - 1\}$, $v_{k_h,p}$ and $v_{k_l,p}$ are fractions of T_c for $k_h \in \{1, \cdots, K_h\}$, $k_l \in \{1, \cdots, K_l\}$ and $p \in \{1, \cdots, P\}$. Denote the L_d-dimensional column vectors

$$\mathbf{c}_{k_h} = \frac{1}{\sqrt{L_h L_l}}[c_{k_h 0}\ c_{k_h 1}\ \cdots\ c_{k_h (L_h-1)}\ \underbrace{0\ \cdots\ 0}_{L_l - zeros}]^T \tag{5.14}$$

and

$$\mathbf{c}_{k_l} = \frac{1}{L_l}[c_{k_l 0}\ c_{k_l 1}\ \cdots\ c_{k_l (L_l-1)}\ \underbrace{0\ \cdots\ 0}_{L_h - zeros}]^T \tag{5.15}$$

Using the technique in Section 4.2, we obtain temporal spreading vectors for low rate users

$$\mathbf{c}^{-1}_{k_l,p} = (1 - v_{k_l,p})\mathbf{T}_L^{L_l - u_{k_l,p}}\mathbf{c}_{k_l} + v_{k_l,p}\mathbf{T}_L^{L_l - u_{k_l,p} - 1}\mathbf{c}_{k_l} \tag{5.16}$$

$$\mathbf{c}^{0}_{k_l,p} = (1 - v_{k_l,p})\mathbf{T}_R^{u_{k_l,p}}\mathbf{c}_{k_l} + v_{k_l,p}\mathbf{T}_R^{u_{k_l,p}+1}\mathbf{c}_{k_l} \tag{5.17}$$

$$\mathbf{c}^1_{k_l,p} = (1 - v_{k_l,p})\mathbf{T}_R^{L_l+u_{k_l,p}}\mathbf{c}_{k_l} + v_{k_l,p}\mathbf{T}_R^{L_l+u_{k_l,p}+1}\mathbf{c}_{k_l} \tag{5.18}$$

where $\mathbf{T}_L$ and $\mathbf{T}_R$ are the acyclic left shift operator and right shift operator, respectively defined in Section 4.2.1. Then, we obtain the following matrix for low rate users for $n \in \{-1, 0, 1\}$

$$C^n_{k_l,p} = \underbrace{\begin{bmatrix} \mathbf{c}^n_{k_l,p} & \cdots & \mathbf{0} \\ \vdots & \ddots & \vdots \\ \mathbf{0} & \cdots & \mathbf{c}^n_{k_l,p} \end{bmatrix}}_{M-columns} \tag{5.19}$$

Similar to the case of single rate systems, the $ML_d \times 3M$ temporal channel matrix for low rate users for $k_l = 1, \cdots, K_l$ and $p = 1, \cdots, P$ can be expressed as

$$C_{k_l,p} = [C^{-1}_{k_l,p} \vdots C^0_{k_l,p} \vdots C^1_{k_l,p}] \tag{5.20}$$

The corresponding $3M \times 3$ spatial matrices for low rate users are given by

$$F_{k_l,p} = \begin{bmatrix} \mathbf{f}_{k_l,p} & \mathbf{0} & \mathbf{0} \\ \mathbf{0} & \mathbf{f}_{k_l,p} & \mathbf{0} \\ \mathbf{0} & \mathbf{0} & \mathbf{f}_{k_l,p} \end{bmatrix} \tag{5.21}$$

The spatial temporal channel matrix for low rate users, for $k_l = 1, \cdots, K_l$ and $p = 1, \cdots, P$, is then given by

$$H_{k_l,p} = C_{k_l,p}F_{k_l,p} \tag{5.22}$$

Denoting the sliding window bit vectors for the i_l-th bit of the k_l-th low rate user as

$$\mathbf{b}^w_{k_l}(i_l) = [b_{k_l}(i_l - 1) \;\; b_{k_l}(i_l) \;\; b_{k_l}(i_l + 1)]^T \tag{5.23}$$

the received discrete-time signal vector (ML_d-dimensional) at the i_l-th bit interval from the low rate users is given by

$$\mathbf{x}_l(i_l) = \sum_{k_l=1}^{K_l} H_{k_l}\mathbf{b}^w_{k_l}(i_l) \tag{5.24}$$

where

$$H_{k_l} = \sum_{p=1}^{P} H_{k_l,p} \tag{5.25}$$

From Figure 5.2, it is observed that r consecutive bits $(b_{k_h}(i_h), b_{k_h}(i_h+1), \cdots, b_{k_h}(i_h+r-1))$ completely lie in the observation interval $T_h + T_l$, and bits $b_{k_h}(i_h-1)$ and $b_{k_h}(i_h+r)$ lie partially in this interval and interfere with the r desired bits. Our goal is to detect $b_{k_h}(i_h)$, $b_{k_h}(i_h+1), \cdots, b_{k_h}(i_h+r-1)$ in the i_l-th observation interval. Referring to (4.12), the sampled data during the observation interval from the mth antenna element can be expressed as an L_d-dimensional column vector for $k_h = 1, \cdots, K_h$, and $m = 1, \cdots, M$

$$\mathbf{x}_{k_h}^m(i_l) = \sum_{p=1}^{P} \{\mathbf{h}_{k_h,p}^{-1,m} b_{k_h}(i_h-1) + \mathbf{h}_{k_h,p}^{0,m} b_{k_h}(i_h) + \cdots + \mathbf{h}_{k_h,p}^{r-1,m} b_{k_h}(i_h+r-1) + \mathbf{h}_{k_h,p}^{r,m} b_{k_h}(i_h+r)\} \tag{5.26}$$

where

$$\mathbf{h}_{k_h,p}^{-1,m} = f_{k_h,p}^m \mathbf{c}_{k_h,p}^{-1}$$

$$\mathbf{h}_{k_h,p}^{0,m} = f_{k_h,p}^m \mathbf{c}_{k_h,p}^{0}$$

$$\mathbf{h}_{k_h,p}^{r_1,m} = f_{k_h,p}^m \mathbf{c}_{k_h,p}^{r_1}, \quad \text{for } r_1 = 1, \cdots, r$$

and the temporal spreading vectors for high-rate users are given by

$$\mathbf{c}_{k_h,p}^{-1} = (1 - v_{k_h,p}) \mathbf{T}_L^{L_h - u_{k_h,p}} \mathbf{c}_{k_h} + v_{k_h,p} \mathbf{T}_L^{L_h - u_{k_h,p} - 1} \mathbf{c}_{k_h} \tag{5.27}$$

$$\mathbf{c}_{k_h,p}^{0} = (1 - v_{k_h,p}) \mathbf{T}_R^{u_{k_h,p}} \mathbf{c}_{k_h} + v_{k_h,p} \mathbf{T}_R^{u_{k_h,p}+1} \mathbf{c}_{k_h} \tag{5.28}$$

for $r_1 = 1, \cdots, r$

$$\mathbf{c}_{k_h,p}^{r_1} = (1 - v_{k_h,p}) \mathbf{T}_R^{r_1 L_h + u_{k_h,p}} \mathbf{c}_{k_h} + v_{k_h,p} \mathbf{T}_R^{r_1 L_h + u_{k_h,p}+1} \mathbf{c}_{k_h} \tag{5.29}$$

We express the temporal spreading vectors of the high-rate users in matrix form for $n \in \{-1, 0, 1, \cdots, r\}$

$$C_{k_h,p}^n = \underbrace{\begin{bmatrix} \mathbf{c}_{k_h,p}^n & \cdots & \mathbf{0} \\ \vdots & \ddots & \vdots \\ \mathbf{0} & \cdots & \mathbf{c}_{k_h,p}^n \end{bmatrix}}_{M-columns} \tag{5.30}$$

Following the same procedure as in Section 4.2.2, the $ML_d \times (r+2)M$ temporal channel matrix of high-rate users is written as

$$C_{k_h,p} = \begin{bmatrix} C_{k_h,p}^{-1} & \vdots & C_{k_h,p}^{0} & \vdots & \cdots & \vdots & C_{k_h,p}^{r} \end{bmatrix} \tag{5.31}$$

and the corresponding $(r+2)M \times (r+2)$ spatial matrix for high-rate users is given by

$$F_{k_h,p} = \underbrace{\begin{bmatrix} \mathbf{f}_{k_h,p} & \cdots & \mathbf{0} \\ \vdots & \ddots & \vdots \\ \mathbf{0} & \cdots & \mathbf{f}_{k_h,p} \end{bmatrix}}_{(r+2)-columns} \tag{5.32}$$

Thus, the spatial temporal channel matrix corresponding to the high-rate users, for $k_h = 1, \cdots, K_h$ and $p = 1, \cdots, P$, is written as

$$H_{k_h,p} = C_{k_h,p} F_{k_h,p} \tag{5.33}$$

Denoting the $r+2$ dimensional sliding window bit vectors for the high-rate users during the i_l-th observation interval

$$\mathbf{b}_{k_h}^w(i_l) = [b_{k_h}(i_h - 1) \;\; b_{k_h}(i_h) \;\; \cdots \;\; b_{k_h}(i_h + r)]^T$$

the received discrete-time signal vector at the i_l-th observation interval from the high-rate users is given by

$$\mathbf{x}_h(i_l) = \sum_{k_h=1}^{K_h} H_{k_h} \mathbf{b}_{k_h}^w(i_l) \tag{5.34}$$

where

$$H_{k_h} = \sum_{p=1}^{P} H_{k_h,p} \tag{5.35}$$

The composite discrete-time signal vector from both high-rate and low-rate users at the i_l-th observation interval is expressed as

$$\mathbf{x}(i_l) = \mathbf{x}_l + \mathbf{x}_h + \mathbf{n}(i_l) = \sum_{k_h=1}^{K_h} H_{k_h} \mathbf{b}_{k_h}^w(i_l) + \sum_{k_l=1}^{K_l} H_{k_l} \mathbf{b}_{k_l}^w(i_l) + \mathbf{n}(i_l) \tag{5.36}$$

where $\mathbf{n}(i_l)$ is the AWGN after sampling with zero mean and covariance $\frac{\sigma^2}{L_d}\mathbf{I}_{ML_d}$.

5.3 Iterative Dual-Rate Receiver

In this section, we derive an iterative receiver structure for the dual rate systems. We assume that the relative time delays are known at the receiver. Applying the SAGE

algorithm to our synchronous equivalent discrete-time model, we obtain joint channel array response vector estimation and bit sequence detection for both high-rate and low-rate users.

5.3.1 Receiver Derivation

We first decouple the received signal using the technique developed in Section 4.4. We choose user index as the index set for multi-user signal decoupling. For high-rate user k_h, for $k_h = 1, \cdots, K_h$, the hidden-data is given by

$$\mathbf{x}^S_{k_h}(i_l) = H_{k_h}\mathbf{b}^w_{k_h}(i_l) + \mathbf{n}(i_l) = \sum_{p=1}^{P} H_{k_h,p}\mathbf{b}^w_{k_h} + \mathbf{n}(i_l) \tag{5.37}$$

The hidden-data corresponding to the low-rate users is, for $k_l = 1, \cdots, K_l$,

$$\mathbf{x}^S_{k_l}(i_l) = H_{k_l}\mathbf{b}^w_{k_l}(i_l) + \mathbf{n}(i_l) = \sum_{p=1}^{P} H_{k_l,p}\mathbf{b}^w_{k_l} + \mathbf{n}(i_l) \tag{5.38}$$

Given the spatial matrix estimates and bit detection results at the jth iteration for all the users except for the k_h-th high rate user, the conditional expectation of $\mathbf{x}^S_{k_h}(i_l)$, for $k_h = 1, \cdots, K_h$ and $i_l = 1, \cdots, N_l$, is obtained as

$$\hat{\mathbf{x}}^S_{k_h}(i_l) = \mathbf{x}(i_l) - \sum_{k_1=1, k_1\neq k_h}^{K_h}\sum_{p=1}^{P} \hat{H}^j_{k_1,p}\hat{\mathbf{b}}^{wj}_{k_1}(i_l) - \sum_{k_l=1}^{K_l}\sum_{p=1}^{P} \hat{H}^j_{k_l,p}\hat{\mathbf{b}}^{wj}_{k_l}(i_l) \tag{5.39}$$

Similarly, the conditional expectation of $\mathbf{x}^S_{k_l}(i_l)$, for $k_l = 1, \cdots, K_l$ and $i_l = 1, \cdots, N_l$, is given by

$$\hat{\mathbf{x}}^S_{k_l}(i_l) = \mathbf{x}(i_l) - \sum_{k_1=1, k_1\neq k_l}^{K_l}\sum_{p=1}^{P} \hat{H}^j_{k_1,p}\hat{\mathbf{b}}^{wj}_{k_1}(i_l) - \sum_{k_h=1}^{K_h}\sum_{p=1}^{P} \hat{H}^j_{k_h,p}\hat{\mathbf{b}}^{wj}_{k_h}(i_l) \tag{5.40}$$

where $\hat{H}^j_{k_h,p} = C_{k_h,p}\hat{F}^j_{k_h,p}$ and $\hat{H}^j_{k_l,p} = C_{k_l,p}\hat{F}^j_{k_l,p}$ for $k_h = 1, \cdots, K_h$, $k_l = 1, \cdots, K_l$ and $p = 1, \cdots, P$.

Using the approach in Section 4.4, we further decouple the multipath signals for high-rate and low-rate users, respectively, for $k_h = 1, \cdots, K_h$, $k_l = 1, \cdots, K_l$ and $i_l = 1, \cdots, N_l$,

$$\mathbf{x}^S_{k_h,p}(i_l) = H_{k_h,p}\mathbf{b}^w_{k_h} + \mathbf{n}(i_l) \tag{5.41}$$

$$\mathbf{x}_{k_l,p}^{S}(i_l) = H_{k_l,p}\mathbf{b}_{k_l}^{w} + \mathbf{n}(i_l) \tag{5.42}$$

The conditional expectations of $\mathbf{x}_{k_h,p}^{S}(i_l)$ and $\mathbf{x}_{k_l,p}^{S}(i_l)$, for $k_h = 1,\cdots,K_h$, $k_l = 1,\cdots,K_l$, $p = 1,\cdots,P$ and $i_l = 1,\cdots,N_l$, are given by

$$\hat{\mathbf{x}}_{k_h,p}^{S}(i_l) = \hat{\mathbf{x}}_{k_h}^{S}(i_l) - \sum_{p_1=1,p_1\neq p}^{P} \hat{H}_{k_h,p_1}\mathbf{b}_{k_h}^{w}$$

and

$$\hat{\mathbf{x}}_{k_l,p}^{S}(i_l) = \hat{\mathbf{x}}_{k_l}^{S}(i_l) - \sum_{p_1=1,p_1\neq p}^{P} \hat{H}_{k_l,p_1}\mathbf{b}_{k_l}^{w}$$

The maximum-likelihood channel array response vector estimates and detected bit sequences are obtained by the same procedure as in Section 4.4.

The SAGE-based iterative channel array response vector estimation and bit sequence detection is summarized as follows:

for $j = 1, 2\cdots$

$k = (j \text{ modulo } K)$

E-step: compute the conditional expectation of hidden-data

if k is corresponding to high rate user k_h

for $i_l = 1,\cdots,N_l$

$$\hat{\mathbf{x}}_{k_h}^{S^{(j+1)}}(i_l) = \mathbf{x}(i_l) - \sum_{k_1=1,k_1\neq k_h}^{K_h}\sum_{p=1}^{P} C_{k_1,p}\hat{F}_{k_1,p}^{j}\hat{\mathbf{b}}_{k_1}^{wj}(i_l) - \sum_{k_l=1}^{K_l}\sum_{p=1}^{P}\hat{H}_{k_l,p}^{j}\hat{\mathbf{b}}_{k_l}^{wj}(i_l) \tag{5.43}$$

for $p = 1,\cdots,P$

$$\hat{\mathbf{x}}_{k_h,p}^{Sj}(i_l) = \hat{\mathbf{x}}_{k_h}^{S^{(j+1)}}(i_l) - \sum_{p_1=1,p_1\neq p}^{P} C_{k_h,p_1}\hat{F}_{k_h,p_1}^{j}\mathbf{b}_{k_h}^{wj}(i_l) \tag{5.44}$$

if k is corresponding to low rate user k_l

for $i_l = 1,\cdots,N_l$

$$\hat{\mathbf{x}}_{k_l}^{S^{(j+1)}}(i_l) = \mathbf{x}(i_l) - \sum_{k_1=1,k_1\neq k_l}^{K_l}\sum_{p=1}^{P} C_{k_1,p}\hat{F}_{k_1,p}^{j}\hat{\mathbf{b}}_{k_1}^{wj}(i_l) - \sum_{k_h=1}^{K_h}\sum_{p=1}^{P}\hat{H}_{k_h,p}^{j}\hat{\mathbf{b}}_{k_h}^{wj}(i_l) \tag{5.45}$$

for $p = 1, \cdots, P$

$$\hat{\mathbf{x}}_{k_l,p}^{Sj}(i_l) = \hat{\mathbf{x}}_{k_l}^{S^{(j+1)}}(i_l) - \sum_{p_1=1, p_1 \neq p}^{P} C_{k_l,p_1} \hat{F}_{k_l,p_1}^{j} \mathbf{b}_{k_l}^{wj}(i_l) \tag{5.46}$$

M-step: compute the channel array response vector estimates

for the high-rate user, compute $\hat{\mathbf{f}}_{k_h,p}$

for $p = 1, \cdots, P$

$$\hat{F}_{k_h,p} = (C_{k_h,p}^H C_{k_h,p})^{-1} C_{k_h,p}^H \sum_{i=1_l}^{N_l} \hat{\mathbf{x}}_{k_h,p}^{Sj}(i_l) \hat{\mathbf{b}}_{k_l}^{wjH}(i_l)][\sum_{i=1_l}^{N_l} \hat{\mathbf{b}}_{k_h}^{wj}(i_l) \hat{\mathbf{b}}_{k_h}^{wjH}(i_l)]^{-1} \tag{5.47}$$

for low rate user, compute $\hat{\mathbf{f}}_{k_l,p}$

for $p = 1, \cdots, P$

$$\hat{F}_{k_l,p} = (C_{k_l,p}^H C_{k_l,p})^{-1} C_{k_l,p}^H \sum_{i=1_l}^{N_l} \hat{\mathbf{x}}_{k_l,p}^{Sj}(i_l) \hat{\mathbf{b}}_{k_l}^{wjH}(i_l)][\sum_{i=1_l}^{N_l} \hat{\mathbf{b}}_{k_l}^{wj}(i_l) \hat{\mathbf{b}}_{k_l}^{wjH}(i_l)]^{-1} \tag{5.48}$$

detect the bit,

for the high-rate user, obtain $\hat{b}_{k_h}(i_l)$,

$k_h = 1, \cdots, K_h$ and $i_l = 1, \cdots, N_l$

$$\hat{\mathbf{b}}_{k_h}^{wj+1}(i_l) = \text{sign}[(\hat{\mathcal{R}}_{k_h k_h}^{j+1})^{-1} \hat{H}_{k_h}^{j+1^H} \hat{\mathbf{x}}_{k_h}^{Sj}(i_l)] \tag{5.49}$$

for the low-rate user, obtain $\hat{b}_{k_l}(i_l)$,

$$\hat{\mathbf{b}}_{k_l}^{wj+1}(i_l) = \text{sign}[(\hat{\mathcal{R}}_{k_l k_l}^{j+1})^{-1} \hat{H}_{k_l}^{j+1^H} \hat{\mathbf{x}}_{k_l}^{Sj}(i_l)] \tag{5.50}$$

$$\begin{aligned} \hat{F}_{k',p}^{j+1} &= \hat{F}_{k',p}^{j}, && k' \neq k \in \{1, \cdots, K_h, 1, \cdots, K_l\} \\ \hat{\mathbf{b}}_{k'}^{wj+1}(i_l)) &= \hat{\mathbf{b}}_{k'}^{wj}(i_l), && k' \neq k \in \{1, \cdots, K_h, 1, \cdots, K_l\} \end{aligned}$$

The convergence of the SAGE-based iterative receiver has been studied in Chapter 3 and verified by simulation in Chapter 4.

5.3.2 Simplified Bit Detection for Wideband CDMA Systems

The information bit detector in (5.49) has multipath interference decorrelation via $(\hat{\mathcal{R}}_{k_h k_h}^{j+1})^{-1}$ which requires $(r+2) \times (r+2)$ matrix inversion. When the rate-ratio r is large, the $O(r^3)$ computational complexity of the matrix inverse will be very high. Since the differences between the relative time delays for different paths are larger than the chip interval for high processing gain (i.e. wideband) CDMA systems, the despreading process can resolve the received signals from different paths for each user. Although the decorrelation via $(\hat{\mathcal{R}}_{k_h k_h}^{j+1})^{-1}$ is eliminated, the despread signals from different paths are still combined to suppress multipath interference and take advantage of time diversity. Therefore, it is expected that a simplified bit detector without a multipath decorrelator would suffer from very little performance degradation in wideband CDMA, since the multipath delay spread is larger than a chip interval.

The algorithm in Section 5.3.1 is modified as follows: the high-rate user signal detector in (5.49) is replaced by

$$\hat{\mathbf{b}}_{k_h}^{wj+1}(i_l) = \text{sign}[\hat{H}_{k_h}^{j+1^H} \hat{\mathbf{x}}_{k_h}^{Sj}(i_l)] \tag{5.51}$$

For the case of the low-rate user signal detector in (5.50), a 3×3 matrix inversion can be avoided by replacing (5.50) by

$$\hat{\mathbf{b}}_{k_l}^{wj+1}(i_l) = \text{sign}[\hat{H}_{k_l}^{j+1^H} \hat{\mathbf{x}}_{k_l}^{Sj}(i_l)] \tag{5.52}$$

The simplified bit detection algorithm can be interpreted as follows: the spatial-temporal channel matrix in (5.34) corresponding to the high-rate user for $k_h = 1, \cdots, K_h$ becomes

$$H_{k_h} = \sum_{p=1}^{P} C_{k_h,p} \mathbf{A}_{k_h,p} \alpha_{k_h,p} \tag{5.53}$$

where

$$\mathbf{A}_{k_h,p} = \underbrace{\begin{bmatrix} \mathbf{a}(\theta_{k_h,p}) & \cdots & \mathbf{0} \\ \vdots & \ddots & \vdots \\ \mathbf{0} & \cdots & \mathbf{a}(\theta_{k_h,p}) \end{bmatrix}}_{(r+2)-column}$$

which is similar to that of single-rate systems. The spatial-temporal channel matrix corresponding to the low-rate user for $k_l = 1, \cdots, K_l$ becomes

$$H_{k_l} = \sum_{p=1}^{P} C_{k_l,p} \mathbf{A}_{k_l,p} \alpha_{k_l,p} \tag{5.54}$$

where

$$\mathbf{A}_{k_l,p} = \begin{bmatrix} \mathbf{a}(\theta_{k_l,p}) & \mathbf{0} & \mathbf{0} \\ \mathbf{0} & \mathbf{a}(\theta_{k_l,p}) & \vdots \\ \mathbf{0} & \mathbf{0} & \mathbf{a}(\theta_{k_l,p}) \end{bmatrix}$$

Thus, high-rate and low-rate users have the identical bit detector structure in each iteration illustrated in Figure 5.3.

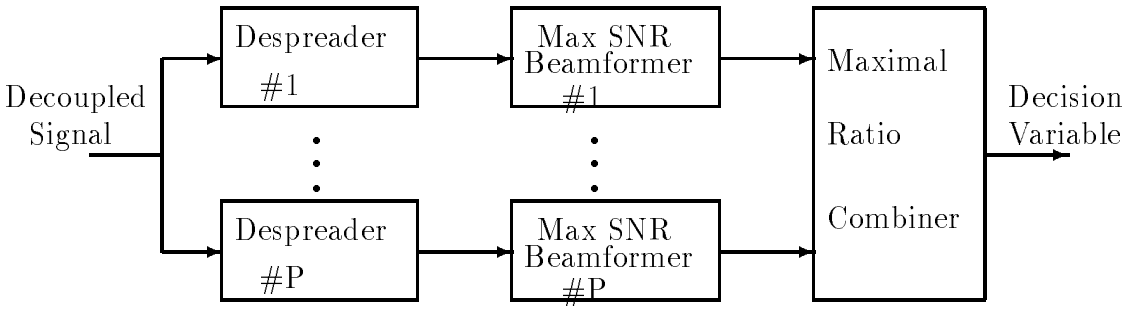

Figure 5.3: Simplified Bit Detection at Each Iteration

5.3.3 Performance Analysis

This section derives a BER lower bound for the SAGE-based receiver in dual-rate systems to assess the simulation results provided in the next section. Similar to the case for the single-rate systems, we again assume that we have cancelled all the multiple access interference in the hidden-data set at the final iteration cycle.

We assume that the spatial-temporal channel matrix for the desired user is known perfectly.

From (5.49) and (5.50) and straightforward application of the technique developed in Section 4.5, we obtain the BER lower bound for high-rate and low-rate users, for $q \in \{h, l\}$,

$$P_{k_q} = [(1-\mu_q)/2]^P \sum_{p=0}^{P-1} \begin{pmatrix} P-1+p \\ p \end{pmatrix} [(1+\mu_q)/2]^p \tag{5.55}$$

where

$$\mu_q = \sqrt{\frac{\bar{\gamma}_q}{(1+\bar{\gamma}_q)}}$$

and

$$\bar{\gamma}_q = \frac{M L_q A_{k_q}^2 \rho_{k_q k_q,11}^{0,0}}{\sigma^2} E[\alpha_{k_q,p}^2]$$

where

$$\rho_{k_q k_q,11}^{0,0} = |\mathbf{c}_{k_q,1}^0|^2$$

and $\mathbf{c}_{k_q,1}^0$ is given in (5.17) and (5.28) for low-rate and high-rate users, respectively. The average SNR for user k_q is denoted by $\bar{\gamma}_q$, L_q is the processing gain corresponding to $q \in \{h, l\}$ for high-rate and low-rate users, respectively, M and P are the numbers of antenna elements and propagation paths, respectively.

5.4 Simulation Results

We consider a dual-rate system with rate-ratio $r = 4$. Gold sequences of length 31 from [52] are assigned to high-rate users. For low-rate users, we obtain length-124 spreading sequences by repeating each length-31 Gold sequence four times:

$$c_{k_l 0}, \cdots, c_{k_l 30}, c_{k_l 0}, \cdots, c_{k_l 30}, c_{k_l 0}, \cdots, c_{k_l 30}, c_{k_l 0}, \cdots, c_{k_l 30}$$

The length-31 Gold sequences for high-rate users and low-rate users are different to avoid the possible confusion at the base-station receiver. In the simulations, we transmit a 100-bit information sequence from each high-rate user and a 25-bit information

sequence for each low-rate user in the same time interval. We assume that the channel attenuations and DOAs remain unchanged during the data-block transmission. One training bit in the first bit position in each sequence is inserted to obtain the initial channel array response vector estimates for either high-rate or low-rate users. A uniform linear array with half-wavelength spacing is used at the base-station and the DOAs are assumed to be uniformly distributed in $[-60°, 60°]$. The time delay of the first path for each active user is uniformly distributed in $(0,\ T_h/2)$ and the time delay of the second path for each user is uniformly distributed in $(T_h/2, T_h)$. Multipath channels are assumed to be Rayleigh-distributed with identical covariance for all paths. We consider CDMA systems with two-element base-station antenna arrays and two propagation paths for all of the following simulations.

In the first example, we consider a system with two high-rate users and two low-rate users. Four iterations are used to obtain the results. Figures 5.4 and 5.5 show the bit-error-rate (BER) performance of the SAGE-based iterative receiver for high-rate and low-rate users, respectively. It is observed that using the simplified bit sequence detection in Section 5.3.2 can achieve comparable performance to the detector having a multipath decorrelator for both high-rate and low-rate users. This is consistent with our claim in Section 5.3.2. Note that the BER performance of the simplified bit sequence detection is slightly better than that of the detector having a multipath decorrelator in some SNR regions. This can be explained as follows: similar to the multi-access interference decorrelator, the multipath decorrelator increases the variance of the background thermal noise, therefore makes its BER performance worse at some SNR points. Since the multipath signals for each user have been identified using despreading, the multipath decorrelator is not necessary. BER performance for high-rate and low-rate users is close to their lower bounds and two lower bounds are equivalent. The BER convergence to the iterative receiver for the high-rate and low-rate users is illustrated in Figures 5.6 and 5.7, respectively. We observe that the BER of the high-rate user converges faster than that of the low-rate user. This means that the BER of the low-rate users is much more sensitive to multi-access interference

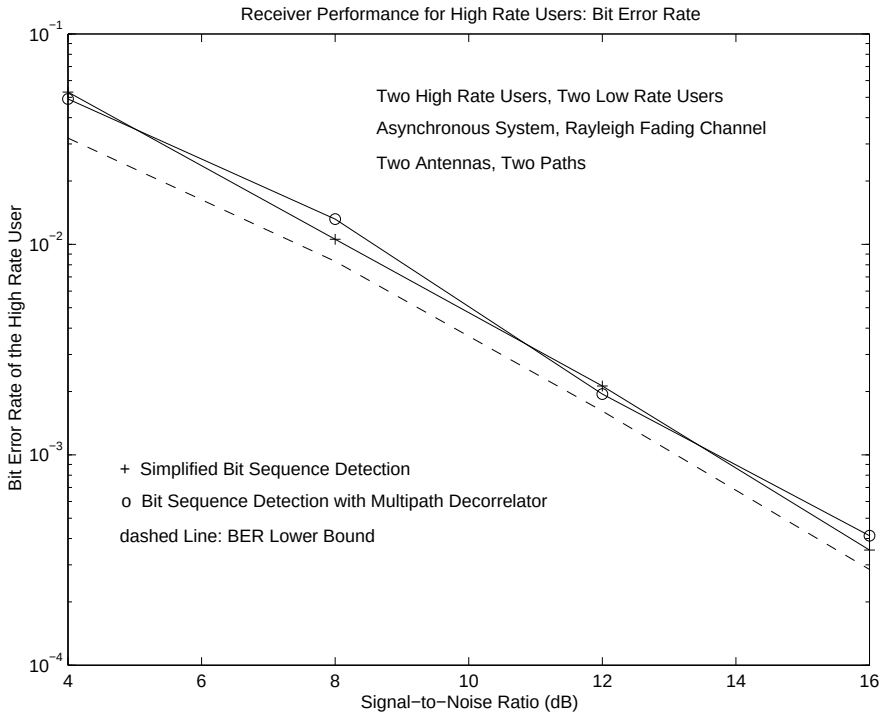

Figure 5.4: Bit Error Rate (BER) of the Desired High Rate User

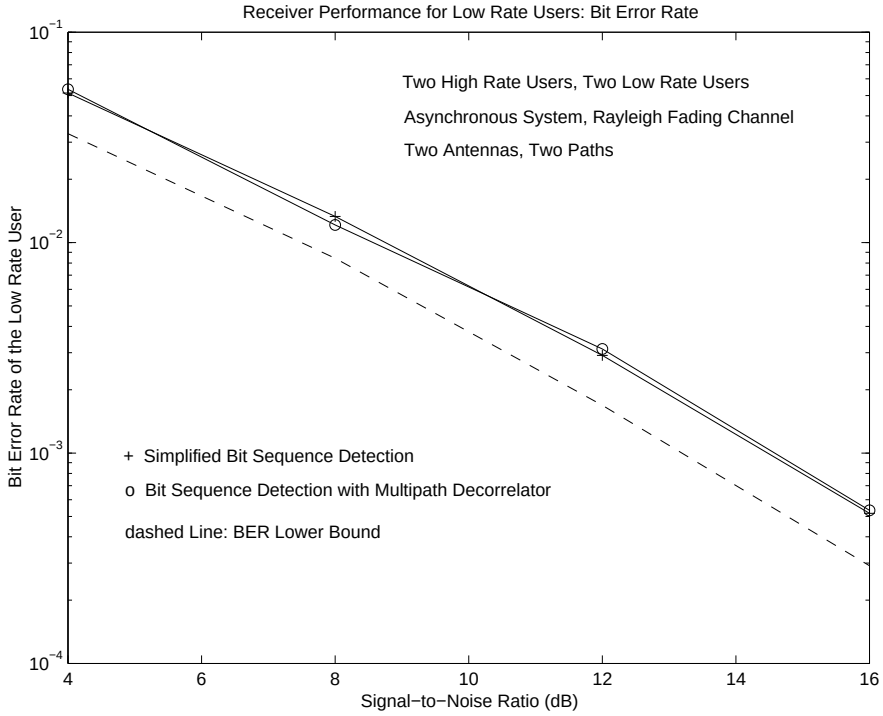

Figure 5.5: Bit Error Rate (BER) of the Desired Low Rate User

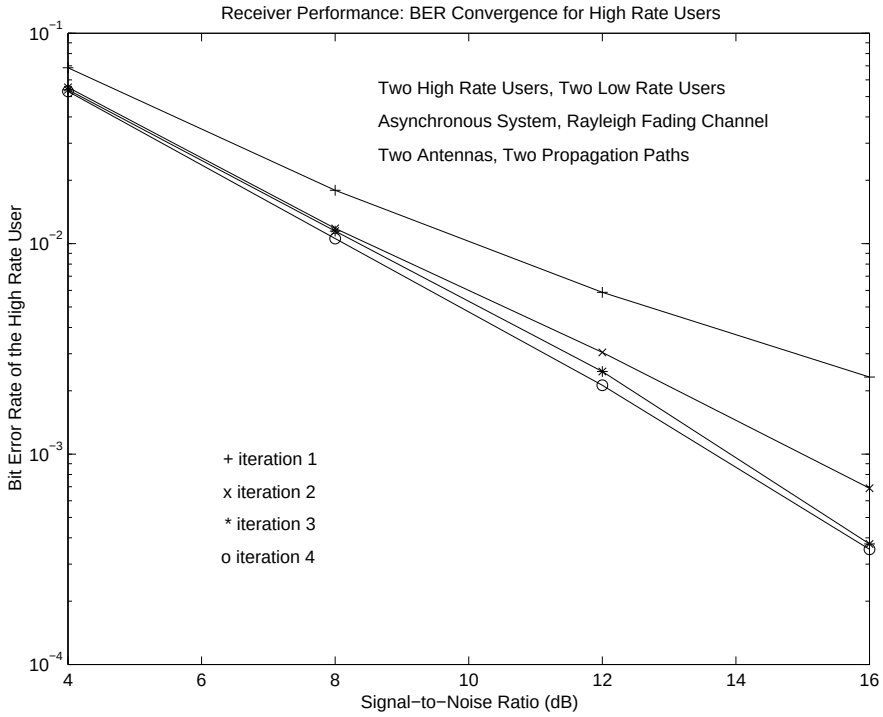

Figure 5.6: BER Convergence of the Desired High Rate User

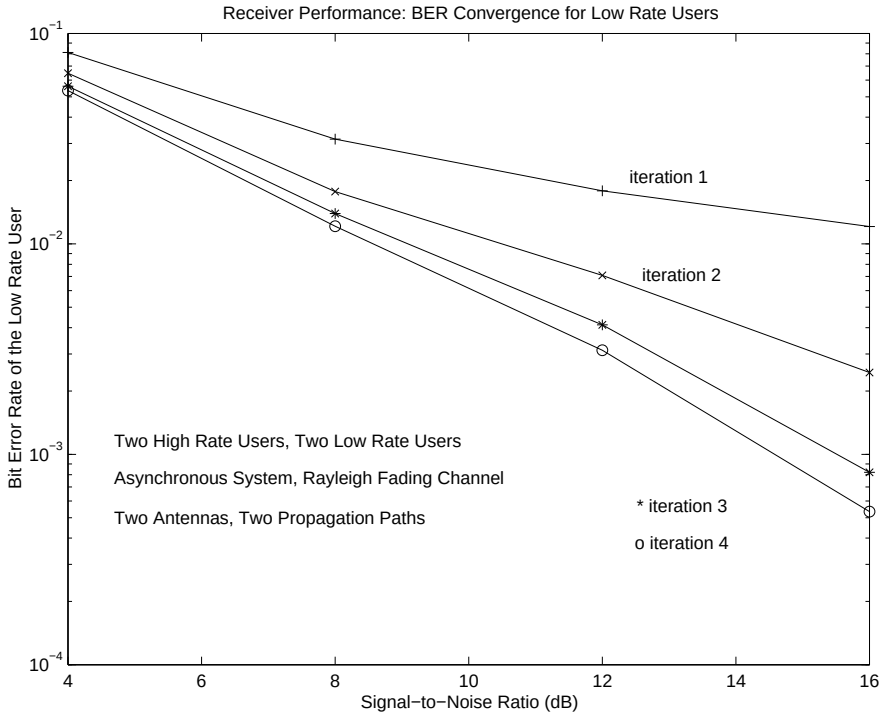

Figure 5.7: BER Convergence of the Desired Low Rate User

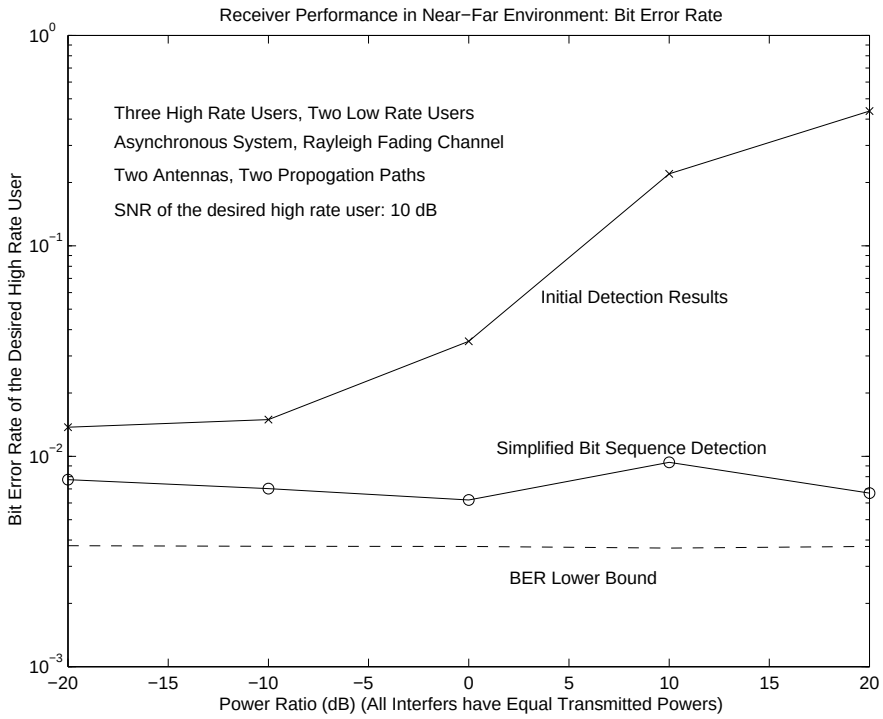

Figure 5.8: BER Performance of the Desired High Rate User in Near-Far Environment

than that of the high-rate users in dual-rate systems. The results are consistent with the findings in [12] that use a conventional single-user receiver with power control.

The second example is used to investigate BER performance of the iterative receiver in near-far environments. There exist three high-rate users and two low-rate users in the system. The SNR of the desired high-rate user is 10 dB. All other users have the same transmitted power and the power ratio changes from -20 dB to 20 dB. From Figure 5.8, we observe that the BER of the desired high rate user does not change with an increase of power of the interfering users. Therefore, the SAGE-based iterative receiver has near-far resistant behavior. Figure 5.9 shows the BER convergence for high-rate users. We see that the iterative receiver achieves near-far resistant BER performance at the expense of more iterations when the interferers become stronger.

In the final example, we consider a system with fixed two low-rate users and increase the number of the high-rate users. The SNRs for all users are the same

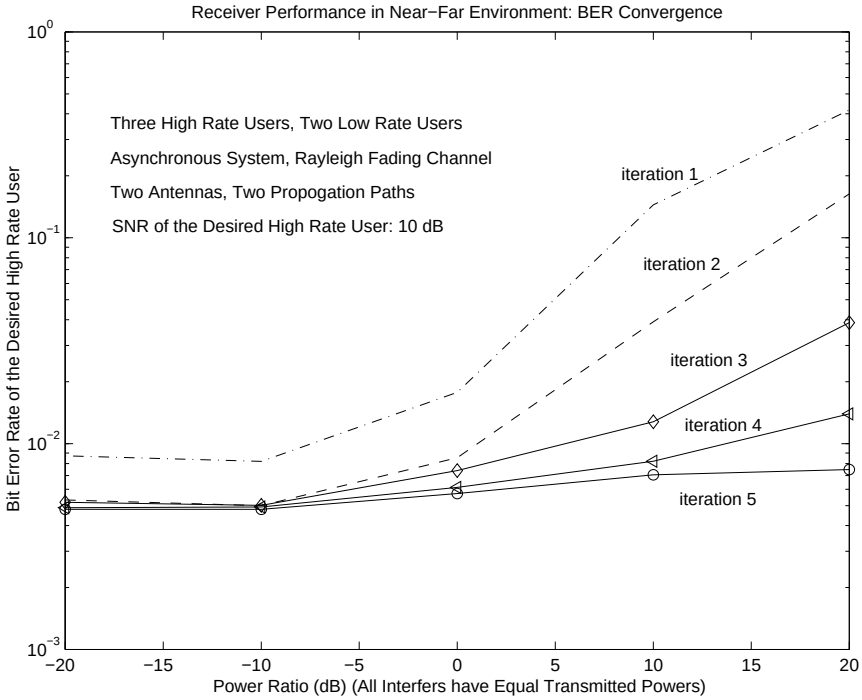

Figure 5.9: BER Convergence of the Desired High Rate User in Near-Far Environment

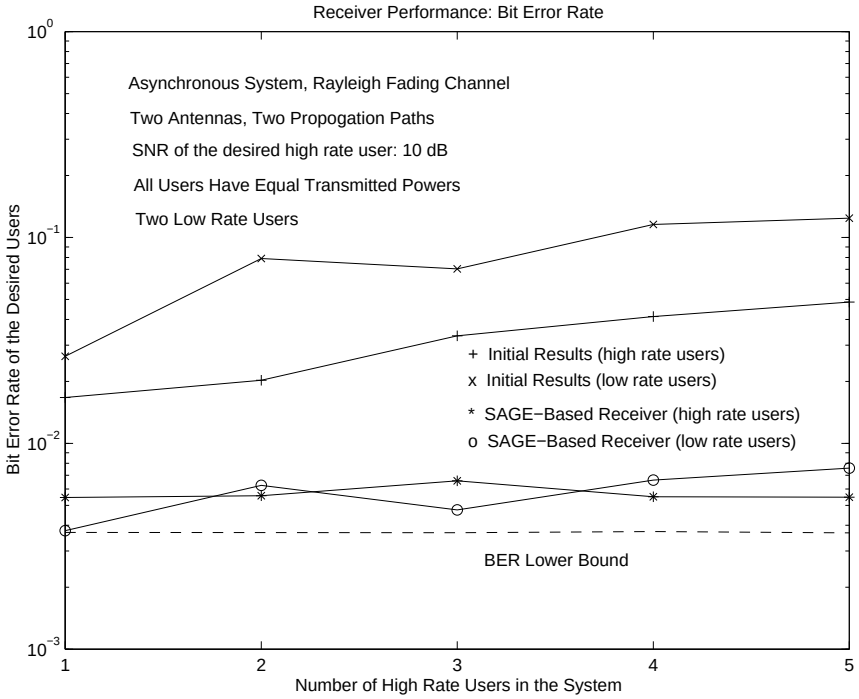

Figure 5.10: BER Performance of the Desired Users as a Function of Increasing Numbers of High Rate Users in the System

and set to be 10 dB. Figure 5.10 compares the BER performance of the high-rate and low-rate users. We observe that the BER performances are comparable and the performance for the high-rate users are slightly better than that of the low-rate users when the number of high-rate users gets large. BER convergences for high-rate and low-rate users are illustrated in Figures 5.11 and 5.12, respectively. Again, the BER of high-rate users converges faster than that of low-rate users.

5.5 Conclusions

We have extended the results in Chapter 4 for single-rate systems to dual rate systems in this chapter. We first developed a synchronous equivalent discrete-time system model for dual rate systems with base-station antenna arrays over asynchronous multipath fading channels. We applied the SAGE algorithm to this dual rate system

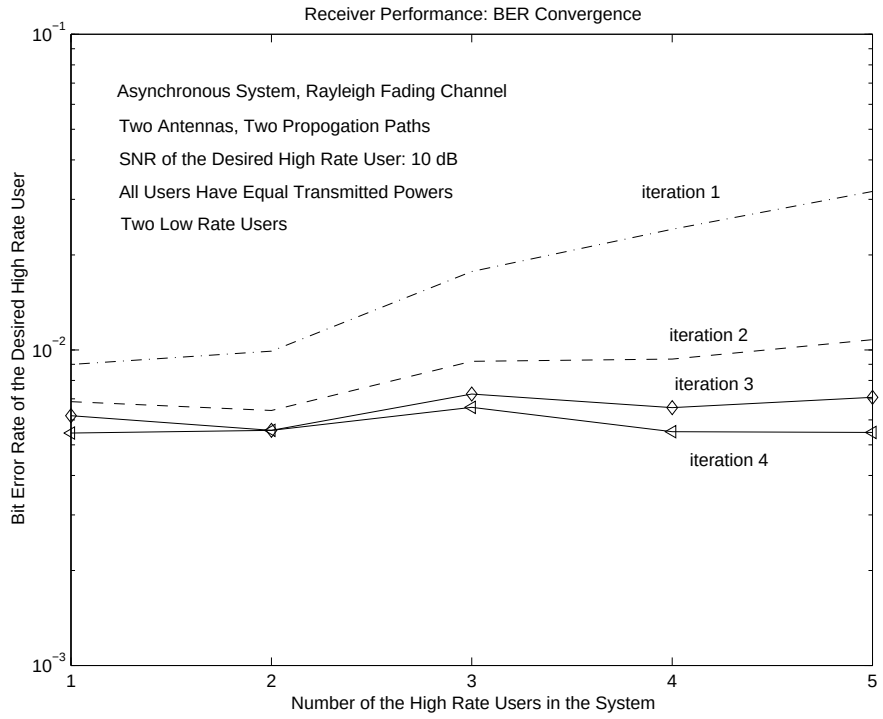

Figure 5.11: BER Convergence of the Desired High Rate User as a Function of Increasing Numbers of High Rate Users in the System

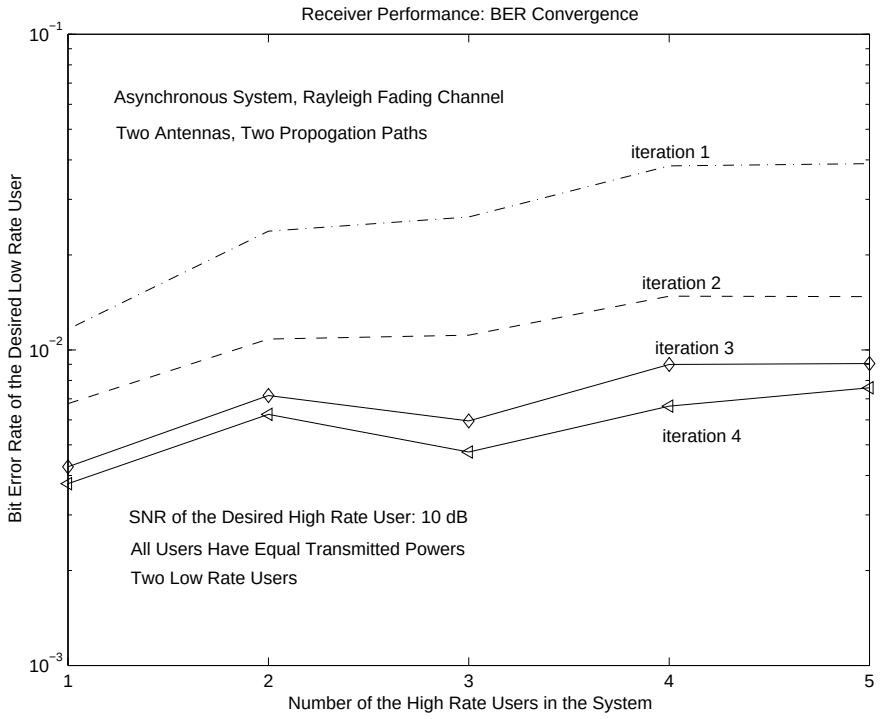

Figure 5.12: BER Convergence of the Desired Low Rate User as a Function of Increasing Numbers of High Rate Users in the System

model and obtained an iterative multi-user receiver for joint channel array response vector estimation and bit sequence detection with known relative time delays for all users. Simulation results show that the BER performance of the SAGE-based iterative receiver is near-far resistant. The BERs for high-rate users and low-rate users are equivalent and the BER of the high-rate user converges faster than that of the low-rate user. It is shown that using simplified bit detection algorithm achieves comparable BER performance to the detector having a multipath decorrelator for wideband CDMA systems. We observe that the BER performance degradation is very small for either high-rate users or low-rate users when the number of the high-rate users in the system gets large.

Chapter 6

Conclusions and Future Work

This chapter summarizes the major contributions in this thesis and presents possible future directions which could be extensions of the research work in this thesis.

6.1 Thesis Summary

This thesis has investigated spatial-temporal signal processing required for implementing channel estimation combined with multi-user signal detection. We considered the CDMA uplink with base-station antenna arrays for fading channels. The objectives of this work were to develop channel estimation and bit sequence detection algorithms for near-far resistant receivers. The computational complexity of the new receiver algorithms are shown to be linear in the number of users.

We first developed a spatial-temporal decorrelator for a synchronous single dominant-path channel and analyzed the decorrelator's asymptotic efficiency in Chapter 3. We found in Section 3.3 that the spatial-temporal decorrelator is near-far resistant and that using a base-station antenna array can significantly increase the asymptotic efficiency for either the spatial-temporal decorrelator or the conventional single-user detector. To jointly estimate channel array response vectors and detect information bit sequences for all active users, we applied the expectation-maximization (EM) and the space alternating generalized expectation-maximization (SAGE) algorithms to CDMA systems and obtained two iterative receiver structures in Sections 3.4 and

3.5, respectively. It has been demonstrated in Section 3.6.1 that the SAGE-based receiver converges faster than the EM-based receiver. We also found that using a base-station antenna array accelerates the receiver's convergence. It is shown that using base-station antenna arrays can improve channel array response vector estimates of the SAGE-based receiver and therefore improve the receiver's bit error rate (BER) performance. We observed that the BER performance of the SAGE-based receiver is near-far resistant and close to the simulated and analytical results for the case of known channels.

To extend the results obtained for synchronous systems to the case of asynchronous multipath systems, we formulate a synchronous equivalent discrete-time system model in Section 4.2. Based on this model, we derived a spatial-temporal decorrelator for asynchronous multipath channels by incorporating a maximal ratio combiner in Section 4.3. It is shown that this decorrelator is near-far resistant. We found that unlike base-station antenna arrays, multipath diversity does not improve asymptotic efficiency for either the spatial-temporal decorrelator or the conventional single-user detector. For given relative time delays, in Section 4.4, we applied the SAGE algorithm to obtain an iterative receiver structure for jointly estimating channel array response vectors and detecting bit sequences for all active users. We introduced double decoupling the multipath received signals to estimate the channel array response vector for each path of each user. It is shown that the SAGE-based receiver for multipath channels is also near-far resistant and the BER performance of the SAGE-based receiver is close to that for known channels. The approximation for analytical BER lower bound derived in Section 4.5 is found to be reasonable. Simulation results show that timing error effect is not significant for the case of equal transmitted powers and in lower SNR regions. However, the near-far resistance of the SAGE-based receiver degrades due to timing errors.

In Section 5.2, we formulated a discrete-time model for dual-rate systems with fixed chip rate and variable processing gain. We obtained an iterative multi-user receiver for joint channel array response vector estimation and bit sequence detection

for dual-rate systems with base-station antenna arrays and asynchronous multipath fading channels by using the techniques developed for the case of single-rate systems in Section 5.3. It is verified that multipath diversity combining is an efficient method to combat multipath interference and improve receiver's BER performance for CDMA systems. We found that using the SAGE-based receiver, the BER performance for both high rate users and low rate users are equivalent and close to the analytical BER lower bound. We have observed that using simplified bit detection algorithm derived in Section 5.3.2 can achieve comparable performance to the detector having a multipath decorrelator for wideband CDMA systems. It is shown that the BER performance of the SAGE-based receiver is near-far resistant and less sensitive to an increase of the number of the inteferers in the system at the expense of more iterations.

6.2 Future Directions

Although this thesis has investigated the problem of joint channel array response vector estimation and bit sequence detection by incorporating array signal processing with multi-user signal detection, there are several issues that remain to be explored. In this section, we discuss several important areas which require further study.

6.2.1 System Capacity Estimation

Due to the computational complexity of simultaneously estimating channel array response vectors and detecting bits for all users, this thesis verified the performance of proposed receivers by simulating a small number of users using bit error rate (BER). It is expected that the improved BER performance can potentially increase system capacity. However, direct system capacity estimation is more effective and straightforward to evaluate the proposed receivers for cellular communications. One possible method to estimate system capacity using proposed receivers is to find the residual interference after the final-stage iteration. By analyzing the residual interference

statistics, we could evaluate system capacity improvement using current methods such as that in [57].

6.2.2 Time Delay Estimation

In this thesis, we have assumed that the relative time delays for all the users are known at the base-station receiver. However, in practical applications, we have to estimate these parameters. Previous study showed that the BER performance of multi-user receivers degrades significantly due to time delay estimation errors for single-antenna single-path systems [3] [5] [63] [111]. In [5], an improved minimum-mean-squared-error (IMMSE) multi-user receiver is proposed taking into account the timing errors. However, numerical results show that the IMMSE receiver performs worse than the MMSE receiver in terms of bit error rate for small timing errors and still suffers from timing errors. Therefore, higher precise approaches to time delay estimation are required to achieve acceptable performance when the time delays are not available.

Time delay estimation for multi-user CDMA systems using subspace-based techniques have been proposed in [2] and [83]. In [47], it is observed that using a base-station antenna array can increase dimension of the noise subspace in [2] and hence increase the number of users in the system whose parameters can be correctly estimated. The application of the EM algorithm to time delay estimation is first reported in [17] for superimposed signals. In [15], joint time delay and channel attenuation estimation methods are proposed for multipath CDMA systems using the EM algorithm and the alternating projection algorithm developed in [112]. Time delay estimation, however, is computationally very complex. It is necessary to investigate efficient estimation schemes for multi-user systems. In [79], polynomial rooting is used to reduce computational complexity of time delay estimation for signal-user CDMA systems. Since our discrete-time model for asynchronous systems is formulated without assumption of priori knowledge of time delays for all the active users, it may be possible to incorporate time delay estimation into the receiver algorithms for both single-rate and multi-rate systems.

6.2.3 Multi-User Receiver in Multi-Cell Systems

Since it is difficult for a base-station to know all the spreading codes used in other cells, multi-user receivers only eliminate the multi-access interference (MAI) from the same cell. Interference from other cells is normally weaker than the MAI from the same cell and is a fraction f of the latter. The bound of capacity increase using multi-user detection is $(1+f)/f$ [11]. For $f = 0.55$, this factor is 2.8 [99]. It is expected that using a base-station antenna array could achieve higher capacity [11]. Therefore, it could be beneficial to investigate performance improvement by incorporating antenna array processing with multi-user signal detection for multi-cell systems.

6.2.4 Multi-user Receiver for Downlink

Much work on multi-user signal detection has been focused on the CDMA uplink (mobile to base-station). Improving downlink (base-station to mobile) capacity is also important. A joint transmitter-receiver structure is proposed based on the minimum mean squared error (MMSE) criterion for uplink multipath channel without base-station antenna array in [28]. However, channel parameter estimation is not addressed.

For antenna array CDMA systems, transmit beamforming can be used to improve system performance for the downlink [21]. The difficulty for CDMA transmit beamforming is that the channel characteristics for uplink and downlink are different in frequency division duplex systems since the estimated channel for uplink cannot be directly used to downlink. However, the directions of arrival (DOAs) for two links remain nearly the same if the channel changes slowly. Therefore, a possible transmit beamformer weight can be obtained from the estimated DOAs. Although we did not address the problem of DOA estimation in this thesis, it is straightforward to obtain DOAs from the estimated channel array response vectors for all active users. Thus, joint channel estimation and downlink multi-user detection by incorporating transmit beamforming could be a possible research direction.

Appendix A

Derivation of the Cramér-Rao Lower Bound (CRLB)

This appendix derives the Cramér-Rao Lower Bound (CRLB) for the channel array response vector estimates. Assumming that we have a block of received signal samples over N information symbols $\{\mathbf{x}(i), 1 \leq i \leq N\}$ and the channel and array response vectors remain unchanged during the block transmission, then the likelihood function of the data samples is given by

$$\Omega(\mathbf{x}(i)|i = 1, \cdots, N) = \frac{1}{\pi^{MLN}(\sigma^2/L)^{MLN}} \exp(-\frac{1}{\sigma^2/L} \sum_{i=1}^{N} [\mathbf{x}(i) - H\mathbf{b}(i)]^H [\mathbf{x}(i) - H\mathbf{b}(i)]) \tag{A.1}$$

The unknown deterministic parameters are background noise covariance σ^2, the real part and imaginary part of channel and array response vectors for K users. Denoting $\mathbf{a} = \bar{\mathbf{a}} + j\check{\mathbf{a}}$, where $\bar{\mathbf{a}}$ and $\check{\mathbf{a}}$ are the real and imagenary parts of $\mathbf{a}$, respectively, the unknown deterministic parameters background noise covariance σ^2, $\bar{\mathbf{a}}$ and $\check{\mathbf{a}}$. The parameter vector is defined as

$$\phi = \begin{bmatrix} \sigma^2 & \bar{\mathbf{a}}^T & \check{\mathbf{a}}^T \end{bmatrix}^T \tag{A.2}$$

Discarding the terms independent of the unknown parameter vecter ϕ, the log-likelihood function is given by

$$\ln \Omega = -MLN \ln \sigma^2 - \frac{L}{\sigma^2} \sum_{i=1}^{N} [\mathbf{x}(i) - H\mathbf{b}(i)]^H [\mathbf{x}(i) - H\mathbf{b}(i)]) \tag{A.3}$$

Now, we compute the derivative of the above log-likelihood function with respect to paramater vector ϕ. The derivative with respect σ^2 is given by

$$\frac{\partial \ln \Omega}{\partial \sigma^2} = -\frac{MLN}{\sigma^2} + \frac{L}{\sigma^4} \sum_{i=1}^{N} \mathbf{n}^H(i)\mathbf{n}(i) \tag{A.4}$$

The derivative of $\ln \Omega$ with respect to $\bar{\mathbf{a}}$ can be obtained by

$$\frac{\partial \ln \Omega}{\partial \bar{\mathbf{a}}} = [\frac{\partial \ln \Omega}{\partial \bar{\mathbf{a}}_1} \cdots \frac{\partial \ln \Omega}{\partial \bar{\mathbf{a}}_K}]^T \tag{A.5}$$

and (for $k = 1, \cdots, K$)

$$\frac{\partial \ln \Omega}{\partial \bar{\mathbf{a}}_k} = [\frac{\partial \ln \Omega}{\partial \bar{a}_1^1} \cdots \frac{\partial \ln \Omega}{\partial \bar{a}_K^M}]^T \tag{A.6}$$

where (for $k = 1, \cdots, K$ and $m = 1, \cdots, M$)

$$\frac{\partial \ln \Omega}{\partial \bar{a}_k^m} = \frac{2L}{\sigma^2} \sum_{i=1}^{N} Re[\mathbf{b}(i)^H \frac{\partial H^H}{\partial \bar{a}_k^m} \mathbf{n}(i)] = \frac{2L}{\sigma^2} \sum_{i=1}^{N} Re[b_k^*(i) \frac{\partial \mathbf{h}_k^H}{\partial \bar{a}_k^m} \mathbf{n}(i)] \tag{A.7}$$

where $Re(x)$ is the real part of x. Recall $\mathbf{h}_k = C_k \mathbf{f}_k$ and $\mathbf{f}_k = A_k \mathbf{a}_k$, then

$$\frac{\partial \mathbf{h}_k^H}{\partial \bar{a}_k^m} = \begin{bmatrix} \mathbf{0}_L^T & \cdots & A_k \mathbf{c}_k^T & \cdots & \mathbf{0}_L^T \end{bmatrix} \tag{A.8}$$

where $\mathbf{0}_L$ is an L-dimentional zero vector.

Denoting the $ML \times M$ channel derivative matrix as (for $k = 1, \cdots, K$)

$$D_k = \begin{bmatrix} A_k \mathbf{c}_k & \mathbf{0}_L & \cdots & \mathbf{0}_L \\ \mathbf{0}_L & A_k \mathbf{c}_k & \ddots & \mathbf{0}_L \\ \vdots & \ddots & \ddots & \vdots \\ \mathbf{0}_L & \cdots & \mathbf{0} & A_k \mathbf{c}_k \end{bmatrix} \tag{A.9}$$

(A.6) can be obtained as

$$\frac{\partial \ln \Omega}{\partial \bar{\mathbf{a}}_k} = \frac{2L}{\sigma^2} \sum_{i=1}^{N} Re[B_k^H(i) D_k^H \mathbf{n}(i)] \tag{A.10}$$

Using the following compact notation

$$D = \begin{bmatrix} D_1 & \cdots & D_K \end{bmatrix} \tag{A.11}$$

and

$$B(i) = \text{diag}[B_1(i), \ \cdots, \ B_K(i)] \tag{A.12}$$

the derivative of log-likelihood function with respect to $\bar{\mathbf{a}}$ is given by

$$\frac{\partial \ln \Omega}{\partial \bar{\mathbf{a}}} = \frac{2L}{\sigma^2} \sum_{i=1}^{N} Re[B^H(i) D^H \mathbf{n}(i)] \tag{A.13}$$

Similarly, the derivative of log-likelihood function with respect to the imaginary part of $\mathbf{a}$, $\breve{\mathbf{a}}$, is given by

$$\frac{\partial \ln \Omega}{\partial \bar{\mathbf{a}}} = \frac{2L}{\sigma^2} \sum_{i=1}^{N} Im[B^H(i) D^H \mathbf{n}(i)] \tag{A.14}$$

where $Im(x)$ represents the imaginary part of x.

The Fisher information matrix is given by [34]

$$\mathbf{I}(\phi) = E[(\frac{\partial \ln \Omega}{\partial \phi})(\frac{\partial \ln \Omega}{\partial \phi})^T] \tag{A.15}$$

First, we can obtain the following result [82]

$$I(\sigma^2) = E[|\frac{\partial \ln \Omega}{\partial \sigma^2}|^2] = \frac{MLN}{\sigma^4} \tag{A.16}$$

and $\frac{\partial \ln \Omega}{\partial \sigma^2}$ is uncorrelated with other two derivative vectors.

Using following relations [82]

$$Re(\mathbf{x}) Re(\mathbf{y}^T) = \frac{1}{2}[Re(\mathbf{x}\mathbf{y}^T + Re(\mathbf{x}\mathbf{y}^H] \tag{A.17}$$

$$Im(\mathbf{x}) Im(\mathbf{y}^T) = -\frac{1}{2}[Re(\mathbf{x}\mathbf{y}^T - Re(\mathbf{x}\mathbf{y}^H] \tag{A.18}$$

$$Re(\mathbf{x}) Im(\mathbf{y}^T) = \frac{1}{2}[Im(\mathbf{x}\mathbf{y}^T - Im(\mathbf{x}\mathbf{y}^H] \tag{A.19}$$

and

$$E[\mathbf{n}(i)\mathbf{n}^T(j)] = 0; \;\; i = 1, \cdots, N \quad and \quad j = 1, \cdots, N \tag{A.20}$$

$$E[\mathbf{n}(i)\mathbf{n}^H(j)] = \delta(i-j)\frac{\sigma^2}{L} I_M; \;\; i = 1, \cdots, N \quad and \quad j = 1, \cdots, N \tag{A.21}$$

where I_M is an $M \times M$ indentity matrix, we obtain

$$\mathbf{I}(\bar{\mathbf{a}}) = E[(\frac{\partial \ln \Omega}{\partial \bar{\mathbf{a}}})(\frac{\partial \ln \Omega}{\partial \bar{\mathbf{a}}})^T] = \frac{2L}{\sigma^2} \sum_{i=1}^{N} Re[B^H(i) D^H DB(i)] \tag{A.22}$$

$$\mathbf{I}(\bar{\mathbf{a}}\breve{\mathbf{a}}) = E[(\frac{\partial \ln \Omega}{\partial \bar{\mathbf{a}}})(\frac{\partial \ln \Omega}{\partial \breve{\mathbf{a}}})^T] = -\frac{2L}{\sigma^2} \sum_{i=1}^{N} Im[B^H(i) D^H DB(i)] \tag{A.23}$$

Denoting signal-to-noise ratio (SNR) $\gamma_k = A_k^2/\sigma^2$ (for $k = 1, \cdots, K$), we can obtain

$$\begin{aligned} G(i) &= B^H(i) D^H D B(i) \\ &= \begin{bmatrix} \gamma_1 \rho_{11} I_M & \sqrt{\gamma_1 \gamma_2}\rho_{12}\mathbf{B}_{12}(i) & \cdots & \sqrt{\gamma_1 \gamma_K}\rho_{1K}\mathbf{B}_{1K}(i) \\ \sqrt{\gamma_1 \gamma_2}\rho_{12}\mathbf{B}_{12}(i) & \gamma_2 \rho_{22} I_M & \ddots & \vdots \\ \vdots & \ddots & \ddots & \vdots \\ \sqrt{\gamma_1 \gamma_K}\rho_{1K}\mathbf{B}_{1K}(i) & \cdots & \cdots & \gamma_K \rho_{KK} I_M \end{bmatrix} \end{aligned}$$

where $\mathbf{B}_{kj}(i) = B_k^H(i) B_j(i)$ (for $i = 1, \cdots, N$ and $j = 1, \cdots, N$). Since G is real, we have

$$\mathbf{I}(\bar{\mathbf{a}}) = \mathbf{I}(\breve{\mathbf{a}}) = \frac{2L}{\sigma^2} \sum_{i=1}^{N} G(i) \tag{A.24}$$

and

$$\mathbf{I}(\bar{\mathbf{a}}\breve{\mathbf{a}}) = \mathbf{0} \tag{A.25}$$

Thus, the Fisher information matrix is given by

$$\mathbf{I}(\phi) = \begin{bmatrix} I(\sigma^2) & \mathbf{0}_{MK}^T & \mathbf{0}_{MK}^T \\ \mathbf{0}_{MK} & \mathbf{I}(\bar{\mathbf{a}}) & \mathbf{0} \\ \mathbf{0}_{MK} & \mathbf{0} & \mathbf{I}(\breve{\mathbf{a}}) \end{bmatrix} \tag{A.26}$$

Using inverse of a partitioned matrix, we can obtain the Cramer-Rao lower bound (CRLB) matrix for channel and array response vectors

$$\mathbf{CRLB}(\mathbf{a}) = \mathbf{I}(\bar{\mathbf{a}})^{-1} + \mathbf{I}(\breve{\mathbf{a}})^{-1} \tag{A.27}$$

Appendix B

Derivation of $\hat{H}_{k,p}$

In this Appendix, we derive the estimate of $H_{k,p}$, $\hat{H}_{k,p}$, in (4.38). Rewrite the log-likelihood function (4.37)

$$\Omega = -\frac{1}{\sigma^2/L}\sum_{i=1}^{N}(\hat{\mathbf{x}}_{k,p}^{Sj}(i) - H_{k,p}\mathbf{b}_k^w(i))^H(\hat{\mathbf{x}}_{k,p}^{Sj}(i) - H_{k,p}\mathbf{b}_k^w(i)) \tag{B.1}$$

Discarding the terms which are independent of $H_{k,p}$, the likelihood function can be written as

$$\Omega = \frac{1}{\sigma^2/L}\sum_{i=1}^{N}[\mathbf{b}_k^{wT}(i)H_{k,p}^H H_{k,p}\mathbf{b}_k^w(i) - 2\hat{\mathbf{x}}_{k,p}^{SjH}(i)H_{k,p}\mathbf{b}_k^w(i)] \tag{B.2}$$

We denote

$$H_{k,p} = \begin{bmatrix} H_{k,p}[1,1] & H_{k,p}[1,2] & H_{k,p}[1,3] \\ \vdots & \vdots & \vdots \\ H_{k,p}[2ML,1] & H_{k,p}[2ML,2] & H_{k,p}[2ML,3] \end{bmatrix} \tag{B.3}$$

where $H_{k,p}[m,n]$, for $m = 1,\cdots,2ML$ and $n = 1,2,3$, is the (m,n)th component of the matrix $H_{k,p}$,

$$\hat{\mathbf{x}}_{k,p}^{Sj}(i) = \begin{pmatrix} \hat{x}_{k,p}^{Sj}(i)[1] & \cdots & \hat{x}_{k,p}^{Sj}(i)[2ML] \end{pmatrix}^T \tag{B.4}$$

For notational consistency, we also denote

$$\mathbf{b}_k^w(i) = (b_k^w(i)[1] \quad b_k^w(i)[2] \quad b_k^w(i)[3])$$

Thus, the likelihood function can be expressed as

$$\begin{aligned}
\Omega = \tfrac{1}{\sigma^2/L}\textstyle\sum_{i=1}^{N} \quad & b_k^w(i)[1]\,(b_k^w(i)[1]\textstyle\sum_{m=1}^{2ML} H_{k,p}^*[m,1]H_{k,p}[m,1] \\
& \qquad +b_k^w(i)[2]\textstyle\sum_{m=1}^{2ML} H_{k,p}^*[m,2]H_{k,p}[m,1] \\
& \qquad +b_k^w(i)[3]\textstyle\sum_{m=1}^{2ML} H_{k,p}^*[m,3]H_{k,p}[m,1]) \\
& +b_k^w(i)[2]\,(b_k^w(i)[1]\textstyle\sum_{m=1}^{2ML} H_{k,p}^*[m,1]H_{k,p}[m,2] \\
& \qquad +b_k^w(i)[2]\textstyle\sum_{m=1}^{2ML} H_{k,p}^*[m,2]H_{k,p}[m,2] \\
& \qquad +b_k^w(i)[3]\textstyle\sum_{m=1}^{2ML} H_{k,p}^*[m,3]H_{k,p}[m,2]) \\
& +b_k^w(i)[3]\,(b_k^w(i)[1]\textstyle\sum_{m=1}^{2ML} H_{k,p}^*[m,1]H_{k,p}[m,3] \\
& \qquad +b_k^w(i)[2]\textstyle\sum_{m=1}^{2ML} H_{k,p}^*[m,2]H_{k,p}[m,3] \\
& \qquad +b_k^w(i)[3]\textstyle\sum_{m=1}^{2ML} H_{k,p}^*[m,3]H_{k,p}[m,3]) \\
& -2\,(b_k^w(i)[1]\textstyle\sum_{m=1}^{2ML}(\hat{x}_{k,p}^{Sj}(i)[m])^* H_{k,p}[m,1] \\
& \qquad +b_k^w(i)[2]\textstyle\sum_{m=1}^{2ML}(\hat{x}_{k,p}^{Sj}(i)[m])^* H_{k,p}[m,2] \\
& \qquad +b_k^w(i)[3]\textstyle\sum_{m=1}^{2ML}(\hat{x}_{k,p}^{Sj}(i)[m])^* H_{k,p}[m,3])
\end{aligned} \tag{B.5}$$

where $H_{k,p}^*[m,n]$ is the complex conjugate of $H_{k,p}[m,n]$ for $m = 1,\cdots,2ML$ and $n = 1,2,3$. To obtain the ML estimate for $H_{k,p}$, we take the derivative of (B.5) with respect to $H_{k,p}$. The derivative is given in a matrix form

$$\frac{\partial\Omega}{\partial H_{k,p}} = \begin{bmatrix} \frac{\partial\Omega}{\partial H_{k,p}[1,1]} & \frac{\partial\Omega}{\partial H_{k,p}[1,2]} & \frac{\partial\Omega}{\partial H_{k,p}[1,3]} \\ \vdots & \vdots & \vdots \\ \frac{\partial\Omega}{\partial H_{k,p}[2ML,1]} & \frac{\partial\Omega}{\partial H_{k,p}[2ML,2]} & \frac{\partial\Omega}{\partial H_{k,p}[2ML,3]} \end{bmatrix} \tag{B.6}$$

For $m = 1,\cdots,2ML$, we obtain

$$\begin{aligned}
\tfrac{\partial\Omega}{\partial H_{k,p}[m,1]} &= \tfrac{2}{\sigma^2/L}\textstyle\sum_{i=1}^{N} \quad b_k^w(i)[1]b_k^w(i)[1]H_{k,p}^*[m,1] + b_k^w(i)[1]b_k^w(i)[2]H_{k,p}^*[m,2] \\
&\qquad +b_k^w(i)[1]b_k^w(i)[3]H_{k,p}^*[m,3] - b_k^w(i)[1]\hat{x}_{k,p}^{Sj}(i)[m])^* \\
&= \tfrac{2}{\sigma^2/L}\textstyle\sum_{i=1}^{N} \quad H_{k,p}^*[m]\mathbf{b}_k^w(i)b_k^w(i)[1] - (\hat{x}_{k,p}^{Sj}(i)[m])^* b_k^w(i)[1]
\end{aligned} \tag{B.7}$$

where $H_{k,p}^*[m] = (H_{k,p}^*[m,1] \;\; H_{k,p}^*[m,2] \;\; H_{k,p}^*[m,3])$ is a 3-dimensional row vector for $m = 1,\cdots,2ML$. Similarly, we have

$$\frac{\partial\Omega}{\partial H_{k,p}[m,2]} = \frac{2}{\sigma^2/L}\sum_{i=1}^{N} H_{k,p}^*[m]\mathbf{b}_k^w(i)b_k^w(i)[2] - (\hat{x}_{k,p}^{Sj}(i)[m])^* b_k^w(i)[2] \tag{B.8}$$

and

$$\frac{\partial \Omega}{\partial H_{k,p}[m,3]} = \frac{2}{\sigma^2/L} \sum_{i=1}^{N} H^*_{k,p}[m]\mathbf{b}^w_k(i)b^w_k(i)[3] - (\hat{x}^{Sj}_{k,p}(i)[m])^* b^w_k(i)[3] \tag{B.9}$$

Therefore, the derivative matrix is obtained as

$$\begin{aligned}\frac{\partial \Omega}{\partial H_{k,p}} = \; & \frac{2}{\sigma^2/L} \sum_{i=1}^{N} \\ & \begin{bmatrix} H^*_{k,p}[1]\mathbf{b}^w_k(i)b^w_k(i)[1] & H^*_{k,p}[1]\mathbf{b}^w_k(i)b^w_k(i)[2] & H^*_{k,p}[1]\mathbf{b}^w_k(i)b^w_k(i)[3] \\ \vdots & \vdots & \vdots \\ H^*_{k,p}[2ML]\mathbf{b}^w_k(i)b^w_k(i)[1] & H^*_{k,p}[2ML]\mathbf{b}^w_k(i)b^w_k(i)[2] & H^*_{k,p}[2ML]\mathbf{b}^w_k(i)b^w_k(i)[3] \end{bmatrix} \\ & - \begin{bmatrix} (\hat{x}^{Sj}_{k,p}(i)[1])^* b^w_k(i)[1] & (\hat{x}^{Sj}_{k,p}(i)[1])^* b^w_k(i)[2] & (\hat{x}^{Sj}_{k,p}(i)[1])^* b^w_k(i)[3] \\ \vdots & \vdots & \vdots \\ (\hat{x}^{Sj}_{k,p}(i)[2ML])^* b^w_k(i)[1] & (\hat{x}^{Sj}_{k,p}(i)[2ML])^* b^w_k(i)[2] & (\hat{x}^{Sj}_{k,p}(i)[2ML])^* b^w_k(i)[3] \end{bmatrix}\end{aligned} \tag{B.10}$$

Eqn. (B.10) can be expressed in a compact form as

$$\frac{\partial \Omega}{\partial H_{k,p}} = \frac{2}{\sigma^2/L} \sum_{i=1}^{N} H^*_{k,p}\mathbf{b}^w_k(i)\mathbf{b}^{wT}_k(i) - (\hat{\mathbf{x}}^{Sj}_{k,p}(i))^* \mathbf{b}^{wT}_k(i) \tag{B.11}$$

Equating (B.11) to zero, and noting that $\mathbf{b}^w_k(i)$ is a real-valued vector, we obtain

$$\hat{H}_{k,p} = [\sum_{i=1}^{N} \hat{\mathbf{x}}^{Sj}_{k,p}(i)\mathbf{b}^{wT}_k(i)][\sum_{i=1}^{N} \mathbf{b}^w_k(i)\mathbf{b}^{wT}_k(i)]^{-1} \tag{B.12}$$

Bibliography

[1] P. Balaban and J. Salz, "Optimum diversity combining and equalization in data transmission with application to cellular mobile radio - Part I: theoretical considerations", *IEEE Transactions on Communications*, vol. 40, no. 5, pp. 885–894, May 1992.

[2] S. E. Bensley and B. Aazhang, "Subspace-based channel estimation for code division multiple access communication systems", *IEEE Transactions on Communications*, vol. 44, no. 8, pp. 1009–1020, Aug. 1996.

[3] R. M. Buehrer, A. Kaul, S. Striglis and B. D. Woerner, "Analysis of DS-CDMA parallel interference cancellation with phase and timing errors", *IEEE Journal on Selected Areas in Communications*, vol. 14, no. 8 pp. 1522–1534, Oct. 1996.

[4] D. S. Chen and S. Roy, "An adaptive multiuser receiver for CDMA systems". *IEEE Journal on Selected Areas in Communications*, vol. 12, no. 5, pp. 808–816, June 1994.

[5] L. Chu and U. Mitra, "Performance analysis of an improved MMSE multiuser receiver for mismatched delay channels", *IEEE Transactions on Communications*, vol. 46, no. 10, pp. 1369–1380, Oct. 1998.

[6] G. W. K. Colman, *An Investigation into the Capacity of Cellular CDMA Communication Systems with Beamforming in Environments with Scatter.* Master thesis, Dept. of Electrical and Computer Engineering, Queen's University, 1998.

[7] D. Dahlhaus, A. Jarosch, B. H. Fleury and R. Heddergott, "Joint demodulation in DS/CDMA systems exploiting the space and time diversity of the mobile radio channel", *Proceedings of the 1997 Sixth IEEE International Symposium on Personal, Indoor and Mobile Radio Communications*, pp. 47–52, Helsinki, Finland, 1997.

[8] A. P. Dempster, N. M. Laird and D. B. Rubin, "Maximum likelihood from incomplete data via the EM algorithm", *Journal of the Royal Statistical Society Series B*, vol. 39, no. 1, pp. 1–38, Nov. 1977.

[9] A. Duel-Hallen, "Decorrelating decision-feedback multiuser detector for synchronous code-division multiple-access channel", *IEEE Transactions on Communications*, vol. 41, no. 2, pp. 285–290, Feb. 1993.

[10] A. Duel-Hallen, "A family of multiuser decision-feedback detectors for asynchronous code-division multiple-access channels", *IEEE Transactions on Communications*, vol. 43, no. 2/3/4, pp. 421–434, Feb./Mar./Apr. 1995.

[11] A. Duel-Hallen, J. Holtzman and Z. Zvonar, "Multiuser detection for CDMA systems", *IEEE Personal Communications*, pp 46–58, Apr. 1995.

[12] A. M. Earnshaw, *An Investigation into Improving Performance of Cellular CDMA Communication Systems with Digital Beamforming.* PhD thesis, Dept. of Electrical and Computer Engineering, Queen's University, 1997.

[13] A. Mark Earnshaw and Steven D. Blostein, "A chip-level IS95-compliant cellular CDMA simulator: Design, implementation, and analysis". Technical report, Department of Electrical and Computer Engineering, Queen's University, 1996. Available from `http://ipcl.ee.queensu.ca`.

[14] R. B. Ertel and P. Cardieri, "Overview of spatial channel models for antenna array communication systems", *IEEE Personal Communications*, pp. 10–22, Feb. 1998.

[15] E. Ertin, U. Mitra and S. Siwamogsatham, "Iterative techniques for DS/CDMA multipath channel estimation", In *1998 Allerton Conference*, Monticello, IL., Sept. 1998.

[16] U. Fawer and B. Aazhang, "A multiuser receiver for code division multiple access communications over multipath channels", *IEEE Transactions on Communications*, vol. 43, no. 2/3/4, pp. 1556-1565, Feb./Mar./Apr. 1995.

[17] M. Feder and E. Weinstein, "Parameter estimation of superimposed signals using the EM algorithm", *IEEE Transactions on Acoustics, Speech, and Signal Processing*, vol. 36, no. 4, pp. 477–489, Apr. 1988.

[18] J. A. Fessler and A. O. Hero, "Complete-data spaces and generalized EM algorithms", In *Proc. IEEE Conf. on Acoustics, Speech, and Signal Processing*, vol. 4, pp. 1–4, 1993.

[19] J. A. Fessler and A. O. Hero, "Space-alternating generalized EM algorithm", *IEEE Transactions on Signal Processing*, vol. 42, no. 10, pp. 2664–2677, Oct. 1994.

[20] C. N. Georghiades and J. C. Han, "Sequence Estimation in the Presence of Random Parameters Via the EM Algorithm", *IEEE Transactions on Communications*, vol. 45, no. 3, pp. 300-308, Mar. 1997.

[21] K. S. Gilhousen, I. M. Jacobs, R. Padovani, A. J. Viterbi, Jr. L. A. Weaver, and C. E. Wheatley III, "On the capacity of a cellular CDMA system". *IEEE Transactions on Vehicular Technology*, 40(2):303–312, 1991.

[22] A. O. Hero and J. A. Fessler, "Asymptotic convergence properties of EM-tpye algorithms", , Technical Report, Communications and Signal Processing Lab., Dept. of Electrical and Computer Engineering, University of Michigan, Ann Arbor, April 1993.

[23] A. O. Hero and J. A. Fessler, "Convergence in norm for alternating expectation-maximization (EM) type algorithms", *Statistica Sinica*, vol. 5, no. 1, pp. 41–54, Jan. 1995.

[24] M. Honig, U. Madhow and S. Verdú, "Blind adaptive multiuser detection". *IEEE Transactions on Information Theory*, vol. 41, no. 4, pp. 944–960, July 1995.

[25] C.-L. I and R. D. Gitlin, "Multi-code CDMA wireless personal communications networks", *Proceedings of IEEE International Conference on Communications*, pp. 1060–1064, Seattle, WA, June 1995.

[26] P. A. Iltis and L. Mailaender, "An adaptive multiuser detector with joint amplitude and delay estimation", *IEEE Journal on Selected Areas in Communications*, vol. 12, no. 5, pp. 774–784, June 1994.

[27] W. C. Jakes, Ed., *Microwave Mobile Communications*, IEEE Press, Reprinted, 1994.

[28] W. M. Jang, B. R. Vojcic and R. L Pickholtz, "Joint transmitter-receiver optimization in synchronous multiuser communications over multipath channels", *IEEE Transactions on Communications*, vol. 46, no. 2, pp. 269–277, Feb. 1998.

[29] D. H. Johnson and D. E. Dudgeon, *Array Signal Pricessing: Concepts and Techniques*, Englewood Cliffs, NJ: Prentice-Hall, 1993.

[30] P. Jung and J. Blanz, "Joint detection with coherent receiver antenna diversity in CDMA mobile radio systems". *IEEE Transactions on Vehicular Technology*, vol. 44, no. 1, pp. 76–88, Feb. 1995.

[31] A. Kajiwara and M. Nakagawa, "Microcellular CDMA system with a linear multiuser interference canceler", *IEEE Journal on Selected Areas in Communications*, vol. 12, no. 4, pp. 605–611, May 1994.

[32] M. Kavehrad and P. McLane, "Performance of a low complexity channel coding and diversity for spread spectrum in indoor wireless communications", *AT&T Technical Journal*, vol. 64, pp. 1927–1964, Oct. 1985.

[33] T. Kawahara and T. Matsumoto, "Joint decorrelating multiuser detection and channel estimation in asynchronous CDMA mobile communications channels". *IEEE Transactions on Vehicular Technology*, vol. 44, no. 3, pp. 506–515, Aug. 1995.

[34] S. M. Kay, *Fundamentals of Statistical Signal Processing: Estimation Theory*, Prentice-Hill, Inc., 1993.

[35] B. H. Khahaj, A. Pauraj and T. Kailath, "2D RAKE receivers for CDMA cellular systems", *Proc. 1994 Globecom*, pp. 400–404, Dec. 1994.

[36] B. H. Khahaj, A. Pauraj and T. Kailath, "Spatio-temporal channel estimation techniques for multiple access spread spectrum systems with antenna arrays", *Proc. 1995 IEEE International Conference on Communications*, pp. 1520–1524, June 1995.

[37] R. Kohno, H. Imai, M. Hatori and S. Pasupathy, "Combination of an adaptive array antenna and a canceller of interference for direct-sequence spread-spectrum multiple-access system", *IEEE Journal on Selected Areas in Communications*, vol. 8, no. 4, pp. 675–681, May 1990.

[38] W. C. Y. Lee, *Mobile Communications Engineering*, McGraw-Hill, 1982.

[39] W. C. Y. Lee, "Overview of cellular CDMA". *IEEE Transactions on Vehicular Technology*, vol. 40, no. 2, pp. 291–302, 1991.

[40] H. Liu and G. Xu, "Smart antenna in wireless systems: uplink multiuser blind channel and sequence detection", *IEEE Transactions on Communications*, vol. 45, no. 2, pp. 187–199, Feb. 1997.

[41] H. Liu and M. D. Zoltowski, "Blind equalization in antenna array CDMA systems", *IEEE Transactions on Signal Processing*, vol. 45, no. 1, pp. 161–172, Jan. 1997.

[42] R. Lupas and S. Verdú, "Linear multiuser detectors for synchronous code-division multiple-access channels". *IEEE Transactions on Information Theory*, vol. 35, no. 1, pp. 123–136, Jan. 1989.

[43] R. Lupas and S. Verdú. "Near-far resistance of multiuser detectors in asynchronous channels". *IEEE Transactions on Communications*, vol. 38, no. 4, pp. 777–781, Apr. 1990.

[44] U. Madhow, "Blind adaptive interference suppression for the near-far resistant acquisition and demodulation of direct-sequence CDMA signals", *IEEE Transactions on Signal Processing*, vol. 45, no. 1, pp. 124–136, Jan. 1997.

[45] U. Madhow, "Blind adaptive interference suppression for direct-sequence CDMA", *Proceedings of the IEEE*, pp. 2049–2069, Oct. 1998.

[46] U. Madhow and M. L. Honig, "MMSE interference suppression for direct-sequence spread-spectrum CDMA". *IEEE Transactions on Communications*, vol. 42, No. 12, pp. 3178–3188, 1994.

[47] R. K. Madyastha and B. Aazhang, "Multiuser reveivers for CDMA communication systems using antenna array", *Proceedings of 32th Annual Allerton Conference on Communication, Control, and Computing*, Monticello, IL, Sept. 1994.

[48] S. L. Miller, "An adaptive direct-sequence code-division multiple-access receiver for multiuser interference rejection", *IEEE Transactions on Communications*, vol. 43, no. 2/3/4, pp. 1746–1755, Feb./Mar./Apr. 1995.

[49] S. Y. Miller and S. C. Schwartz, "Integrated spatial-temporal detectors for asynchronous Gaussian multiple-access channels", *IEEE Transactions on Communications*, vol. 43, no. 2/3/4, pp. 396–411, Feb./Mar./Apr. 1995.

[50] U. Mitra, "Comparison of maximum-likelihood-based detection for two multi-rate access schemes for CDMA signals", *IEEE Transactions on Communications*, vol. 47, no. 1, pp. 64–77, Jan. 1999.

[51] U. Mitra, D. Slock and C. Escudero, "Blind identification schemes for multi-channel DS/SS systems". In *1997 International Conference on Information Sciences and Systems*, Johns Hopkins University, 1997.

[52] A. M. Monk, M. Davis and L. B. Milstein, "A noise-whitening approach to multiple access noise rejection - part I: theory and background", *IEEE Journal on Selected Areas in Communications*, vol. 12, no. 5, pp. 817–827, June 1994.

[53] Robert A. Monzingo and Thomas W. Miller. *Introduction to Adaptive Arrays.* John Wiley & Sons, Inc., 1980.

[54] T. Moon, "The Expectation-Maximization algorithm", *IEEE Signal Processing Magazine*, pp. 47–60, Nov. 1996.

[55] T. K. Moon, Z. Xie, C. K. Rushforth and R. T. Short, "Parameter estimation in a multi-user communication system", *IEEE Transactions on Communications*, vol. 42, no. 8, pp. 2553–2559, Aug. 1994.

[56] Shimon Moshavi. "Multi-user detection for DS-CDMA communications". *IEEE Communications Magazine*, vol. 34, no. 10, pp. 124–136, Oct. 1996.

[57] Ayman F. Naguib. *Adaptive Antennas for CDMA Wireless Networks.* PhD thesis, Dept. of Electrical Engineering, Stanford University, 1995.

[58] Ayman F. Naguib and Arogyaswami Paulraj. "Performance of wireless CDMA with M-ary orthogonal modulation and cell site antenna arrays". *IEEE Journal on Selected Areas in Communications*, vol. 14, no. 9, pp. 1770–1783, 1996.

[59] Ayman F. Naguib, Arogyaswami Paulraj, and Thomas Kailath. "Capacity improvement with base-station antenna arrays in cellular CDMA". *IEEE Transactions on Vehicular Technology*, vol. 43, no.3, pp. 691–698, 1994.

[60] L. B. Nelson and H. V. Poor, "Iterative multiuser receivers for CDMA channels: an EM-Based approach", *IEEE Transactions on Communications*, vol. 44, no. 12, pp. 1700–1710, Dec. 1996.

[61] B. C. Ng, M. Cedervall and A. Paulraj, "A structured channel estimator for maximum likelihood sequence detection". *IEEE Communications Letter*, vol. 1, no. 2, pp. 52–55, Mar. 1997. .

[62] A. Papoulis. *Probability, Random Variables, and Stochastic Processes.* McGraw-Hill, Inc., 1984.

[63] S. Parkvall, E. Strom and B. Ottersten, "The impact of timimg errors on the performance of linear DS-CDMA receivers", *IEEE Journal on Selected Areas in Communications*, vol. 14, no. 8 pp. 1660–1668, Oct. 1996.

[64] P. Patel and J. Holtzman, "Analysis of a simple successive interference cancellation scheme in DS/CDMA system", *IEEE Journal on Selected Areas in Communications*, vol. 12, no. 5, pp. 796–807, June 1994.

[65] P. Patel and J. Holtzman, "Performance comparison of a DS/CDMA system using a successive interference cancellation (IC) scheme and a parallel IC scheme under fading". In *1994 International Conference on Communications*, pp. 510–515, 1994.

[66] A. J. Paulraj and C. B. Papadias, "Space-time processing for wireless communications", *IEEE Signal Processing Magazine*, pp. 49–83, Nov. 1997.

[67] S. U. Pillai, *Array Signal Processing.* Springer-Verlag, 1989.

[68] H. V. Poor. *An Intriduction to Signal Detection and Estimation.* Springer-Verlag, 1994.

[69] J. G. Proakis. *Digital Communications*, 3rd Ed., McGraw-Hill, Inc., 1995.

[70] Qualcomm Inc. "Mobile station-base compatibility standard for dual-mode wideband spread system", 1993.

[71] P. B. Rapajic and B. S. Vucetic, "Adaptive receiver structures for asynchronous CDMA systems", *IEEE Journal on Selected Areas in Communications*, vol. 12, no. 4, pp. 685–697, June 1994.

[72] M. Saquib, R. Yates and N. Mandayam, "Decorrelating detectors for a dual rate synchronous DS/CDMA channel", *Proceedings of the IEEE Vehicular Technology Conference*, Atlanta, GA, May 1996.

[73] M. Saquib, R. Yates and N. Mandayam, "A decision feedback decorrelator for a dual rate synchronous DS/CDMA system", *Proceedings of 1996 IEEE Global Telecommunications Conference*, London, Nov. 1996.

[74] M. Saquib and R. Yates, "A two stage decorrelator for a dual rate synchronous DS/CDMA system", *Proceedings of 1997 IEEE International Conference on Communications*, Montreal, June 1997.

[75] M. Saquib, R. Yates and A. Ganti, "An ansynchronous decentralized multi-rate decorrelator", *Proceedings of the Conference on Information Science ans Systems*, pp. 462–467, Johns Hopkins University, March 1997.

[76] J. B. Schodorf and D. B. Williams, "Array processing techniques for multiuser detection". *IEEE Transactions on Communications*, Vol. 45, No. 11, pp. 1375–1378, Nov. 1997.

[77] M. Schwartz, W. R. Bennett and S. Stein, *Communication Systems and Techniques*, McGraw-Hill, 1995.

[78] I. Sharfer and A. O. Hero, "Optimum multiuser CDMA detector using grouped coordinate ascent and the DWT", *Proceedings of the IEEE 1997 Workshop in Signal Processing Advances in Wireless Communications*, Paris, Apr. 1997.

[79] I. Sharfer and A. O. Hero, "A maxmum likelihood digital receiver using coordinate ascent and the discrete wavelet transform", *IEEE Transactions on Signal Processing*, vol. 46, no. 12, Dec. 1998.

[80] W. Y. Shiu and S. D. Blostein, "Adaptive digital beamforming in cellular CDMA systems using noniterative signal subspace tracking". In *1997 International Conference on Communications*, pp. 652–656, 1997.

[81] A. C. K. Soong and W. A. Krzymien, "A novel CDMA multiuser interference cancellation receiver with reference symbol aided estimation of channel parameters". *IEEE Journal on Selected Areas in Communications*, vol. 14, no. 8, pp. 1536–1547, Oct. 1996.

[82] P. Stoica and A. Nehorai, "Music, maximum likelihood, and Cramer-Rao bound", *IEEE Transactions on Acoustics, Speech, and Signal Processing*, vol. 37, no. 5, pp. 720–741, May 1989.

[83] E. Strom, S. Parkvall, S. Miller and B. Ottersten, "Propagation delay estimation in asynchronous direct-sequence code-division multiple access systems", *IEEE Transactions on Communications*, vol. 44, no. 1, pp. 84–93, Jan. 1996.

[84] G. L. Stuber, *Principle of Mobile Communication*, Kluwer Academic, 1996.

[85] S. C. Swales, M. A. Beach, D. J. Edwards, and J. P. McGeehan, "The performance enhancement of multibeam adaptive base-station antennas for cellular land mobile radio systems". *IEEE Transactions on Vehicular Technology*, vol. 39, no. 1, pp. 56–67, Jan. 1990.

[86] S. Talwar, M. Viberg and A. Paulraj, "Blind separation of synchronous co-channel digital signals using an antenna array. part I: algorithm". *IEEE Transactions on Signal Processing*, vol. 44, no. 5, pp. 1184–1197, May 1996.

[87] Telecommunications Industry Association (TIA), *The cdma2000 ITU-R RTT Candidate Submission*, 1998.

[88] J. S. Thompson, P. M. Grant and B. Mulgrew, "Smart antenna arrays for CDMA systems", *IEEE Personal Communications*, pp 15–25, Oct. 1996.

[89] M. Torlak and G. Xu, "Blind multi-user channel estimation in asynchronous CDMA systems". *IEEE Transactions on Signal Processing*, vol. 45, no. 1, pp. 137–147, Jan. 1997.

[90] M. C. Vanderveen, A-J. van der Veen and A. Paulraj, "Estimation of multipath parameters in wireless communications". *IEEE Transactions on Signal Processing*, vol. 46, no. 3, pp. , Mar. 1998.

[91] M. K. Varanasi and B. Aazhang, "Multistage detection in asynchronous code-division multiple-access communications", *IEEE Transactions on Communications*, vol. 38, no. 4, pp. 509–519, Apr. 1990.

[92] M. K. Varanasi and B. Aazhang, "Near-optimum detection in synchronous code-division multiple-access communications", *IEEE Transactions on Communications*, vol. 39, no. 5, pp. 725–736, May 1991.

[93] S. Vansudevan and M. K. Varanasi, "Achieving Near-optimum asymptotic efficiency and fading resistance over the tiem-varying Rayleigh-faded CDMA channel", *IEEE Transactions on Communications*, vol. 44, no. 9, pp. 1130–1143, Sept. 1996.

[94] S. Verdú, *Optimum Multi-user Signal Detection.* PhD thesis, Dept. of Electrical & Computer Engineering, University of Illinois, Urbana-Champaihn, 1984.

[95] S. Verdú, "Minimum probability of error for asynchronous Gaussian multiple-access channels". *IEEE Transactions on Information Theory*, vol. 32, no. 1, pp. 85–96, Jan. 1986.

[96] S. Verdú, "Optimum multi-user asymptotic efficiency", *IEEE Transactions on Communications*, vol. 34, no. 9, pp. 890–897, Sept. 1986.

[97] S. Verdú, "Adaptive multiuser detection". in *Code Division Multiple Access Communicatoins*, S. D. Glisic and P. A. Leppanen, Eds., Dordrecht: Kluwer, 1995.

[98] A. J. Viterbi, "Very low rate convolutional codes for maximum theoretical performance of spread-spectrum multiple-access channels", *IEEE Journal on Selected Areas in Communications*, vol. 8, no. 4, pp. 641–649, May 1990.

[99] A. J. Viterbi, "The orthogonal-random wave form dichotomy for digital mobile personal communications", *IEEE Personal Communications*, First Quarter, pp. 18–24, 1994.

[100] A. J. Viterbi. *CDMA: Principles of Spread Spectrum Communication.* Addison-Wesley, 1995.

[101] R. Wang and S. D. Blostein, "Maximum likelihood multi-user CDMA receiver for base-station antenna arrays using EM algorithm", *Proceedings of 19th Biennial Symposium on Communications*, Kingston, ON, June 1998.

[102] X. Wang and H. V. Poor, "Blind multiuser detection: a subspace approach". *IEEE Transactions on Information Theory*, vol. 44, no. 2, pp. 677–690, March 1998.

[103] S. S. H. Wijayasuriya, G. H. Norton and J. P. McGeehan, "A sliding window decorrelating receiver for multiuser DS-CDMA mobile radio networks". *IEEE Transactions on Vehicular Technology*, vol. 45, no. 3, pp. 503–521, Aug. 1996.

[104] J. H. Winters, "Optimum combining in digital mobile radio with cochannel interference", *IEEE Journal on Selected Areas in Communications*, vol. 2, no. 4, pp. 528–539, July 1984.

[105] J. H. Winters, "Signal acquisition and tracking with adaptive arrays in the digital mobile radio system IS-54 with flat fading". *IEEE Transactions on Vehicular Technology*, vol. 42, no. 4, pp. 377–384, Nov. 1993.

[106] C. F. J. Wu, "On the convergence properties of the EM algorithm", *Annals of Statistics*, vol. 11, no. 1, pp. 95–103, Jan. 1983.

[107] Z. Xie, R. T. Short and C. K. Rushforth, "A family of suboptimum detectors for coherent multiuser communications", *IEEE Journal on Selected Areas in Communications*, vol. 8, no. 4, pp. 683–690, May 1990.

[108] Z. Xie, C. K. Rushforth and R. T. Short and T. K. Moon, "Joint signal detection and parameter estimation in multiuser communications", *IEEE Transactions on Communications*, vol. 41, no. 7, pp. 1208–1215, Aug. 1993.

[109] M. D. Yacoub, *Foundations of Mobile Radio Engineering*, CRC Press, 1993.

[110] Y. C. Yoon and H. Leib, "Matched filters with interference suppression capabilities for DS-CDMA", *IEEE Journal on Selected Areas in Communications*, vol. 14, no. 8, pp. 1510–1521, Oct. 1996.

[111] F. Zheng and S. K. Barton, "On the performance of near-far resistant CDMA detectors in the presence of synchronization errors", *IEEE Transactions on Communications*, vol. 43, no. 12, pp. 3037–3045, Dec. 1995.

[112] I. Ziskind and M. Wax, "Maximum likelihood localization of multiple sources by alternating projection", *IEEE Transactions on Signal Processing*, vol. 36, no. 10, pp. 1553–1560, Oct. 1988.

[113] Z. Zvonar, "Combined multiuser detection and diversity reception for wireless CDMA systems", *IEEE Transactions on Vehicular Technology*, vol. 45, no. 1, pp. 205–211, Feb. 1996.

[114] Z. Zvonar and D. Brady, "Multiuser detection in single-path fading channels", *IEEE Transactions on Communications*, vol. 42, no. 2/3/4, pp. 1729–1739, Feb./Mar./Apr. 1994.

[115] Z. Zvonar and D. Brady, "Suboptimal multiuser detector for frequency-selective Rayleigh fading synchrous CDMA channels", *IEEE Transactions on Communications*, vol. 43, no. 2/3/4, pp. 154–157, Feb./Mar./Apr. 1995.

Vita

Ruifeng Wang

EDUCATION

Ph.D.	Electrical and Computer Engineering, Queen's University	1995–99
M.Sc.	Telecommunications & Control, Northern Jiaotong University	1986–89
B.Sc	Telecommunications & Control, Northern Jiaotong University	1982–86

AWARD

Queen's Graduate Awards	1995–99
Queen's Graduate Fellowship	1996–97

EXPERIENCE

Senior Member of Technical Staff (1999-), COM DEV, Cambridge, Ontario

Research Assistant (1995–1999), Electrical & Computer Engineering, Queen's University

Teaching Assistant (1995–1996), Electrical & Computer Engineering, Queen's University

Hardware Design Engineer (1989–1995), The Sixth Research Institute, Ministry of Electronics Industry, Beijing, China

Research Assistant (1986–1989), Signal & Systems Lab, Northern Jiaotong University

PUBLICATIONS

Ruifeng Wang and Steven D. Blostein, "Iterative Multiuser Receivers for Antenna Array CDMA Systems over Asynchronous Multipath Fading Channels", Submitted to *IEEE Journal on Selected Areas in Communications: Wireless Communications Series*, March, 1999.

Ruifeng Wang and Steven D. Blostein, "A Spatial-Temporal Decorrelating Receiver for CDMA Systems with Base-Station Antenna Arrays", Submitted to *IEEE Transactions on Communications*, October 1998.

Ruifeng Wang and Steven D. Blostein, "Spatial-Temporal CDMA Receiver Structures for Rayleigh Fading Channels", *1999 International Conference on Communications*, Vancouver, June, 1999.

Ruifeng Wang and Steven D. Blostein, "Maximum Likelihood Multi-User CDMA Receiver for Base-Station Antenna Arrays Using EM Algorithm", *Proc. 19th Biennial Symposium on Communications*, Kingston, June, 1998, pp.110–114.